Enantioselective Modification of Sulfonamides and Sulfonamide-Containing Drugs via Carbene Organic Catalysis

Runjiang Song+[a], Yingguo Liu+[a], Pankaj Kumar Majhi+[a], Ng Pei Rou[a], Lin Hao[a], Jun Xu[b,a], Weiyi Tian*[b], Long Zhang[c], Hongmei Liu[c], Xinglong Zhang*[d], Yonggui Robin Chi*[a,e]

[a] Division of Chemistry & Mathematical Science, School of Physical & Mathematical Sciences, Nanyang Technological University, Singapore 637371, Singapore
Email: robinchi@ntu.edu.sg
[b] Guizhou University of Traditional Chinese Medicine, Guiyang 550025, China
Email: tianweiyi@gzy.edu.cn
[c] Institute of Nervous System Diseases, Xuzhou Medical University, Xuzhou 221002, P. R. China
[d] Institute of High Performance Computing, A*STAR (Agency for Science, Technology and Research), 138632, Singapore
Email: zhang_xinglong@ihpc.a-star.edu.sg
[e] Key Laboratory of Green Pesticide and Agricultural Bioengineering,Ministry of Education, Guizhou University, Huaxi District, Guiyang 550025, China
[+] These authors contributed equally to this work.

Table of Content

I. General Information

Commercially available materials purchased form TCI or Sigma Aldrich was used as received. All reactions were carried out under an argon atmosphere with dry solvents under anhydrous conditions, unless otherwise noted. THF were distilled from sodium-benzophenone. Flash chromatography was performed using silica gel (200- 300 mesh). Reactions were monitored by thin layer chromatography (TLC). Visualization was achieved under a UV lamp (254nm and 365 nm). ^{1}H and ^{13}C NMR were recorded on Bruker BBFO 400 MHz NMR, Bruker AV400 MHz NMR spectrometer with TMS as the internal standard and were calibrated using residual undeuterated solvent as an internal reference ($CDCl_3$: ^{1}H NMR = 7.26, ^{13}C NMR = 77.16). The following abbreviations were used to explain the multiplicities: s = singlet, d = doublet, t = triplet, q = quartet, m = multiplet, br = broad. Coupling constants (J) are reported in Hertz (Hz). High resolution Mass spectra (HRMS) were recorded by using Finnigan MAT 95 XP mass spectrometer (Thermo Electron Corporation). The determination of ee was performed via chiral HPLC analysis using Shimadzu LC-20AD HPLC workstation. Optical rotations were measured using a 1 mL cell with a 1 dm path length on a Jasco P-1030 polarimeter and are reported as follows: $[\alpha]^{rt}{}_{D}$ (c in g per 100 mL solvent). Melting points were determined via SRS OptiMelt MPA100.

II. Condition Optimization[a]

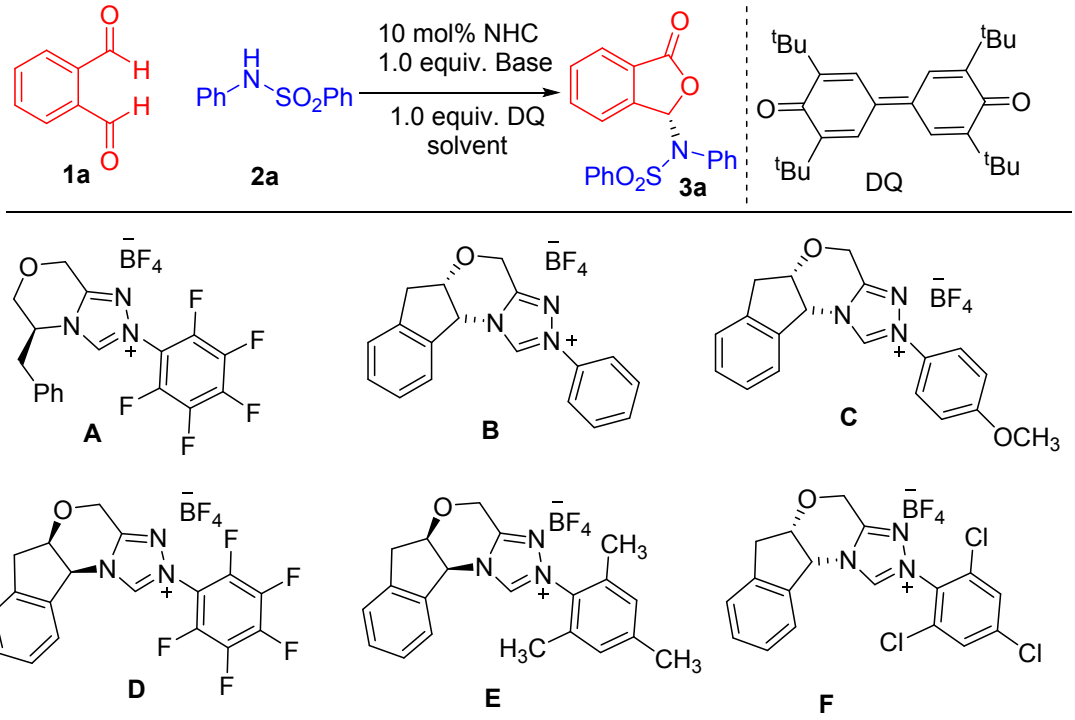

Entry	NHC	Base	Solvent	Yield(%)	e.r.
1	A	DBU	CH_2Cl_2	77	46:54
2	B	DBU	CH_2Cl_2	84	53:47
3	C	DBU	CH_2Cl_2	88	60:40
4	D	DBU	CH_2Cl_2	66	16:84
5	E	DBU	CH2Cl2	68	14:86
6	F	DBU	CH_2Cl_2	92	86:14
7	F	DIEA	CH_2Cl_2	82	97:3
8	F	Et_3N	CH_2Cl_2	83	96:4
9	F	DMAP	CH_2Cl_2	83	96:4
10	F	DABCO	CH_2Cl_2	81	97:3

11	F	K_2CO_3	CH_2Cl_2	76	97:3
12	F	Cs_2CO_3	CH_2Cl_2	79	96:4
13	F	$LiOH.H_2O$	CH_2Cl_2	92	99:1
14	F	$LiOH.H_2O$	Tolune	89	97:3
15	F	$LiOH.H_2O$	$PhCF_3$	80	97:3
16	F	$LiOH.H_2O$	EtOAc	61	90:10
17	F	$LiOH.H_2O$	MeCN	58	88:12
18	F	$LiOH.H_2O$	THF	74	92:8
19	F	$LiOH.H_2O$	Acetone	54	89:11

[a] Reaction condition: **1** (0.1 mmol), **2** (0.15 1 mmol), **NHC** (0.01 mmol), Base (0.1 mmol), **DQ** (0.1 mmol) = 3,3',5,5'-tetra-tert-butyldiphenoquinone, solvent (2 mL). DBU = 1,8-Diazabicyclo [5.4.0] undec-7-ene. DIEA = N, N-Diisopropylethylamine. EtOAc = ethyl acetate. DABCO = 1,4-diazabicyclo[2.2.2]octane. Yields were isolated yields after SiO_2 column chromatography. The e.r. was determined via chiral-phase HPLC analysis.

III. Experimental Procedure

1. General procedure for the synthesis of Benzosulfonamides

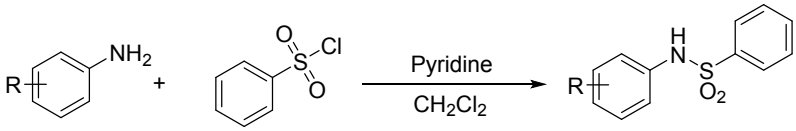

To a mixture of **amine** (1.00 eq) and pyridine (3.00 eq) solvated in CH_2Cl_2 (50 mL), **benzenesulfonyl chloride** (1.10 eq) was added portionwise. The resulting mixture stirred at room temperature, when complete (monitered by TLC), was quenched using 2*N* HCl. Mixture washed with CH_2Cl_2 organic fractions combined, was evaporated in vacuo. Crude product was then isolated by column chromatography. The resulting benzosulfonamide product was collected from fractions, solvent evaporated, and isolated as solid.

2. General procedure for the synthesis of 3-(*N*-substituted) aminophthalides

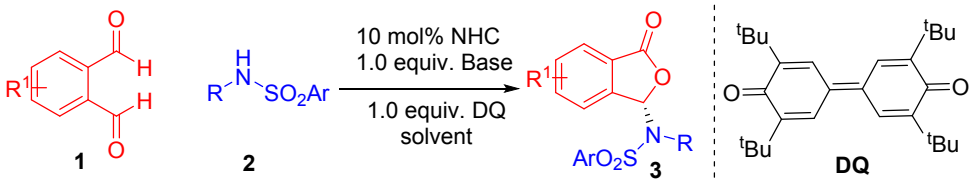

A dry 10 mL Schlenk tube with stir bar was charged with phthalaldehydes (**1**) (0.10 mmol, 1.0 equiv.), NHC **F** (4.8 mg, 10 mol%), benzosulfonamides (**2**) (0.15 mmol, 1.5 equiv.), DQ (40.8 mg, 0.1 mmol, 1equiv.) and $LiOH{\cdot}H_2O$ (4.2 mg, 0.1 mmol, 1.0 equiv.). The tube was evacuated and refilled with nitrogen. Then dry CH_2Cl_2 (2 ml) was added to the reaction mixture. The resulting mixture was stirred at room temperature for 12 h when the substrate was consumed completely (monitored by TLC). The mixture was concentrated under vacuum and purified by column chromatography on silica gel (hexane/ethyl acetate) or CH_2Cl_2/Hexane to afford desired product **3**, which was confirmed by ^{1}H NMR, ^{13}C NMR spectra, and the enantiomeric excess was determined by chiral HPLC.

3. Bioactivity assay for investigation of MIC of 6c, 7, 8

Dissolve the **6c**, **7**, **8** into the DMSO to produce the 20 mg / mL stock solution. Dilute the *E. coli.* (ATCC25922) standard stock solution with LB (Luria-Bertani) liquid nutrient medium (2 x 10^7 CFU/ml).

To each of the 7 sterilized 1.5 mL EP tubes were added 1 mL of sterilized LB (Luria-Bertani) liquid nutrient medium, respectively. 1 ml of **6c** stock solution was added into the first tube and the remaining 6 tubes were prepared with gradient dilution method. The resulted **6c** test solution concentrations were 20 mg / mL, 10 mg / mL, 5 mg / mL, 2.5 mg / mL, 1.2g mg / mL, 0.625 mg / mL, 0.313 mg / mL. The **7** and **8** were subjected to the same dilution procedure. Measure 500 μL of the diluted *E. Coli* solution into each of EP tubes with **6c**, **7** ,**8** of different concentrations, respectively. Shake, mix well and place them into 37 °C incubator for 30 min. After incubation, 20 μL of resulted mixture from these EP tubes was inoculated onto LB culture plate. These plates were allowed to stand for 15 min and kept upside down in the 37 °C incubator for 12 h. each drug was done with 3 plates. Observe the plates and count the number of the CFUs. These procedures were done in three biological replicates.

EP tubes No.	**1**	**2**	**3**	**4**	**5**	**6**	**7**
Dilution factor	1:2	1:4	1:8	1:16	1:32	1:64	1:128
Content (mg / mL)	20	10	5	2.5	1.25	0.625	0.313

Table S1. The gradient dilution of 6c, 7 and 8 and corresponding content

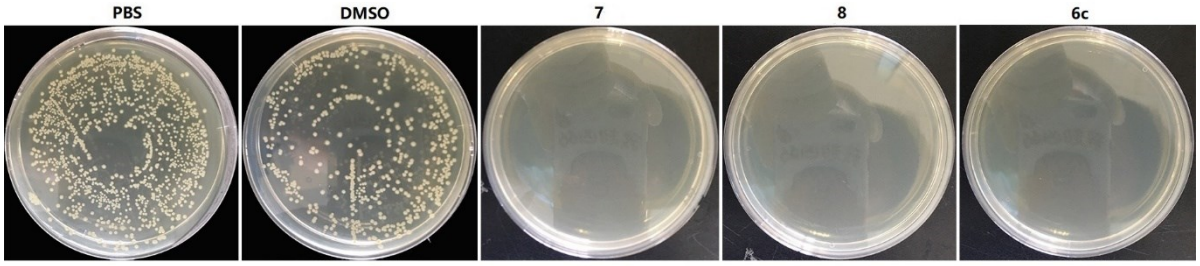

Figure S1. The culture plates at 2.5 mg / mL of 6c, 7, 8 with PBS and DMSO as control experiments

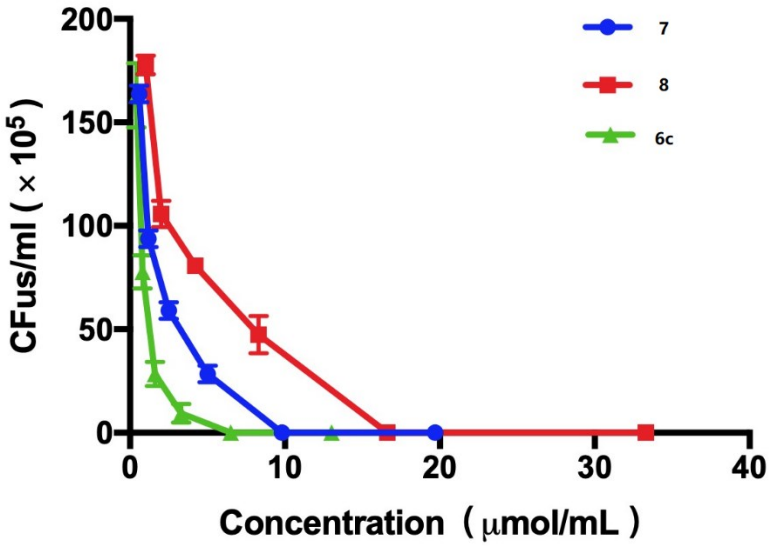

Figure S2. Bioactivity assay for investigation of MIC of 6c, 7, 8. Note: n= 3 biological replicates, Mean ±SD

IV. Crystal structure of 3a

The product **3a** was recrystallize via vaporization of CH_2Cl_2/hexane solvent, colourless crystal was observed, and absolute configuration was determined by X-Ray structure analysis. Supplementary information of the crystal is available under CCDC number 2045331, which could be accessible at free of charge from The Cambridge Crystallographic Data Centre via www.ccdc.cam.ac.uk.

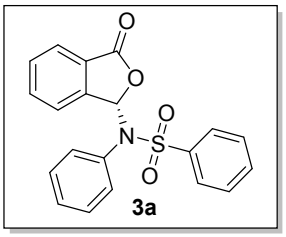
O
O
N
S
O
O
3a

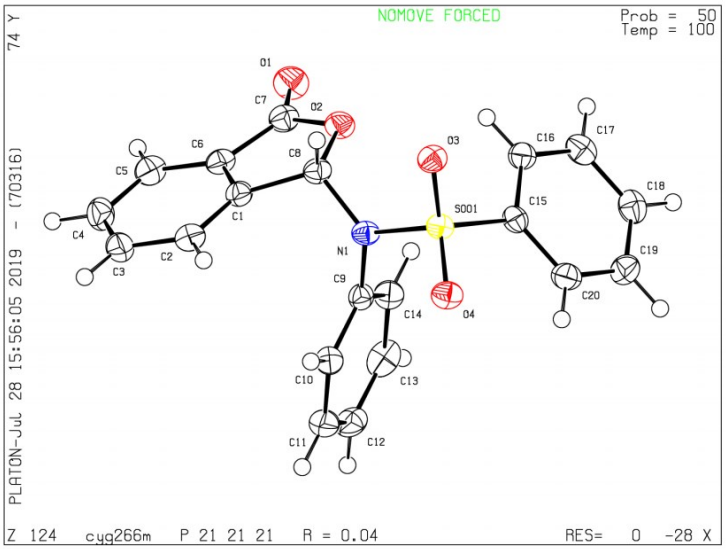
NOMOVE FORCED
Prob = 50
Temp = 100
74 Y
PLATON-Jul 28 15:56:05 2019 - (70316)
O1
C7
O2
C6
C8
O3
C16
C17
C5
C18
C1
S001
C15
C4
N1
C19
C3
C2
C9
C14
O4
C20
C10
C13
C11
C12
Z 124 cyg266m P 21 21 21 R = 0.04
RES= 0 -28 X

V Computational Methods

Geometry optimizations for conformational sampling in the gas phase were carried out using the GFN1-xTB method[1] as implemented in Entos Qcore Version 0.7.[2] The resulting cluster structures were further optimized using global hybrid functional M06-2X[3] with Karlsruhe-family basis set of double-ζ valence def2-SVP[4,5] for all atoms as implemented in *Gaussian 16* rev. B.01.[6] Single point (SP) corrections were performed using M06-2X functional and def2-TZVP[4] basis set for all atoms. The implicit SMD continuum solvation model[7] was used to account for the solvent effect of dichloromethane (CH_2Cl_2) on the conformer free energies. Gibbs energies were evaluated at the room temperature, as was used in the experiments, using a quasi-RRHO treatment of vibrational entropies.[8,9] Vibrational entropies of frequencies below 100 cm^{-1} were obtained according to a free rotor description, using a smooth damping function to interpolate between the two limiting descriptions. The free energies were further corrected using standard concentration of 1 mol/L, which was used in solvation calculations. Conformer Gibbs energies evaluated at SMD(DCM)-M06-2X/def2-TZVP//M06-2X/def2-SVP level of theory are given and quoted in kcal mol^{-1}. (See section on conformational sampling for more details; *vide infra*).

For reaction mechanistic studies, geometries are optimized in implicit SMD(CH_2Cl_2) solvent at M06-2X/def2-SVP level of theory. Minima and transition structures on the potential energy surface (PES) were confirmed as such by harmonic frequency analysis, showing respectively zero and one imaginary frequency, at the same level of theory. The Gibbs energies obtained were further corrected with SMD(CH_2Cl_2)-M06-2X/def2-TZVP single-point energy evaluations. The final SMD(CH_2Cl_2)-M06-2X/def2-TZVP//SMD(CH_2Cl_2)-M06-2X/def2-SVP energies are used for discussion of reaction mechanisms throughout the main text and in this supporting information.

Non-covalent interactions (NCIs) were analyzed using NCIPLOT[10] calculations. The *.wfn* files for NCIPLOT were generated at M06-2X/def2-SVP level of theory. NCI indices calculated with NCIPLOT were visualized at a gradient isosurface value of $s = 0.5$ au. These are colored according to the sign of the second eigenvalue (λ_2) of the Laplacian of the density ($\nabla^2\rho$) over the range of –0.1 (blue = attractive) to +0.1 (red = repulsive). Molecular orbitals are visualized using an isosurface value of 0.05 au throughout. All molecular structures and molecular orbitals were visualized using *PyMOL* software.[11]

1. Conformational considerations

To determine the most stable form of the key acyl azolium intermediate **II** involved in the reaction, we performed a thorough conformational sampling. We generated a set of rotamers by performing 5-fold rotations about four key dihedral angles (in red) as shown in the Chemdraw structure in Figure S3. This

set of total 625 rotamers were then cleaned by removing those species having overlapping atoms within 0.5 Å radius. These were performed using the script in the study of conformational effects on physical-organic descriptors by Brethomé *et al.*[12] A total of 52 resulting rotamers were then subject to geometry optimization using GFN1-xTB in Entos Qcore. The xTB-optimized structures were then clustered using the clustering_traj.py[13] with an RMSD cutoff of 1.0 Å (excluding H atoms) to give 6 distinct conformers, which were reoptimized at DFT M06-2X/def2-SVP level. The Gibbs energies of the resulting structures were corrected using single-point M06-2x/def2-TZVP in SMD(CH_2Cl_2). Their relative solvent-corrected Gibbs energies are given in Figure S3. As would be expected, the most stable conformers (**II-c1** and **II-c2**) benefit from π–π interaction between the phenyl ring on imine substrate (**1a**) and the aryl ring on NHC ligand. Conformer **II-c3** is less stable as it loses the π–π interaction although it gains some CH–π interaction.

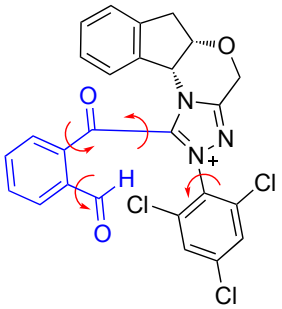

II-c1	**II-c2**	**II-c3**
ΔΔG = 0.0	3.8	4.2
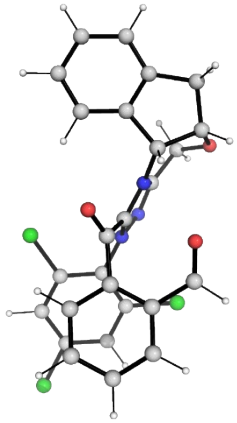	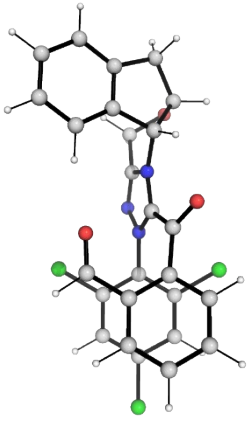	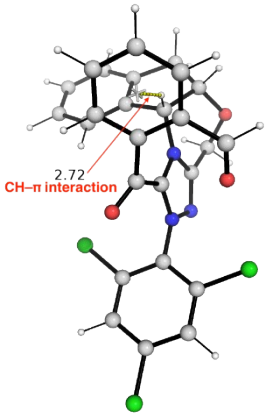
II-c4	**II-c5**	**II-c6**
ΔΔG = 4.8	5.4	6.5

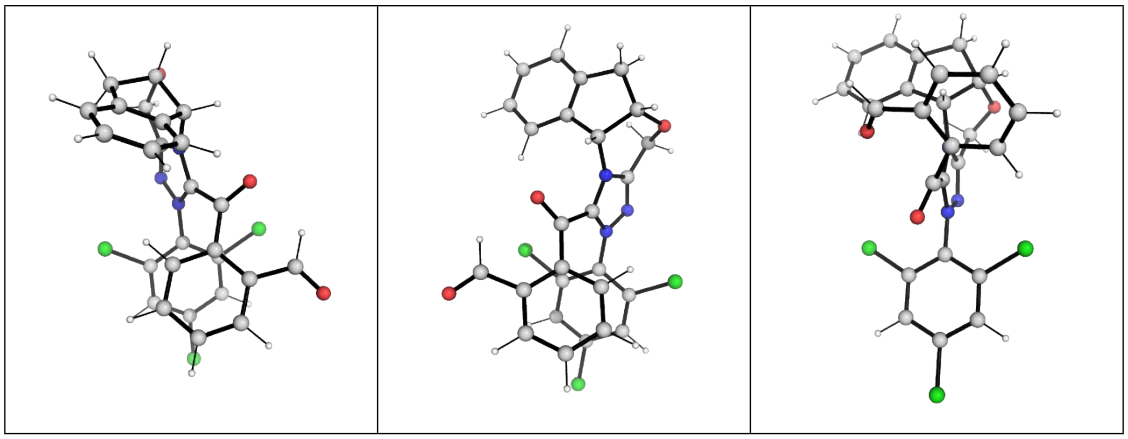

Figure S3. Chemdraw and DFT optimized conformer structures of key acyl azolium intermediate **II**. Relative Gibbs energies are calculated at SMD(CH_2Cl_2)-M06-2X/def2-TZVP//M06-2X/def2-SVP level of theory. Their units are given in kcal mol^{-1}.

For subsequent calculations for mechanistic studies, the most stable conformers **II-c1** and **II-c2** are used for geometry optimization in implicit SMD(CH_2Cl_2) solvent and their Gibbs energies further corrected using single-point M06-2X/def2-TZVP energy in implicit SMD(CH_2Cl_2) solvent. Both of these conformers are involved in the stereoselective C–N bond formation as for each conformer, only one face is available for attack as their other face is shielded from attack by the 2,4,6-trichlorophenyl moiety of NHC. For example, conformer **II-c1** (also named *(Si)*-**II**) can only undergo *Si*-face attack as its *Re*-face is shielded; similarly, conformer **II-c2** (also named *(Re)*-**II**) can only undergo *Re*-face attack.

For N-phenyl benzenesulfonamide substrate, the X-ray crystal structure was taken from The Cambridge Crystallographic Data Centre (CCDC Number: 607421) as the initial structure for DFT geometry optimization.

2. Role of Li^+ ion in the reaction

First, we consider possible reaction pathways in which Li^+ ion does not participate directly, after deprotonation of N-phenyl benzenesulfonamide substrate by LiOH. For the reaction between the deprotonated sulfonamide and acyl azolium intermediate **II**, the reaction complex was first optimized in the solvent phase. Subsequently, a relaxed PES scan along the N-atom of the deprotonated sulfonamide and the carbonyl carbon of the acyl azolium intermediate **II** was performed in implicit CH_2Cl_2 solvent (scanning coordinate shown in Scheme S-1). These scans show that there is only a very small barrier (< 1 kcal mol^{-1}) for the attack of the amide anion to the aldehyde group in the absence of Li^+ ion (for both the *Re*-face attack, Figure S4(i) and the *Si*-face attack, Figure S4(ii)). The scans also show that once the C–N bond is formed, the subsequent oxyanion attacks into the adjacent carbonyl group directly, forming the cyclized product immediately without a barrier (Figure S4).

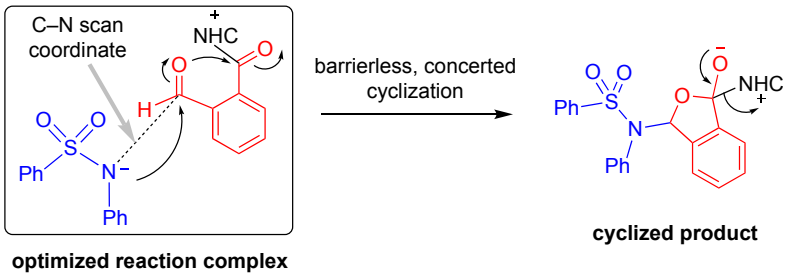

Scheme S-1. Reaction pathway between deprotonated sulfonamide and acyl azolium intermediate **II** in the absence of Li^+ ion (overall neutral reaction). The C–N coordinate for relaxed PES scan is shown.

The lack of a high activation barrier for the reaction between deprotonated sulfonamide anion and the positively charged acyl azolium intermediate is perhaps unsurprising as their reaction is highly favored by electrostatic interactions in dichloromethane solvent (low dielectric constant of 8.93; cf. dielectric constant of water = 80.4). Thus, in the absence of Li^+ ion, the product selectivity will be determined by the conformer distribution of the acyl azolium intermediate **II-c1** and **II-c2**. Since **II-c1** is more thermodynamically stable than **II-c2**, this mechanism (no Li^+ ion involvement) predicts that *Si*-face attack would be favored, which is inconsistent with experimental observation where the *Re*-face attack product is observed. Therefore, a mechanism involving the role of Li^+ ion is important for our consideration.

For completeness, the comparative Gibbs energy profiles for this mechanism without Li^+ ion involvement calculated at SMD(CH_2Cl_2)-M06-2X/def2-TZVP//SMD(CH_2Cl_2) -M06-2X/def2-SVP level of theory is show in Figure S5. From this free Gibbs energy profile, we can see that the addition of deprotonated sulfonamide into the *(Si)*-face has an overall barrier of 3.0 kcal mol^{-1}, arising from the loss of NHC from the cyclized product; the addition to the *(Re)*-face has a barrier of 6.1 kcal mol^{-1}. Thus, without Li^+ ion involvement, the reaction will favor the *(Si)*-face addition by 3.1 kcal mol^{-1}, translating to an enantioselective ratio (e.r.) of 99.5 : 0.5 in favor of *(R)*-phthalidyl sulfonamide product (see reference[14], for example, for computing enantioselectivity from DFT calculations). Therefore, without the participation of Li^+ ion, the opposite enantioselectivity will be observed as the conformer for *(Si)*-face is more thermodynamically stable and its cyclization and NHC regeneration are kinetically faster.

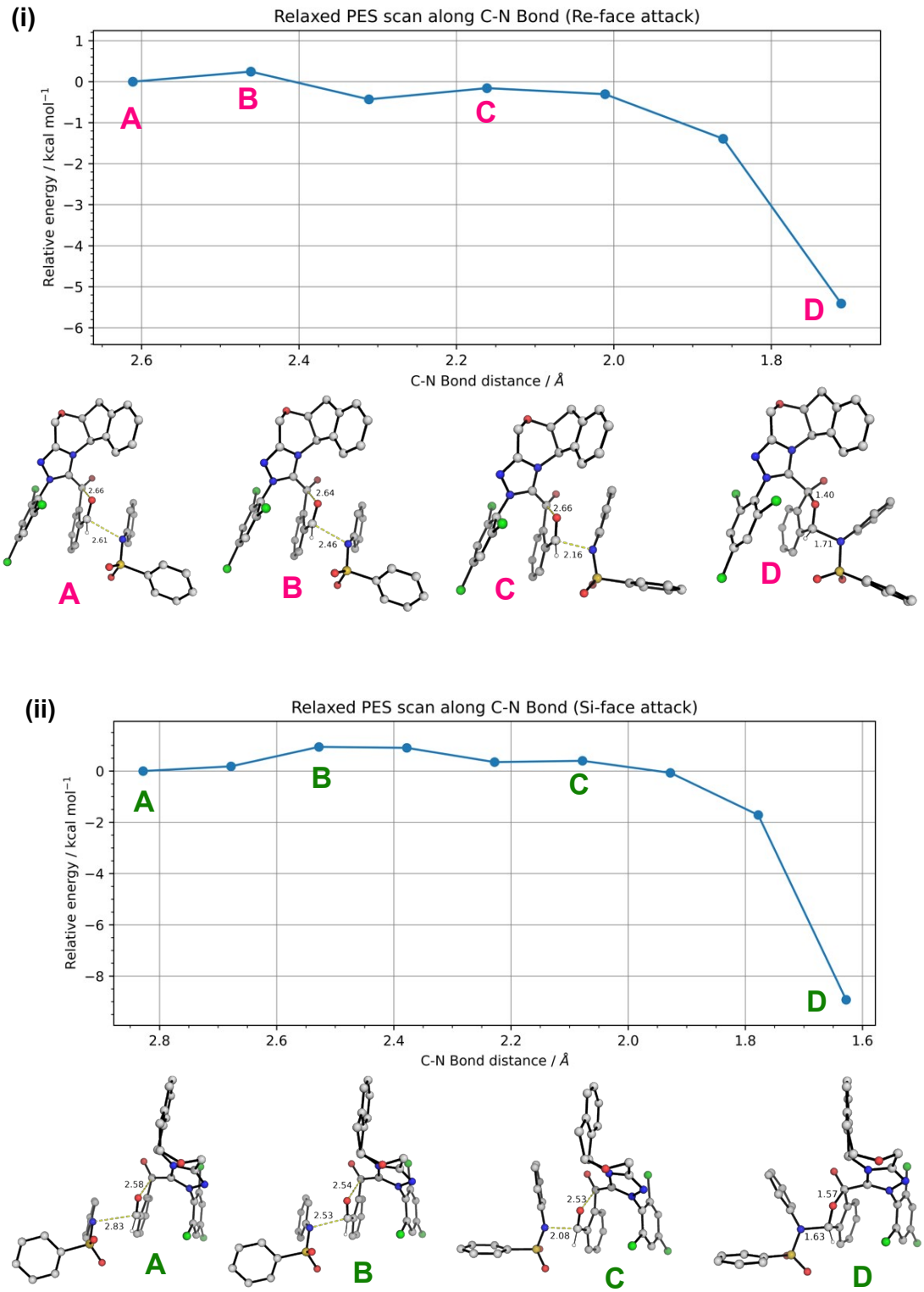

Figure S4. Relaxed potential energy surface (PES) scan for the first C–N bond formation for (i) *Re*-face attack and (ii) *Si*-face attack in the absence of Li^+ ion computed at SMD(CH_2Cl_2)-M06-2X/def2-SVP level of theory. Energies are taken relative to their respective reactant complexes (structures at point A) and their units are given in kcal mol^{-1}. These PES scans give an upper bound of C–N bond formation transition states (TSs) at < 1 kcal mol^{-1}, indicating very flat PES at this region in the absence of Li^+ ion.

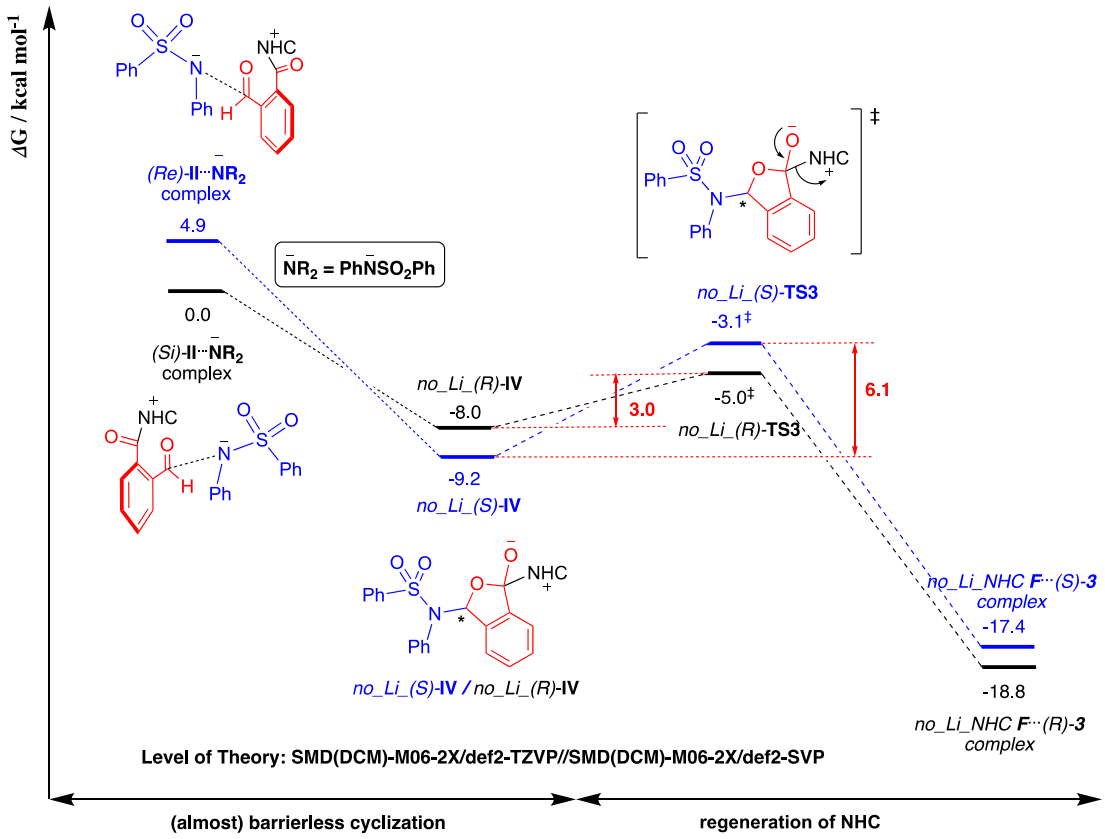

Figure S5. Gibbs energy profile computed at SMD(CH_2Cl_2)-M06-2X/def2-TZVP// SMD(CH_2Cl_2)- M06-2X/def2-SVP level of theory for the reaction between NHC-bound intermediate **II** and deprotonated sulfonamide in the absence of Li^+ ion.

3. Key transition state (TS) structures with Li^+ ion participation

For completeness, we compare the factors influencing the energetic differences between key TSs (*(Re)/(Si)*-**TS1** and *(Re)/(Si)*-**TS3**), although we note that **TS3**s are the turnover-frequency (TOF) determining transition state (TDTS).[15] Figure S6 shows their DFT-optimized structures, highest occupied molecular orbitals (HOMOs) and non-covalent interaction (NCI) plots.

For the formation of C–N bond in the first step (**TS1**), the addition to the *Re*-face is more favorable by 5.3 kcal mol^{-1} due to more NCIs arising from the coordination of Li^+ ion to the aromatic ring (cation-π interaction). The electron distributions in their HOMOs are similar, as the lone pair nitrogen attacks into the π* orbital of the carbonyl group, indicating similar orbital interactions as the C–N bond is formed; the bond forming distances are also similar (1.95Å in *(Re)*-**TS1** and 1.97Å in *(Si)*-**TS1**; within 0.02 Å).

(Re)-**TS1**	*(Si)*-**TS1**
$\Delta G^{\ddagger}$ = 8.0 kcal mol^{-1}	$\Delta G^{\ddagger}$ = 13.3 kcal mol^{-1}

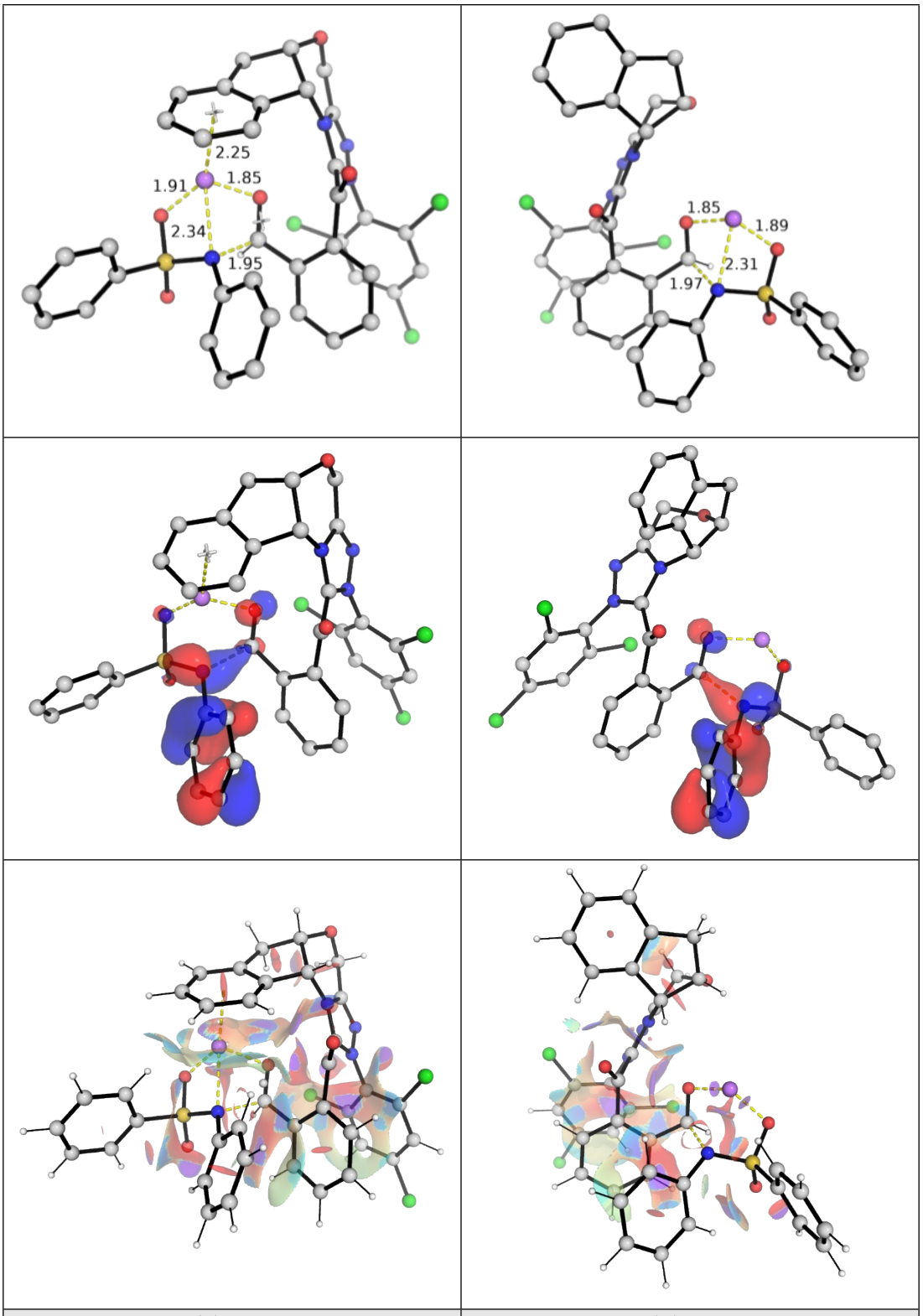

(S)-**TS3**	*(R)*-**TS3**
$\Delta G^{\ddagger}$ = 13.7 kcal mol^{-1}	$\Delta G^{\ddagger}$ = 19.1 kcal mol^{-1}

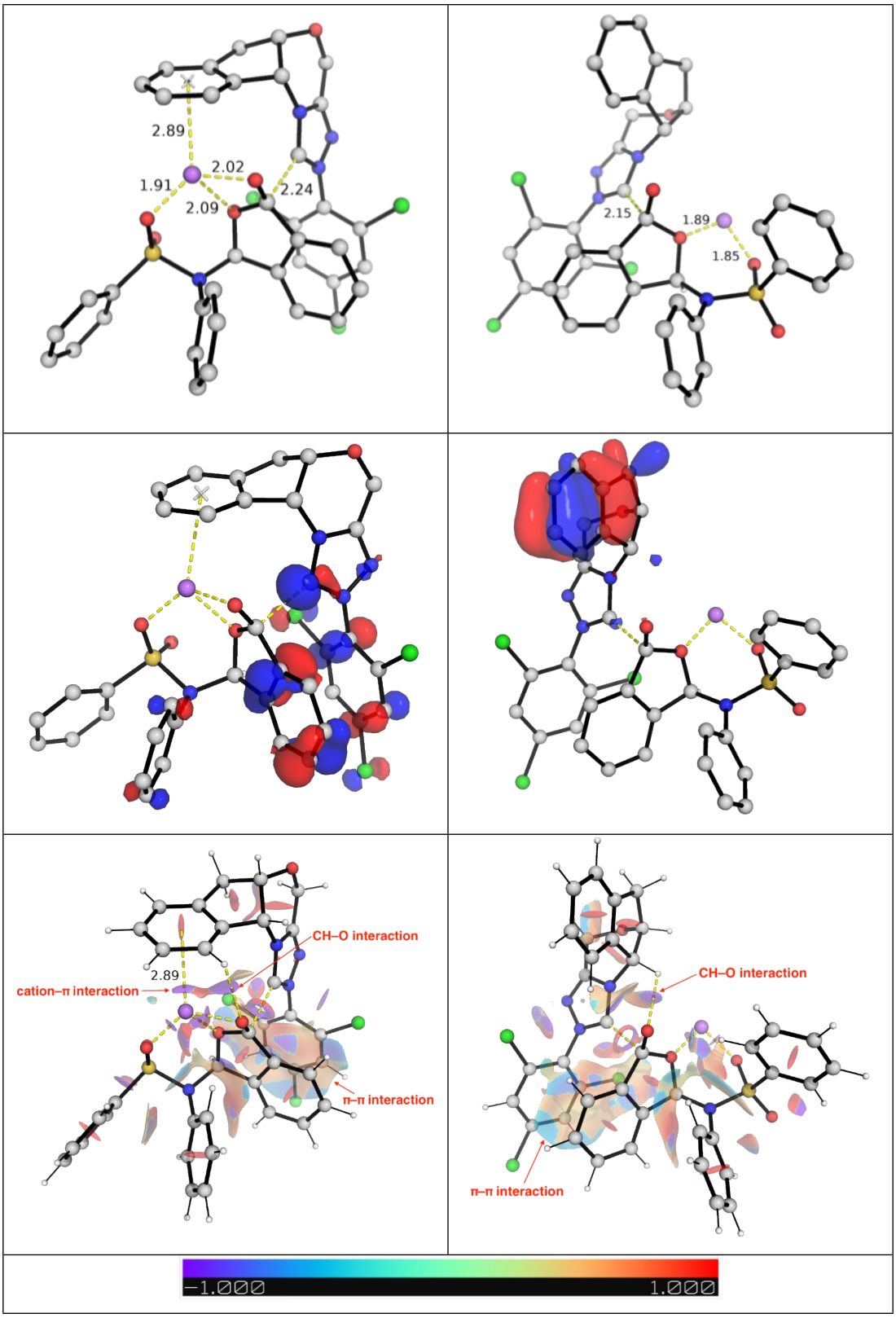

Figure S6. Optimized TS structures, their HOMO (isosurface value = 0.05 au) and NCI plots for the key transition states (TSs) for the reaction between acyl azolium intermediate **II** conformers **II-c1** (prone to *Si*-face attack) and **II-c2** (prone to *Re*-face attack) and lithium sulfonamide. Key bond distances are given in Å. Activation barriers are given in kcal mol^{-1}.

For the TDTSs, orbital interactions are more favorable in *(S)*-**TS3** than in *(R)*-**TS3**, as the σ*(C–C) orbital is directly involved in the HOMO of the former but not the latter. *(S)*-**TS3** is also a later transition state

as the breaking C–C bond distance (2.24Å) is much longer than that in *(R)*-**TS3** (2.15Å). The additional cation-π interaction in *(S)*-**TS3,** which is absent in *(R)*-**TS3**, further contributes to the stability of this TS (albeit diminished due to long Li–π distance of 2.89Å). Taken the orbital and non-covalent interactions together, *(S)*-**TS3** is lower in activation barrier than *(R)*-**TS3** by 5.4 kcal mol^{-1}.

The cation-π interaction in *(S)*-**TS3** is critical as the lack of it in another TS conformer, *(S)*-**TS3-c2** (Figure S7), gives a higher barrier (by 2 kcal mol^{-1}) than *(S)*-**TS3** where the cation-π interaction is present. The presence of cation-π interaction also stabilize the intermediate (**S-IV** vs **S-IV-c2**) and product complexes (**NHC-S-3-complex** vs **NHC-S-3-complex-c2**) by *ca.* 8–14 kcal mol^{-1} (Figure S7).

4. Other optimized structures with Li^+ ion participation

Re-II-Li-amide-complex	**S-III**	**S-TS2**
ΔG = -1.6	1.9	4.9
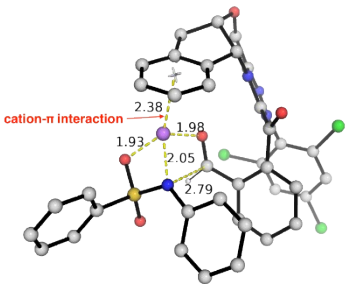	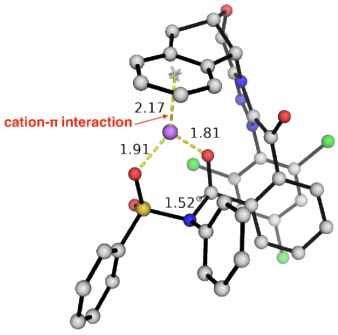	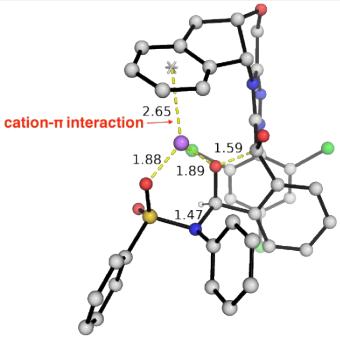
S-IV	**NHC-S-3-complex**	**S-IV-c2**
ΔG = 0.7	-11.4	9.3
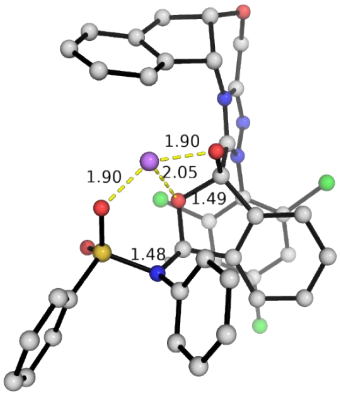	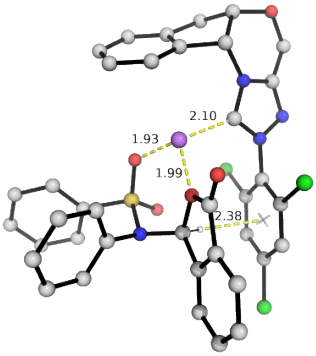	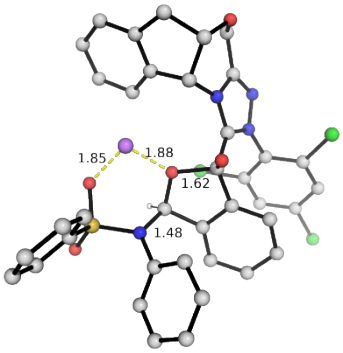
S-TS3-c2	**NHC-S-3-complex-c2**	
ΔG = 15.7	3.4	

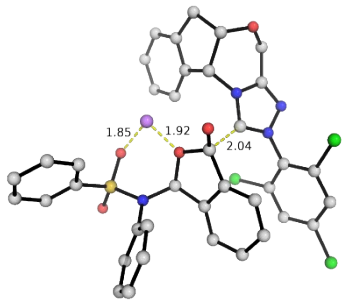	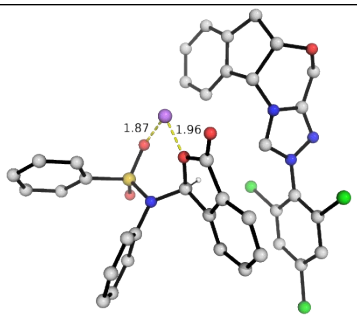	
Si-II-Li-amide-complex	**R-III**	**R-TS2**
ΔG = 3.8	5.8	9.0
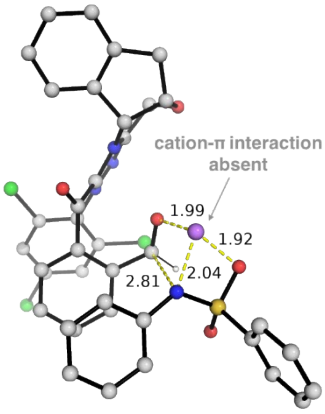	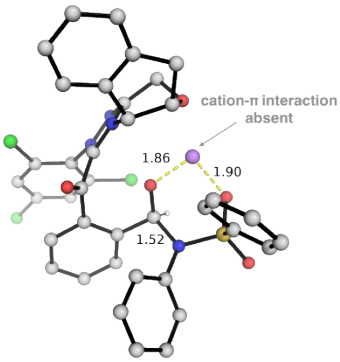	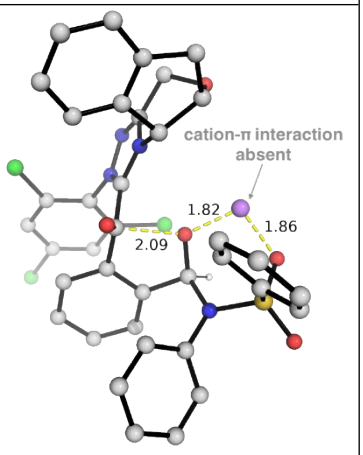
R-IV	**NHC-R-3-complex**	
ΔG = 8.7	-10.3	
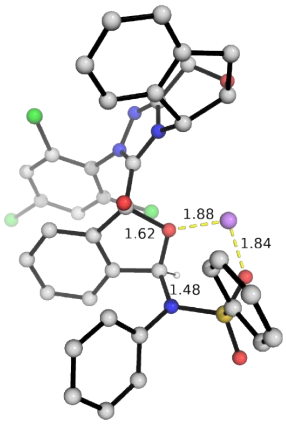	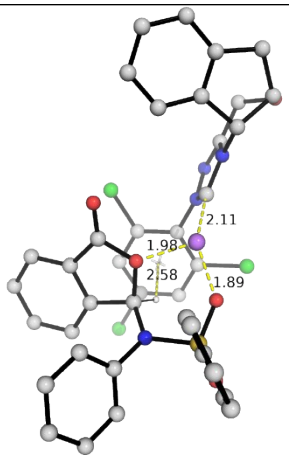	

Figure S7. Other DFT-optimized structures for the reaction between acyl azolium intermediate and lithium sulfonamide. Key bond distances are given in Å. Gibbs energies are given in kcal mol^{-1}.

5. Use of DBU in place of Li^+ ion participation

When protonated DBU, **DBUH**$^+$, is used in place of Li^+ ion, it was found that the *(S)*-**TS3-DBU** is favored over *(R)*-**TS3-DBU** by 0.5 kcal mol^{-1} (Figure S8). This calculated barrier difference in the TDTSs translates to an enantiomeric ratio (e.r.) of 70:30 for *S:R* enantiomeric products. We note that the experimentally observed e.r. of 86:14 corresponds to a barrier difference of 1.0 kcal mol^{-1}, which already falls into the heaven of chemical accuracy, making its exact agreement with computation difficult.

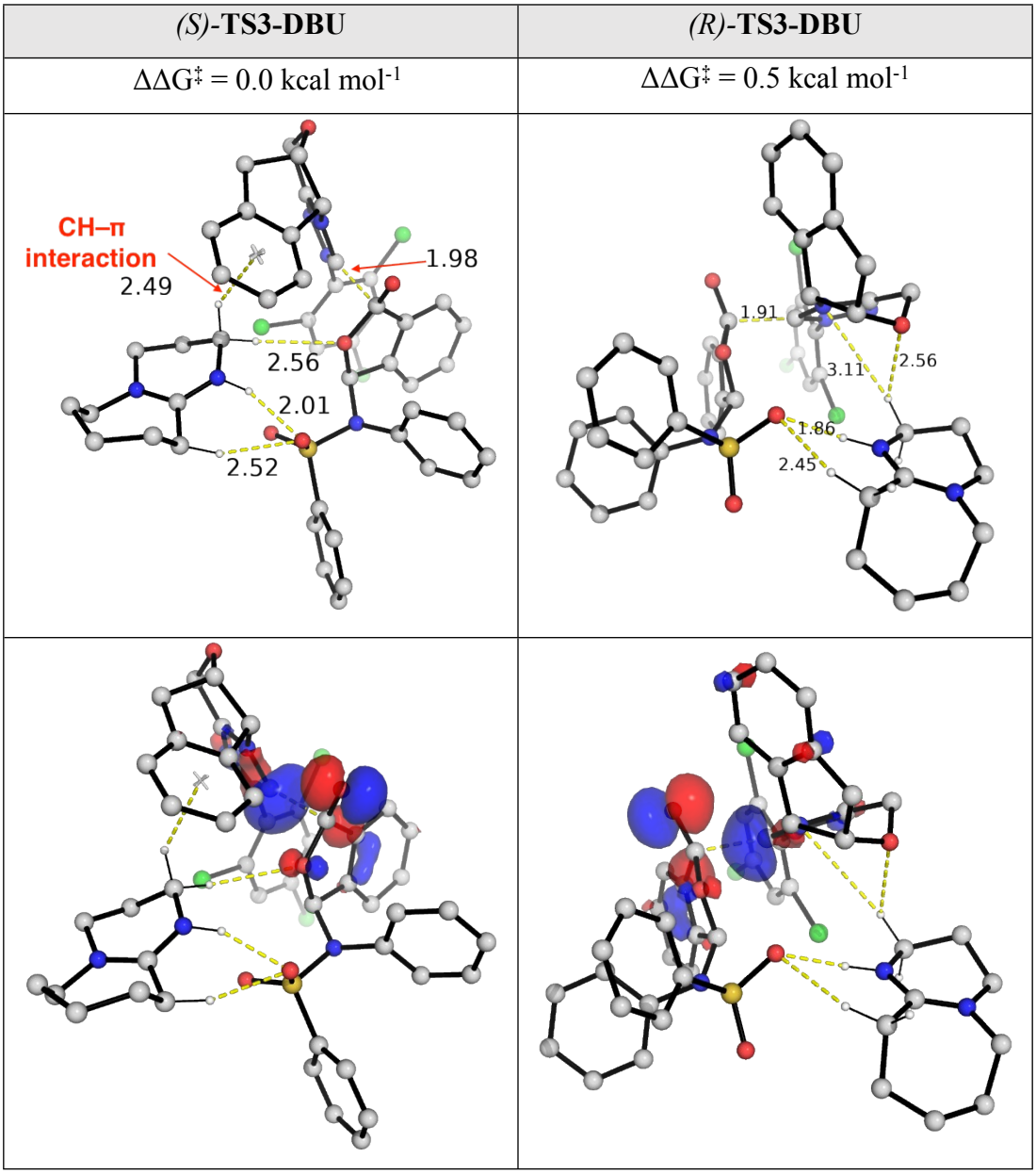

Figure S8. Optimized TS structures and their HOMO (isosurface value = 0.05 au) for the TDTSs with **DBUH**$^+$ in place of Li^+ ion. Relative activation barriers are given in kcal mol^{-1}.

Our calculated value of 0.5 kcal mol^{-1}, although benefits from cancellation of errors, could still fall within the accuracy of the method. Thus, we can only conclude qualitatively that **DBUH**$^+$ can stabilize *(S)*-**TS3-**

DBU better than *(R)*-**TS3-DBU** (the TDTSs) in a way similar to, but less efficient than Li^+ ion (both TSs have similar HOMO structures).

6. Optimized structures and absolute energies, zero-point energies

Geometries of all optimized structures (in .xyz format with their associated energy in Hartrees) are included in a separate folder named *final_xyz_structures* with an associated readme.txt file. All these data have been deposited with this Supporting Information and uploaded to zenodo.org (DOI: 10.5281/zenodo.4409538).

Absolute values (in Hartrees) for SCF energy, zero-point vibrational energy (ZPE), enthalpy and quasi-harmonic Gibbs free energy (at 298.15K) for M06-2X/def2-SVP optimized conformers (intermediate **II-c1** to **II-c8**) and SMD(CH_2Cl_2)-M06-2X/ def2-SVP optimized structures (mechanistic study with and without Li^+ ion) are given below. Single point corrections in SMD(CH_2Cl_2) using M06-2X/def2-TZVP functional are also included.

Structure	E/au	ZPE/au	H/au	T.S/au	qh-G/au	SP M06-2X/def2TZVP
II-c1	-2769.256458	0.385637	-2768.8417	0.08733	-2768.92275	-2771.340557
II-c2	-2769.253414	0.386164	-2768.8385	0.085218	-2768.918501	-2771.335742
II-c3	-2769.243215	0.385649	-2768.8285	0.087561	-2768.909579	-2771.333778
II-c4	-2769.242577	0.385917	-2768.8276	0.0876	-2768.908751	-2771.33293
II-c5	-2769.240971	0.385567	-2768.8264	0.087169	-2768.907342	-2771.331798
II-c6	-2769.240687	0.385521	-2768.826	0.088955	-2768.907782	-2771.329355
Li_amide	-1073.329428	0.200344	-1073.114	0.054545	-1073.166191	-1074.272205
Si-II	-2769.342222	0.385354	-2768.9279	0.085587	-2769.008202	-2771.341036
Re-II	-2769.339156	0.385754	-2768.9247	0.084696	-2769.004424	-2771.336673
Re-II-Li-amide-complex	-3842.708353	0.587944	-3842.0761	0.122213	-3842.186661	-3845.640211
Re-TS1	-3842.699114	0.588772	-3842.0673	0.116579	-3842.174502	-3845.627887

S-III	-3842.714195	0.590206	-3842.0818	0.114271	-3842.187237	-3845.639988
S-TS2	-3842.711847	0.590289	-3842.0797	0.113548	-3842.184274	-3845.63581
S-IV	-3842.719735	0.591285	-3842.0861	0.114823	-3842.191653	-3845.642986
S-TS3	-3842.694656	0.588947	-3842.0631	0.116576	-3842.169613	-3845.619147
NHC-S-3-complex	-3842.733711	0.590231	-3842.1	0.119146	-3842.208212	-3845.659601
S-IV-c2	-3842.701179	0.590074	-3842.0682	0.117425	-3842.17549	-3845.626864
S-TS3-c2	-3842.689598	0.589207	-3842.0578	0.117145	-3842.164591	-3845.616018
NHC-S-3-complex-c2	-3842.7047	0.589239	-3842.0715	0.121507	-3842.181247	-3845.634063
Si-II-Li-amide-complex	-3842.697002	0.587348	-3842.065	0.123577	-3842.1765	-3845.630373
Si-TS1	-3842.687274	0.58813	-3842.0558	0.118778	-3842.164171	-3845.617886
R-III	-3842.709308	0.59123	-3842.0751	0.117333	-3842.182542	-3845.63353
R-TS2	-3842.703021	0.590378	-3842.0705	0.11336	-3842.175517	-3845.629172
R-IV	-3842.703356	0.590713	-3842.0701	0.115463	-3842.176214	-3845.629255
R-TS3	-3842.684893	0.589347	-3842.0529	0.117596	-3842.160044	-3845.610463
NHC-R-3-complex	-3842.729178	0.590089	-3842.0954	0.120768	-3842.204594	-3845.656959
no_Li_Si-II-amide-complex	-3835.212724	0.584256	-3834.5848	0.122247	-3834.70705	-3834.694902
no_Li_R-IV	-3835.24097	0.587907	-3834.6115	0.113657	-3834.72518	-3834.715945
no_Li_R-TS3	-3835.232057	0.585722	-3834.6044	0.118847	-3834.72326	-3834.711082
no_Li_NHC-R-3-complex	-3835.252354	0.5867	-3834.6227	0.121032	-3834.74377	-3834.731136
no_Li_Re-II-amide-complex	-3835.209936	0.584528	-3834.582	0.120578	-3834.70261	-3834.691098

no_Li_S-IV	-3835.244744	0.587847	-3834.6152	0.114793	-3834.73003	-3834.72
no_Li_S-TS3	-3835.232123	0.586677	-3834.6039	0.115598	-3834.71945	-3834.708846
no_Li_NHC-S-3-complex	-3835.246852	0.586745	-3834.6171	0.123437	-3834.74052	-3834.726711
S-TS3-DBU	-4297.283862	0.849318	-4296.3815	0.141084	-4296.508312	-4300.716229
R-TS3-DBU	-4297.283392	0.849507	-4296.3807	0.14172	-4296.507872	-4300.71544

VI. References

Full reference for Gaussian software:

Gaussian 16, Revision B.01, Frisch, M. J.; Trucks, G. W.; Schlegel, H. B.; Scuseria, G. E.; Robb, M. A.; Cheeseman, J. R.; Scalmani, G.; Barone, V.; Mennucci, B.; Petersson, G. A.; Nakatsuji, H.; Caricato, M.; Li, X.; Hratchian, H. P.; Izmaylov, A. F.; Bloino, J.; Zheng, G.; Sonnenberg, J. L.; Hada, M.; Ehara, M.; Toyota, K.; Fukuda, R.; Hasegawa, J.; Ishida, M.; Nakajima, T.; Honda, Y.; Kitao, O.; Nakai, H.; Vreven, T.; Montgomery Jr., J. A.; Peralta, J. E.; Ogliaro, F.; Bearpark, M.; Heyd, J. J.; Brothers, E.; Kudin, K. N.; Staroverov, V. N.; Kobayashi, R.; Normand, J.; Raghavachari, K.; Rendell, A.; Burant, J. C.; Iyengar, S. S.; Tomasi, J.; Cossi, M.; Rega, N.; Millam, J. M.; Klene, M.; Knox, J. E.; Cross, J. B.; Bakken, V.; Adamo, C.; Jaramillo, J.; Gomperts, R.; Stratmann, R. E.; Yazyev, O.; Austin, A. J.; Cammi, R.; Pomelli, C.; Ochterski, J. W.; Martin, R. L.; Morokuma, K.; Zakrzewski, V. G.; Voth, G. A.; Salvador, P.; Dannenberg, J. J.; Dapprich, S.; Daniels, A. D.; Farkas, Ö.; Foresman, J. B.; Ortiz, J. V; Cioslowski, J.; Fox, D. J. Gaussian, Inc., Wallingford CT, 2016.

(1) Grimme, S.; Bannwarth, C.; Shushkov, P. A Robust and Accurate Tight-Binding Quantum Chemical Method for Structures, Vibrational Frequencies, and Noncovalent Interactions of Large Molecular Systems Parametrized for All Spd-Block Elements (Z = 1-86). *J. Chem. Theory Comput.* **2017**, *13* (5), 1989–2009.

(2) Manby, F. R.; Miller, T. F.; Bygrave, P. J.; Ding, F.; Dresselhaus, T.; Buccheri, A.; Bungey, C.; Lee, S. J. R.; Meli, R.; Steinmann, C.; et al. Entos : A Quantum Molecular Simulation Package. *ChemRxiv.* **2019**.

(3) Zhao, Y.; Truhlar, D. G. The M06 Suite of Density Functionals for Main Group Thermochemistry, Thermochemical Kinetics, Noncovalent Interactions, Excited States, and Transition Elements: Two New Functionals and Systematic Testing of Four M06-Class Functionals and 12 Other Function. *Theor. Chem. Acc.* **2008**, *120* (1), 215–241.

(4) Weigend, F.; Ahlrichs, R. Balanced Basis Sets of Split Valence, Triple Zeta Valence and

Quadruple Zeta Valence Quality for H to Rn: Design and Assessment of Accuracy. *Phys. Chem. Chem. Phys.* **2005**, *7* (18), 3297–3305.

(5) Weigend, F. Accurate Coulomb-Fitting Basis Sets for H to Rn. *Phys. Chem. Chem. Phys.* **2006**, *8* (9), 1057–1065.

(6) Frisch, M. J. .; Trucks, G. W. .; Schlegel, H. B. .; Scuseria, G. E. .; Robb, M. A. .; Cheeseman, J. R. .; Scalmani, G. .; Barone, V. .; Petersson, G. A. .; Nakatsuji, H. .; et al. Gaussian 16, Revision B.01. 2016.

(7) Marenich, A. V.; Cramer, C. J.; Truhlar, D. G. Universal Solvation Model Based on Solute Electron Density and on a Continuum Model of the Solvent Defined by the Bulk Dielectric Constant and Atomic Surface Tensions. *J. Phys. Chem. B* **2009**, *113* (18), 6378–6396.

(8) Grimme, S. Supramolecular Binding Thermodynamics by Dispersion-Corrected Density Functional Theory. *Chem.: Eur. J.* **2012**, *18* (32), 9955–9964.

(9) Funes-Ardoiz, I.; Paton, R. S. GoodVibes v1.0.1 http://doi.org/10.5281/zenodo.56091.

(10) Contreras-García, J.; Johnson, E. R.; Keinan, S.; Chaudret, R.; Piquemal, J. P.; Beratan, D. N.; Yang, W. NCIPLOT: A Program for Plotting Noncovalent Interaction Regions. *J. Chem. Theory Comput.* **2011**, *7* (3), 625–632.

(11) Schrödinger, L. *The PyMOL Molecular Graphics Development Component, Version 1.8*; 2015.

(12) Brethomé, A. V.; Fletcher, S. P.; Paton, R. S. Conformational Effects on Physical-Organic Descriptors: The Case of Sterimol Steric Parameters. *ACS Catal.* **2019**, *9* (3), 2313–2323.

(13) Cezar, H. M. Clustering Traj https://github.com/hmcezar/clustering-traj.

(14) Peng, Q.; Duarte, F.; Paton, R. S. Computing Organic Stereoselectivity - from Concepts to Quantitative Calculations and Predictions. *Chem. Soc. Rev.* **2016**, *45* (22), 6093–6107.

(15) Kozuch, S.; Shaik, S. How to Conceptualize Catalytic Cycles? The Energetic Span Model. *Acc. Chem. Res.* **2011**, *44* (2), 101–110.

VII. Characterization of products

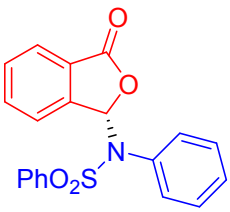

3a

(S)-N-(3-oxo-1,3-dihydroisobenzofuran-1-yl)-N-phenylbenzenesulfonamide (3a): White solid, 33.6 mg, 92% yield.

^{1}H NMR (400 MHz, CDCl3) δ 7.79 (d, J = 7.4 Hz, 2H), 7.67 – 7.60 (m, 5H), 7.52 (t, J = 7.8 Hz, 2H), 7.41 (dt, J = 8.0, 4.1 Hz, 1H), 7.13 (t, J = 7.4 Hz, 1H), 7.05 (t, J = 7.6 Hz, 2H), 6.88 (d, J = 7.6 Hz, 2H).

^{13}C NMR (101 MHz, CDCl3) δ 168.3, 143.7, 139.0, 138.0, 136.4, 134.4, 133.5, 133.3, 133.0, 131.1, 130.5, 129.3, 129.0, 128.9, 128.4, 127.2, 125.4, 125.3, 123.8, 121.7, 87.9 ppm.

HRMS (ESI, m/z): calcd. for $C_{20}H_{16}NO_4S^+$ $[M+H]^+$: 366.0795, found 366.0794.

$[\alpha]^{21}_{D}$ = -255.2 (c = 0.60 in $CHCl_3$)

HPLC analysis: 99:1 e.r. (Chiralcel IA, 10:90 iPrOH/Hexane, 0.6 mL/min), Rt (major) = 24.8 min, Rt (minor) = 20.1 min.

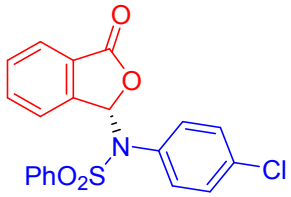

3b

(S)-N-(4-chlorophenyl)-N-(3-oxo-1,3-dihydroisobenzofuran-1-yl)benzenesulfonamide (3b): White solid, 36.8 mg, 92% yield.

^{1}H NMR (400 MHz, CDCl3) δ 7.79 (dd, J = 8.4, 1.1 Hz, 2H), 7.70 – 7.59 (m, 5H), 7.53 (t, J = 7.8 Hz, 2H), 7.45 (t, J = 7.4 Hz, 1H), 7.03 (d, J = 8.8 Hz, 2H), 6.82 (d, J = 8.7 Hz, 2H).

^{13}C NMR (101 MHz, CDCl3) δ 167.9, 143.5, 137.7, 135.5, 134.5, 133.7, 132.3, 131.9, 130.73, 129.2, 129.1, 128.4, 127.1, 125.5, 123.6, 87.7 ppm.

HRMS (ESI, m/z): calcd. for $C_{20}H_{15}ClNO_4S^+$ $[M+H]^+$: 400.0405, found 400.0408.

$[\alpha]^{21}$ D = -304.0 (c = 0.45 in $CHCl_3$)

HPLC analysis: 97:3 e.r. (Chiralcel IA, 10:90 iPrOH/Hexane, 0.6 mL/min), Rt (major) = 16.6 min, Rt (minor) = 28.4 min.

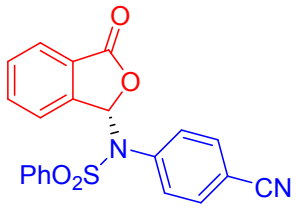

3c

(S)-N-(4-cyanophenyl)-N-(3-oxo-1,3-dihydroisobenzofuran-1-yl)benzenesulfonamide (3c): Yellow solid, 31.6 mg, 81% yield.

^{1}H NMR (400 MHz, CDCl3) δ 7.77 (d, J = 8.1 Hz, 2H), 7.72 – 7.58 (m, 5H), 7.55 (q, J = 7.8, 6.4 Hz, 2H), 7.46 (t, J = 7.4 Hz, 1H), 7.37 (d, J = 7.4 Hz, 2H), 7.03 (d, J = 7.4 Hz, 2H).

^{13}C NMR (101 MHz, CDCl3) δ 167.7, 143.1, 138.0, 137.4, 134.8, 134.0, 132.8, 131.8, 130.9, 129.3, 128.3, 127.0, 125.7, 123.5, 117.4, 113.4, 87.5 ppm.

HRMS (ESI, m/z): calcd. for $C_{21}H_{15}N_2O_4S^+$ $[M+H]^+$: 391.0747, found 391.0747.

$[\alpha]^{21}_D$ = 91.4 (c = 1.00 in $CHCl_3$)

HPLC analysis: 96:4 e.r. (Chiralcel IA, 20:80 iPrOH/Hexane, 0.6 mL/min), Rt (major) = 48.5 min, Rt (minor) = 23.9 min.

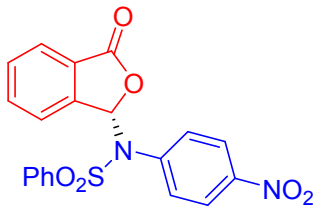

3d

(S)-N-(4-nitrophenyl)-N-(3-oxo-1,3-dihydroisobenzofuran-1-yl)benzenesulfonamide (3d): Yellow solid, 40.6 mg, 99% yield.

^{1}H NMR (400 MHz, $CDCl_3$) δ 7.93 (d, J = 9.0 Hz, 2H), 7.81 – 7.77 (m, 2H), 7.72 – 7.60 (m, 5H), 7.56 (t, J = 7.8 Hz, 2H), 7.46 (t, J = 7.3 Hz, 1H), 7.11 (d, J = 8.9 Hz, 2H).

^{13}C NMR (101 MHz, $CDCl_3$) δ 167.6, 147.8, 143.0, 139.6, 137.4, 134.8, 134.1, 132.0, 131.0, 129.3, 128.3, 127.0, 125.7, 124.1, 123.5, 87.5 ppm.

HRMS (ESI, m/z): calcd. for $C_{20}H_{15}N_2O_4S^+$ $[M+H]^+$: 411.0645, found 411.0648.

$[\alpha]^{21}_D$ = -225.9(c = 1.23 in $CHCl_3$)

HPLC analysis: 97:3 e.r. (Chiralcel IA, 10:90 iPrOH/Hexane, 0.6 mL/min), Rt (major) = 26.4 min, Rt (minor) = 51.5 min.

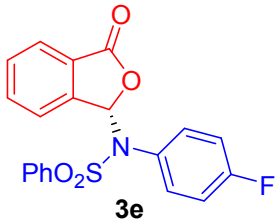

3e

(S)-N-(4-fluorophenyl)-N-(3-oxo-1,3-dihydroisobenzofuran-1-yl)benzenesulfonamide (7): White solid, 27.9 mg, 73% yield.

^{1}H NMR (400 MHz, $CDCl_3$) δ 7.80 (d, J = 7.5 Hz, 2H), 7.69 – 7.60 (m, 5H), 7.53 (t, J = 7.8 Hz, 2H), 7.44 (t, J = 7.2 Hz, 1H), 6.86 (dd, J = 8.5, 5.0 Hz, 2H), 6.74 (t, J = 8.6 Hz, 2H).

^{13}C NMR (101 MHz, $CDCl_3$) δ 167.9, 163.9, 161.4, 143.6, 137.8, 134.4, 133.6, 133.0, 132.9, 130.6, 129.2, 129.0, 128.4, 127.2, 125.5, 123.6, 116.1, 115.8, 87.7 ppm.

HRMS (ESI, m/z): calcd. for $C_{20}H_{15}ClN_2O_4S^+$ $[M+H]^+$: 384.0700, found 384.0702.

$[\alpha]^{21}_D$ = -251.4 (c = 1.50 in $CHCl_3$)

HPLC analysis: 98:2 e.r. (Chiralcel IA, 10:90 iPrOH/Hexane, 0.6 mL/min), Rt (major) = 16.7 min, Rt (minor) = 25.4 min.

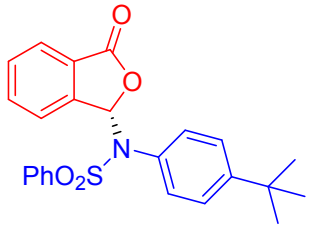

3f

(S)-N-(4-(tert-butyl)phenyl)-N-(3-oxo-1,3-dihydroisobenzofuran-1-yl)benzenesulfonamide (3f): Yellow solid, 29.9 mg, 71% yield.

^{1}H NMR (400 MHz, $CDCl_3$) δ 7.82 – 7.78 (m, 2H), 7.64 (dd, J = 9.1, 5.8 Hz, 5H), 7.52 (t, J = 7.8 Hz, 2H), 7.41 (dt, J = 7.9, 4.1 Hz, 1H), 7.04 (d, J = 8.7 Hz, 2H), 6.78 (d, J = 8.6 Hz, 2H), 1.13 (s, 9H).

^{13}C NMR (101 MHz, $CDCl_3$) δ 168.3, 152.3, 143.9, 138.3, 134.3, 133.4, 130.5, 130.4, 130.3, 128.9, 128.4, 127.2, 125.8, 125.3, 123.7, 88.0, 34.5, 31.0 ppm.

HRMS (ESI, m/z): calcd. for $C_{24}H_{24}NO_4S^+$ $[M+H]^+$: 422.1421, found 422.1421.

$[\alpha]^{21}_D$ = -234.4(c = 0.72 in $CHCl_3$)

HPLC analysis: 98:2 e.r. (Chiralcel IA, 10:90 iPrOH/Hexane, 0.6 mL/min), Rt (major) = 13.3 min, Rt (minor) = 18.6 min.

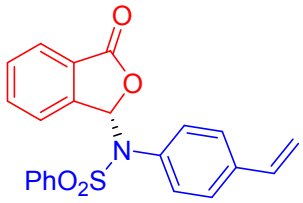

3g

(S)-N-(3-oxo-1,3-dihydroisobenzofuran-1-yl)-N-(4-vinylphenyl)benzenesulfonamide (3g): Yellow solid, 31.7 mg, 81% yield.

^{1}H NMR (400 MHz, $CDCl_3$) δ 7.82 – 7.78 (m, 2H), 7.68 – 7.60 (m, 5H), 7.52 (t, J = 7.8 Hz, 2H), 7.45 – 7.39 (m, 1H), 7.08 (d, J = 8.5 Hz, 2H), 6.83 (d, J = 8.4 Hz, 2H), 6.50 (dd, J = 17.6, 10.9 Hz, 1H), 5.61 (d, J = 17.6 Hz, 1H), 5.21 (d, J = 11.0 Hz, 1H).

^{13}C NMR (101 MHz, $CDCl_3$) δ 168.1, 143.8, 138.4, 138.1, 135.5, 134.4, 133.5, 132.7, 131.2, 130.5, 129.0, 128.4, 127.3, 126.6, 125.4, 123.7, 115.6, 87.9 ppm.

HRMS (ESI, m/z): calcd. for $C_{22}H_{18}NO_4S^+$ $[M+H]^+$: 392.0951, found 392.0951.

$[\alpha]^{21}_D$ = -260.2 (c = 0.82 in $CHCl_3$)

HPLC analysis: 98:2 e.r. (Chiralcel IA, 10:90 iPrOH/Hexane, 0.6 mL/min), Rt (major) = 18.5 min, Rt (minor) = 30.8 min.

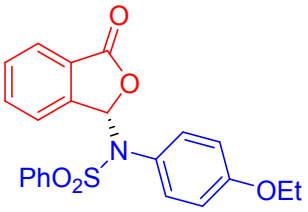

3h

(S)-N-(4-ethoxyphenyl)-N-(3-oxo-1,3-dihydroisobenzofuran-1-yl)benzenesulfonamide (3h): off white solid, 32.3 mg, 79% yield.

^{1}H NMR (400 MHz, $CDCl_3$) δ 7.82 – 7.77 (m, 2H), 7.64 (dd, J = 14.6, 7.0 Hz, 5H), 7.51 (t, J = 7.8 Hz, 2H), 7.44 – 7.39 (m, 1H), 6.75 (d, J = 8.5 Hz, 2H), 6.52 (d, J = 9.1 Hz, 2H), 3.83 (q, J = 7.0 Hz, 2H), 1.30 (t, J = 7.0 Hz, 3H).

^{13}C NMR (101 MHz, $CDCl_3$) δ 168.3, 159.2, 143.9, 138.1, 134.3, 133.4, 132.3, 130.4, 128.9, 128.4, 127.2, 125.3, 125.3, 123.7, 114.4, 88.0, 63.4, 14.6 ppm.

HRMS (ESI, m/z): calcd. for $C_{22}H_{20}NO_5S^+$ $[M+H]^+$: 410.1057, found 410.1058.

$[\alpha]^{21}_D$ = -204.7 (c = 0.62 in $CHCl_3$)

HPLC analysis: 97:3 e.r. (Chiralcel IA, 10:90 iPrOH/Hexane, 0.6 mL/min), Rt (major) = 19.1 min, Rt (minor) = 33.9 min

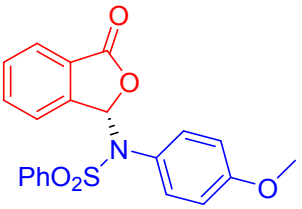

3i

(S)-N-(4-methoxyphenyl)-N-(3-oxo-1,3-dihydroisobenzofuran-1-yl)benzenesulfonamide (3i): White Solid, 36.8 mg, 93% yield.

^{1}H NMR (400 MHz, $CDCl_3$) δ 7.82 – 7.76 (m, 2H), 7.68 – 7.59 (m, 5H), 7.51 (t, J = 7.4 Hz, 2H), 7.43 – 7.39 (m, 1H), 6.76 (d, J = 7.8 Hz, 2H), 6.52 (d, J = 8.2 Hz, 2H), 3.63 (s, 3H).

^{13}C NMR (101 MHz, $CDCl_3$) δ 168.3, 159.8, 143.9, 138.1, 134.3, 133.4, 132.3, 130.4, 128.9, 128.4, 127.2, 125.5, 125.3, 123.7, 114.0, 88.0, 55.2 ppm.

HRMS (ESI, m/z): calcd. for $C_{21}H_{18}NO_5S^+$ $[M+H]^+$: 396.0900, found 396.0902.

$[\alpha]^{21}_D$ = -115.6 (c = 0.39 in $CHCl_3$)

HPLC analysis: 97:3 e.r. (Chiralcel IA, 10:90 iPrOH/Hexane, 0.6 mL/min), Rt (major) = 26.7 min, Rt (minor) = 44.5 min.

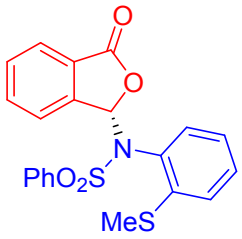

3j

(S)-N-(2-(methylthio)phenyl)-N-(3-oxo-1,3-dihydroisobenzofuran-1-yl)benzenesulfonamide (3j): Yellow solid, 20.2 mg, 49% yield

^{1}H NMR (400 MHz, $CDCl_3$) δ 8.15 (d, J = 7.8 Hz, 1H), 7.86 – 7.81 (m, 2H), 7.67 (dd, J = 10.7, 4.2 Hz, 1H), 7.56 (ddd, J = 13.7, 12.3, 6.9 Hz, 5H), 7.40 (t, J = 7.5 Hz, 1H), 7.10 (dtd, J = 9.6, 8.0, 1.4 Hz, 2H), 6.77 – 6.71 (m, 1H), 6.54 (dd, J = 8.0, 1.2 Hz, 1H), 2.38 (s, 3H).

^{13}C NMR (101 MHz, CDCl3) δ 168.2, 142.7, 138.0, 133.7, 133.4, 131.5, 130.6, 130.2, 129.9, 129.0, 128.9, 127.0, 126.8, 124.8, 124.6, 124.4, 88.8, 15.9 ppm.

HRMS (ESI, m/z): calcd. for $C_{21}H_{17}NO_4S_2H^+$ $[M+H]^+$: 412.0672, found 412.0670.

$[\alpha]^{21}_D$ = -174.8 (c = 0.49 in $CHCl_3$)

HPLC analysis: 99:1 e.r. (Chiralcel IA, 10:90 iPrOH/Hexane, 0.6 mL/min), Rt (major) = 24.7 min, Rt (minor) = 37.6 min.

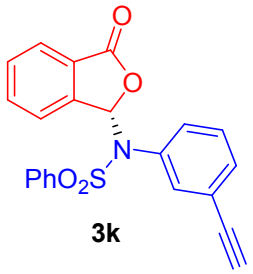

3k

(S)-N-(3-ethynylphenyl)-N-(3-oxo-1,3-dihydroisobenzofuran-1-yl)benzenesulfonamide (3k): White solid, 23.7 mg, 61% yield

^{1}H NMR (400 MHz, $CDCl_3$) δ 7.79 (dd, J = 8.4, 1.1 Hz, 2H), 7.69 – 7.59 (m, 5H), 7.56 – 7.51 (m, 2H), 7.46 – 7.41 (m, 1H), 7.25 (dt, J = 7.7, 1.2 Hz, 1H), 7.07 (s, 1H), 6.99 (t, J = 7.9 Hz, 1H), 6.82 (d, J = 8.1 Hz, 1H), 3.01 (s, 1H).

^{13}C NMR (101 MHz, $CDCl_3$) δ 168.0, 143.4, 137.7, 134.9, 134.5, 133.7, 133.6, 132.9, 131.2, 130.6, 129.1, 128.9, 128.4, 127.1, 125.5, 123.6, 123.2, 87.7, 81.8, 78.6 ppm.

HRMS (ESI, m/z): calcd. for $C_{22}H_{15}NO_4SH^+$ $[M+H]^+$: 390.0795, found 390.0791.

$[\alpha]^{21}_D$ = -264.9 (c = 0.45 in $CHCl_3$)

HPLC analysis: 98:2 e.r. (Chiralcel IA, 10:90 iPrOH/Hexane, 0.6 mL/min), Rt (major) = 21.0 min, Rt (minor) = 27.3 min.

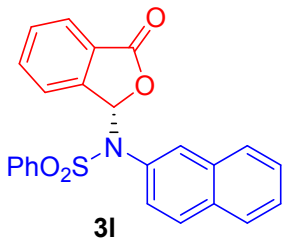

3l

(S)-N-(naphthalen-2-yl)-N-(3-oxo-1,3-dihydroisobenzofuran-1-yl) benzenesulfonamide (3l): White solid, 26.6 mg, 64%

^{1}H NMR (500 MHz, $CDCl_3$) δ 8.51 (d, J = 8.5 Hz, 1H), 7.82 (d, J = 7.4 Hz, 2H), 7.79 (s, 1H), 7.67 – 7.58 (m, 5H), 7.52 (t, J = 7.7 Hz, 3H), 7.45 (t, J = 7.2 Hz, 1H), 7.29 – 7.20 (m, 1H), 7.19 (t, J = 7.4 Hz, 1H), 7.01 (t, J = 7.8 Hz, 1H), 6.72 (d, J = 7.4 Hz, 1H).

^{13}C NMR (126 MHz, $CDCl_3$) δ 168.3, 142.8, 137.3, 134.3, 133.7, 133.7, 132.9, 130.4, 130.4, 130.2, 129.0, 128.9, 128.1, 127.8, 127.1, 126.7, 126.5, 125.0, 124.6, 124.4, 123.5, 88.8 ppm.

HRMS (ESI, m/z): calcd. for $C_{24}H_{17}NO_4SH^+$ $[M+H]^+$: 416.0951, found 416.0951.

$[\alpha]^{21}$ D = -67.5 (c = 0.37 in $CHCl_3$)

HPLC analysis: 97:3 e.r. (Chiralcel IA, 10:90 iPrOH/Hexane, 0.6 mL/min), Rt (major) = 19.9 min, Rt (minor) = 28.2 min.

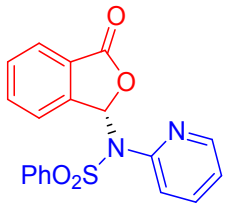

3m

(S)-N-(3-oxo-1,3-dihydroisobenzofuran-1-yl)-N-(pyridin-2-yl)benzenesulfonamide (3m): White solid, 19.8 mg, 54% yield.

^{1}H NMR (400 MHz, $CDCl_3$) δ 8.26 (s, 1H), 8.07 – 8.02 (m, 2H), 7.97 (d, J = 7.4 Hz, 1H), 7.87 (d, J = 9.2 Hz, 1H), 7.75 – 7.64 (m, 3H), 7.57 – 7.47 (m, 4H), 7.23 (dd, J = 7.0, 1.1 Hz, 1H), 6.52 (td, J = 6.9, 1.1 Hz, 1H).

^{13}C NMR (101 MHz, $CDCl_3$) δ 167.5, 155.6, 145.1, 143.1, 140.9, 135.8, 132.2, 131.8, 131.6, 128.8, 126.4, 126.1, 125.4, 124.4, 118.5, 111.1, 83.7 ppm.

HRMS (ESI, m/z): calcd. for $C_{19}H_{14}N_2O_4SH^+$ $[M+H]^+$: 367.0747, found 367.0739.

$[\alpha]^{21}_D$ = 485.3 (c = 0.23 in $CHCl_3$)

HPLC analysis: 90:10 e.r. (Chiralcel AD-H, 20:80 iPrOH/Hexane, 0.6 mL/min), Rt (major) = 72.5 min, Rt (minor) = 58.4 min.

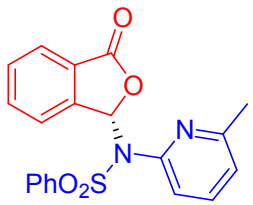

3n

(S)-N-(6-methylpyridin-2-yl)-N-(3-oxo-1,3-dihydroisobenzofuran-1-yl)benzenesulfonamide (3n): White solid, 24.3 mg, 64% yield.

^{1}H NMR (400 MHz, $CDCl_3$) δ 7.89 (d, J = 7.6 Hz, 2H), 7.74 (d, J = 7.6 Hz, 1H), 7.58 (t, J = 7.4 Hz, 1H), 7.54 (s, 1H), 7.52 – 7.45 (m, 4H), 7.38 (dt, J = 15.6, 7.6 Hz, 2H), 7.08 (d, J = 7.9 Hz, 1H), 6.78 (d, J = 7.6 Hz, 1H), 2.10 (s, 3H).

^{13}C NMR (101 MHz, $CDCl_3$) δ 168.6, 158.0, 148.5, 143.8, 138.7, 137.8, 133.7, 133.4, 130.1, 128.8, 128.5, 128.3, 124.7, 123.4, 122.1, 119.7, 87.5, 23.6 ppm.

HRMS (ESI, m/z): calcd. for $C_{20}H_{16}N_2O_4SH^+$ $[M+H]^+$: 381.0904, found 381.0900.

$[\alpha]^{21}_D$ = -152.8 (c = 0.29 in $CHCl_3$)

HPLC analysis: 96:4 e.r. (Chiralcel IA, 10:90 iPrOH/Hexane, 0.6 mL/min), Rt (major) = 22.5 min, Rt (minor) = 26.1 min.

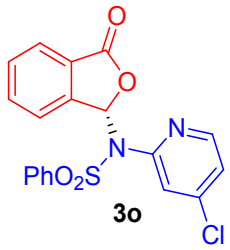

3o

(S)-N-(4-chloropyridin-2-yl)-N-(3-oxo-1,3-dihydroisobenzofuran-1-yl)benzenesulfonamide (3o): white solid, 30.1 mg, 75% yield.

^{1}H NMR (400 MHz, $CDCl_3$) δ 8.12 (s, 1H), 8.02 (d, J = 6.9 Hz, 2H), 7.95 (t, J = 4.8 Hz, 2H), 7.76 – 7.65 (m, 3H), 7.54 (tt, J = 14.3, 7.0 Hz, 3H), 7.17 (d, J = 7.5 Hz, 1H), 6.49 (dd, J = 7.5, 2.1 Hz, 1H)

^{13}C NMR (101 MHz, $CDCl_3$) δ 167.2, 154.8, 149.5, 144.7, 142.6, 135.9, 132.8, 132.1, 131.8, 128.9, 126.4, 126.2, 125.3, 124.3, 117.0, 112.7, 83.6 ppm.

HRMS (ESI, m/z): calcd. for $C_{19}H_{13}ClN_2O_4SH^+$ $[M+H]^+$: 401.0357, found 401.0360.

$[\alpha]^{21}$ D = 287.9 (c = 1.55 in $CHCl_3$)

HPLC analysis: 94:6 e.r. (Chiralcel IA, 10:90 iPrOH/Hexane, 0.6 mL/min), Rt (major) = 98.1 min, Rt (minor) = 82.8 min.

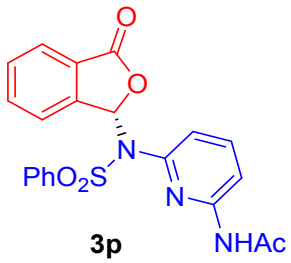

(S)-N-(6-(N-(3-oxo-1,3-dihydroisobenzofuran-1-yl)phenylsulfonamido)pyridin-2-yl)acetamide (3p): white solid, 18.2 mg, 43% yield.

^{1}H NMR (400 MHz, $CDCl_3$) δ 7.88 (d, J = 8.1 Hz, 1H), 7.84 – 7.79 (m, 2H), 7.73 (d, J = 7.6 Hz, 1H), 7.64 – 7.53 (m, 4H), 7.50 (t, J = 7.7 Hz, 4H), 7.44 (t, J = 7.4 Hz, 1H), 7.02 (d, J = 7.7 Hz, 1H), 2.07 (s, 3H).

^{13}C NMR (101 MHz, $CDCl_3$) δ 169.0, 168.7, 150.2, 147.1, 143.3, 140.1, 138.3, 134.2, 133.6, 130.5, 128.9, 128.3, 128.2, 124.9, 123.4, 119.4, 112.9, 87.5, 24.5 ppm.

HRMS (ESI, m/z): calcd. for $C_{21}H_{17}N_3O_5SH^+$ $[M+H]^+$: 424.2962, found 424.2961.

$[\alpha]^{21}$ D = -300.1 (c = 0.5 in $CHCl_3$)

HPLC analysis: 97:3 e.r. (Chiralcel IA, 10:90 iPrOH/Hexane, 0.6 mL/min), Rt (major) = 26.5 min, Rt (minor) = 29.9 min.

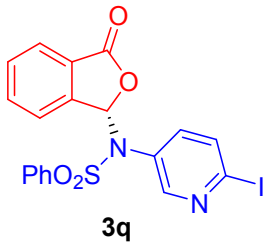

(S)-N-(6-iodopyridin-3-yl)-N-(3-oxo-1,3-dihydroisobenzofuran-1-yl)benzenesulfonamide (3q): yellow solid, 39.4 mg, 80% yield.

^{1}H NMR (400 MHz, $CDCl_3$) δ 7.90 (d, J = 2.6 Hz, 1H), 7.83 – 7.78 (m, 2H), 7.74 – 7.66 (m, 3H), 7.62 – 7.54 (m, 4H), 7.50 (t, J = 7.5 Hz, 1H), 7.44 (d, J = 8.4 Hz, 1H), 6.80 (dd, J = 8.4, 2.7 Hz, 1H).

^{13}C NMR (101 MHz, $CDCl_3$) δ 167.4, 152.7, 143.0, 139.5, 137.3, 135.0, 134.1, 131.1, 130.5, 129.4, 128.3, 126.9, 125.9, 123.3, 118.7, 87.3 ppm.

HRMS (ESI, m/z): calcd. for $C_{19}H_{13}IN_2O_4SH^+$ $[M+H]^+$: 492.9713, found 492.9719.

$[\alpha]^{21}$ $_D$ = -251.8 (c = 0.44 in $CHCl_3$)

HPLC analysis: 97:3 e.r. (Chiralcel IA, 10:90 iPrOH/Hexane, 0.6 mL/min), Rt (major) = 41.9 min, Rt (minor) = 71.9 min.

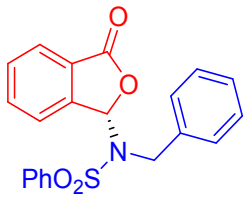

5a

(S)-N-benzyl-N-(3-oxo-1,3-dihydroisobenzofuran-1-yl)benzenesulfonamide (5a): Off white solid, 24.7 mg, 65% yield.

^{1}H NMR (400 MHz, Acetone-d_6) δ 8.10 (d, J = 7.5 Hz, 2H), 7.87 – 7.70 (m, 4H), 7.56 (t, J = 7.5 Hz, 1H), 7.49 – 7.42 (m, 1H), 7.19 – 7.06 (m, 5H), 7.00 (d, J = 7.1 Hz, 2H), 4.43 (d, J = 16.0 Hz, 1H), 3.87 (d, J = 16.0 Hz, 1H).

^{13}C NMR (101 MHz, Acetone-d_6) δ 168.0, 144.5, 140.0, 137.3, 134.4, 134.1, 131.0, 130.0, 128.6, 128.5, 127.7, 127.5, 125.3, 124.8, 88.0, 47.2 ppm.

HRMS (ESI, m/z): calcd. for $C_{21}H_{17}NO_4SH^+$ $[M+H]^+$: 380.0951, found 380.0948.

$[\alpha]^{21}_D$ = -57.5 (c = 0.75 in $CHCl_3$)

HPLC analysis: 95:5 e.r. (Chiralcel IA, 10:90 iPrOH/Hexane, 0.6 mL/min), Rt (major) = 24.1 min, Rt (minor) = 49.7 min.

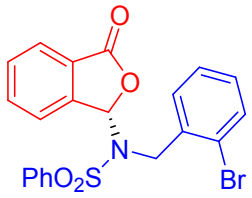

5b

(S)-N-(2-bromobenzyl)-N-(3-oxo-1,3-dihydroisobenzofuran-1-yl)benzenesulfonamide (5b): Yellow solid, 22.4 mg, 49% yield.

^{1}H NMR (400 MHz, $CDCl_3$) δ 8.03 (ddd, J = 7.1, 3.1, 1.9 Hz, 2H), 7.82 – 7.77 (m, 2H), 7.73 – 7.67 (m, 1H), 7.66 – 7.60 (m, 2H), 7.38 (dd, J = 14.3, 6.7 Hz, 2H), 7.28 – 7.20 (m, 2H), 7.09 (dd, J = 8.0, 1.2 Hz, 1H), 7.01 – 6.93 (m, 2H), 4.33 (d, J = 16.6 Hz, 1H), 4.05 (d, J = 16.5 Hz, 1H).

^{13}C NMR (101 MHz, $CDCl_3$) δ 168.1, 142.8, 138.2, 133.7, 133.4, 132.8, 130.5, 130.4, 129.4, 128.8, 128.7, 128.1, 127.1, 126.8, 125.5, 123.8, 87.3, 42.8 ppm.

HRMS (ESI, m/z): calcd. for $C_{21}H_{16}BrNO_4SH^+$ $[M+H]^+$: 458.0056, found 414.0053.

$[\alpha]^{21}_D$ = -135.3 (c = 0.33 in $CHCl_3$)

HPLC analysis: 97:3 e.r. (Chiralcel IA, 10:90 iPrOH/Hexane, 0.6 mL/min), Rt (major) = 25.0 min, Rt (minor) = 28.9 min.

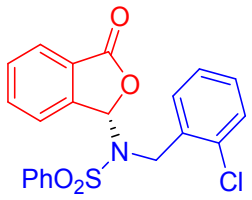

5c

(S)-N-(2-chlorobenzyl)-N-(3-oxo-1,3-dihydroisobenzofuran-1-yl)benzenesulfonamide (5c): White solid, 31 mg, 75% yield.

^{1}H NMR (400 MHz, $CDCl_3$) δ 8.02 (d, J = 7.5 Hz, 2H), 7.78 – 7.72 (m, 2H), 7.69 (t, J = 7.4 Hz, 1H), 7.61 (t, J = 7.6 Hz, 2H), 7.42 – 7.32 (m, 2H), 7.20 (dt, J = 15.7, 7.5 Hz, 2H), 7.01 (t, J = 8.5 Hz, 2H), 6.87 (d, J = 7.9 Hz, 1H), 4.31 (d, J = 16.4 Hz, 1H), 4.07 (d, J = 16.4 Hz, 1H).

^{13}C NMR (101 MHz, $CDCl_3$) δ 168.1, 142.8, 138.2, 133.7, 133.4, 132.8, 130.5, 130.4, 129.4, 128.8, 128.7, 128.0, 127.0, 126.8, 125.5, 123.8, 87.3, 42.8 ppm.

HRMS (ESI, m/z): calcd. for $C_{21}H_{16}ClNO_4SH^+$ $[M+H]^+$: 414.0561, found 414.0560.

$[\alpha]^{21}_D$ = -148.1 (c = 0.26 in $CHCl_3$)

HPLC analysis: 96:4 e.r. (Chiralcel IA, 10:90 iPrOH/Hexane, 0.6 mL/min), Rt (major) = 26.0 min, Rt (minor) = 23.1 min.

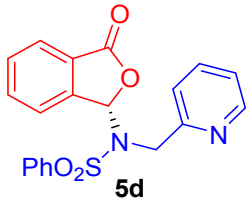

5d

(S)-N-(3-oxo-1,3-dihydroisobenzofuran-1-yl)-N-(pyridin-2-ylmethyl)benzenesulfonamide (5d): white solid, 24.7 mg, 65% yield.

^{1}H NMR (400 MHz, $CDCl_3$) δ 8.11 (s, 1H), 8.02 (d, J = 7.6 Hz, 2H), 7.81 (d, J = 7.6 Hz, 1H), 7.68 (t, J = 7.4 Hz, 1H), 7.60 (t, J = 7.6 Hz, 2H), 7.54 (t, J = 7.6 Hz, 1H), 7.48 (d, J = 7.7 Hz, 1H), 7.43 (t, J = 7.5 Hz, 1H), 7.37 (s, 1H), 7.33 (t, J = 7.5 Hz, 1H), 7.11 (d, J = 7.7 Hz, 1H), 7.04 – 6.99 (m, 1H), 4.39 (d, J = 16.5 Hz, 1H), 3.88 (d, J = 16.5 Hz, 1H).

^{13}C NMR (101 MHz, $CDCl_3$) δ 168.0, 156.2, 148.4, 143.3, 138.3, 136.3, 133.8, 133.7, 130.5, 129.4, 128.0, 127.1, 125.6, 123.8, 122.2, 87.5, 48.5 ppm.

HRMS (ESI, m/z): calcd. for $C_{20}H_{16}N_2O_4SH^+$ $[M+H]^+$: 381.0904, found 381.0903.

$[\alpha]^{21}_D$ = -119.3 (c = 1.00 in $CHCl_3$)

HPLC analysis: 96:4 e.r. (Chiralcel IA, 10:90 iPrOH/Hexane, 0.6 mL/min), Rt (major) = 76.1 min, Rt (minor) = 94.1 min.

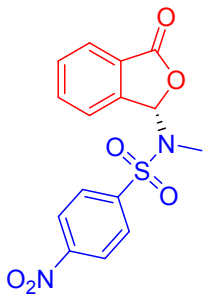

5e

(S)-N-methyl-4-nitro-N-(3-oxo-1,3-dihydroisobenzofuran-1-yl)benzenesulfonamide (5e): white solid, 17.8 mg, 51% yield.

^{1}H NMR (400 MHz, $CDCl_3$) δ 8.45 (d, J = 8.9 Hz, 2H), 8.18 (d, J = 8.9 Hz, 2H), 7.93 (d, J = 7.5 Hz, 1H), 7.85 – 7.79 (m, 1H), 7.68 (t, J = 7.6 Hz, 2H), 7.30 (s, 1H), 2.43 (s, 3H).

^{13}C NMR (101 MHz, $CDCl_3$) δ 167.5, 150.6, 143.2, 143.1, 135.2, 131.3, 129.5, 127.1, 126.1, 124.5, 123.3, 87.3, 28.3 ppm.

HRMS (ESI, m/z): calcd. for $C_{15}H_{12}N_2O_6SH^+$ $[M+H]^+$: 349.0489, found 349.0475.

$[\alpha]^{21}_{D}$ = -236.5 (c = 1.00 in $CHCl_3$)

HPLC analysis: 94:6 e.r. (Chiralcel IB, 10:90 iPrOH/Hexane, 0.6 mL/min), Rt (major) = 69.5 min, Rt (minor) = 86.0 min.

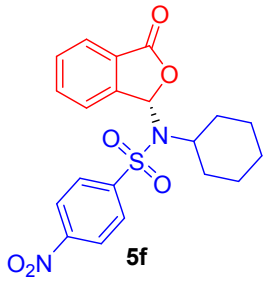

5f

(S)-N-cyclohexyl-4-nitro-N-(3-oxo-1,3-dihydroisobenzofuran-1-yl)benzenesulfonamide (5f): white solid, 23.7 mg, 57% yield.

^{1}H NMR (400 MHz, $CDCl_3$) δ 8.40 (d, J = 8.9 Hz, 2H), 8.16 (d, J = 8.9 Hz, 2H), 7.96 (d, J = 7.6 Hz, 1H), 7.78 (td, J = 7.5, 0.9 Hz, 1H), 7.65 (dd, J = 17.7, 7.6 Hz, 2H), 7.02 (s, 1H), 3.13 (s, 1H), 1.81 – 1.61 (m, 4H), 1.56 – 1.36 (m, 3H), 1.14 – 0.88 (m, 3H).

^{13}C NMR (101 MHz, $CDCl_3$) δ 168.0, 150.3, 146.8, 145.3, 134.7, 130.8, 128.9, 127.1, 125.9, 124.4, 123.3, 86.9, 59.2, 33.6, 32.2, 26.4, 26.3, 24.9 ppm.

HRMS (ESI, m/z): calcd. for $C_{20}H_{20}N_2O_6SH^+$ $[M+H]^+$: 417.1115, found 417.1103.

$[\alpha]^{21}_{D}$ = -53.5 (c = 0.40 in $CHCl_3$)

HPLC analysis: 93:7 e.r. (Chiralcel IB, 10:90 iPrOH/Hexane, 0.6 mL/min), Rt (major) = 42.3 min, Rt (minor) = 56.4 min.

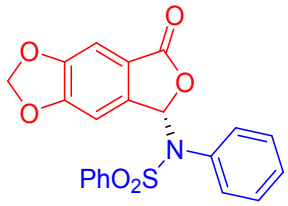

5g

(S)-N-(7-oxo-5,7-dihydro-[1,3]dioxolo[4,5-f]isobenzofuran-5-yl)-N-phenylbenzenesulfonamide (5g): white solid, 33.1 mg, 81% yield.

^{1}H NMR (400 MHz, $CDCl_3$) δ 7.76 (dd, J = 8.4, 1.1 Hz, 2H), 7.65 – 7.59 (m, 1H), 7.54 – 7.45 (m, 3H), 7.21 – 7.15 (m, 1H), 7.11 (t, J = 7.6 Hz, 2H), 6.94 (d, J = 4.6 Hz, 2H), 6.92 – 6.88 (m, 2H), 6.06 (dd, J = 8.8, 1.0 Hz, 2H).

^{13}C NMR (101 MHz, $CDCl_3$) δ 167.6, 153.8, 150.2, 140.2, 138.1, 133.4, 131.1, 129.3, 128.9, 128.4, 121.4, 103.9, 103.1, 102.8, 87.1 ppm.

HRMS (ESI, m/z): calcd. for $C_{21}H_{15}NO_6SH^+$ $[M+H]^+$: 410.0693, found 410.0678.

$[\alpha]^{21}$ D = -138.9 (c = 1.00 in $CHCl_3$)

HPLC analysis: 94:6 e.r. (Chiralcel IA, 10:90 iPrOH/Hexane, 0.6 mL/min), Rt (major) = 41.6 min, Rt (minor) = 49.6 min.

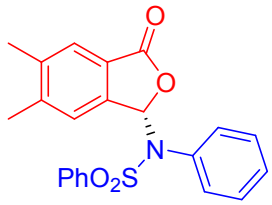

5h

(S)-N-(5,6-dimethyl-3-oxo-1,3-dihydroisobenzofuran-1-yl)-N-phenylbenzenesulfonamide: White solid, 31.5 mg, 80% yield.

^{1}H NMR (400 MHz, $CDCl_3$) δ 7.80 – 7.73 (m, 2H), 7.61 (t, J = 7.5 Hz, 1H), 7.54 (s, 1H), 7.49 (t, J = 7.8 Hz, 2H), 7.36 (d, J = 8.8 Hz, 2H), 7.15 – 7.09 (m, 1H), 7.05 (t, J = 7.5 Hz, 2H), 6.89 (d, J = 7.4 Hz, 2H), 2.32 (s, 3H), 2.20 (s, 3H).

^{13}C NMR (101 MHz, $CDCl_3$) δ 168.6, 144.7, 141.8, 139.8, 138.2, 133.5, 133.4, 131.2, 129.2, 129.0, 128.8, 128.4, 125.7, 125.1, 124.2, 87.6, 20.8, 20.0 ppm.

HRMS (ESI, m/z): calcd. for $C_{22}H_{19}NO_4SH^+$ $[M+H]^+$: 394.1108, found 394.1109

HPLC analysis: 90:10 e.r. (Chiralcel IA, 10:90 iPrOH/Hexane, 0.6 mL/min), Rt (major) = 23.3 min, Rt (minor) = 28.4 min.

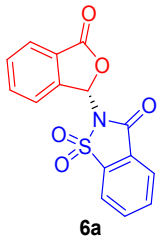

6a

(S)-2-(3-oxo-1,3-dihydroisobenzofuran-1-yl)benzo[d]isothiazol-3(2H)-one 1,1-dioxide (6a): white solid, 30 mg, 95% yield.

^{1}H NMR (400 MHz, $CDCl_3$) δ 8.12 – 8.05 (m, 1H), 8.05 – 7.98 (m, 1H), 7.97 – 7.88 (m, 1H), 7.92 – 7.83 (m, 2H), 7.78 (td, J = 7.5, 1.2 Hz, 1H), 7.78 – 7.66 (m, 2H), 7.30 (s, 1H).

^{13}C NMR (101 MHz, $CDCl_3$) δ 167.60, 158.6, 141.0, 138.0, 135.8, 134.7, 134.5, 131.4, 127.4, 126.1, 126.0, 125.8, 124.2, 121.1, 79.4 ppm.

HRMS (ESI, m/z): calcd. for $C_{15}H_9NSO_5H^+$ $[M+H]^+$: 316.0274, found 316.0271.

$[\alpha]^{21}_D$ = -48.7 (c = 1.20 in $CHCl_3$)

HPLC analysis: 85:15 e.r. (Chiralcel IA, 20:80 iPrOH/Hexane, 0.6 mL/min), Rt (major) = 84.0 min, Rt (minor) = 58.3 min.

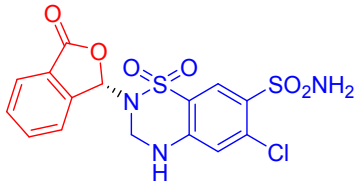

6b

(S)-6-chloro-2-(3-oxo-1,3-dihydroisobenzofuran-1-yl)-3,4-dihydro-2H-benzo[e][1,2,4]thiadiazine-7-sulfonamide 1,1-dioxide (6b): White Solid, 34.3 mg, 80% yield.

^{1}H NMR (400 MHz, Acetone-d_6) δ 8.27 (s, 1H), 7.98 – 7.89 (m, 2H), 7.85 – 7.75 (m, 2H), 7.15 (s, 2H), 7.09 (s, 1H), 6.77 (s, 1H), 5.12 (d, J = 14.9 Hz, 1H), 4.58 (dd, J = 14.9, 4.0 Hz, 1H).

^{13}C NMR (101 MHz, Acetone-d_6) δ 167.1, 146.5, 143.1, 135.8, 135.1, 131.3, 129.4, 127.5, 126.3, 125.4, 123.9, 119.5, 118.0, 87.9, 55.1 ppm.

HRMS (ESI, m/z): calcd. for $C_{15}H_{12}ClN_3O_6S_2H^+$ $[M+H]^+$: 429.9929, found 429.9927.

$[\alpha]^{21}_D$ = -180.5 (c = 0.935 in Acetone)

HPLC analysis: 91:9 e.r. (Chiralcel OD, 30:70 iPrOH/Hexane, 0.6 mL/min), Rt (major) = 30.8 min, Rt (minor) = 41.1 min.

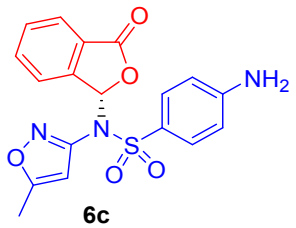

6c

(S)-4-amino-N-(5-methylisoxazol-3-yl)-N-(3-oxo-1,3-dihydroisobenzofuran-1-yl)benzenesulfonamide (6c): white solid, 23.9 mg, 62% yield.

^{1}H NMR (400 MHz, $CDCl_3$) δ 7.80 (d, J = 7.8 Hz, 1H), 7.66 – 7.57 (m, 3H), 7.54 – 7.47 (m, 2H), 7.45 (d, J = 3.2 Hz, 1H), 6.59 (dd, J = 9.0, 2.2 Hz, 2H), 5.98 (s, 1H), 4.37 (s, 2H), 2.20 (s, 3H).

^{13}C NMR (101 MHz, $CDCl_3$) δ 170.7, 168.3, 156.5, 152.2, 143.2, 134.4, 130.6, 130.4, 127.8, 125.3, 124.3, 123.1, 113.9, 101.2, 86.9, 12.5 ppm.

HRMS (ESI, m/z): calcd. for $C_{18}H_{15}N_3O_5SH^+$ $[M+H]^+$: 386.0805, found 386.0801.

$[\alpha]^{21}_{D}$ = -244.6 (c = 0.7 in $CHCl_3$)

HPLC analysis: 93:7 e.r. (Chiralcel IA, 20:80 iPrOH/Hexane, 0.6 mL/min), Rt (major) = 39.7 min, Rt (minor) = 52.6 min.

VIII. NMR and HPLC Spectra

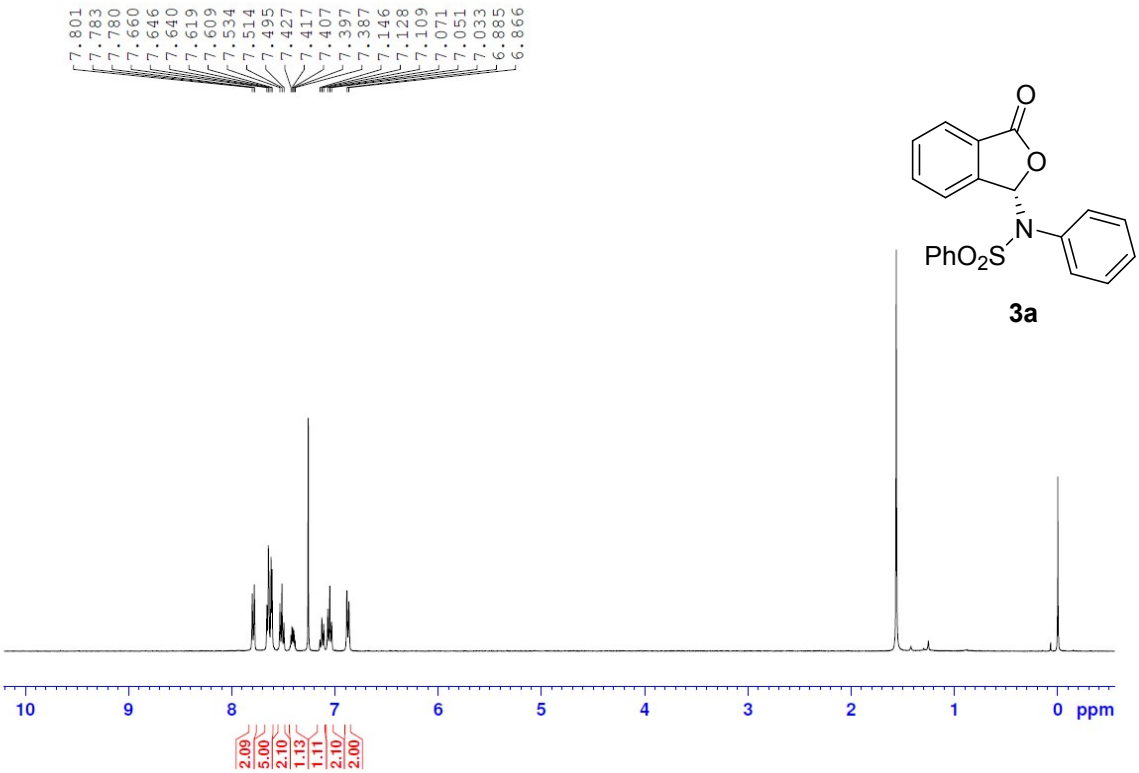

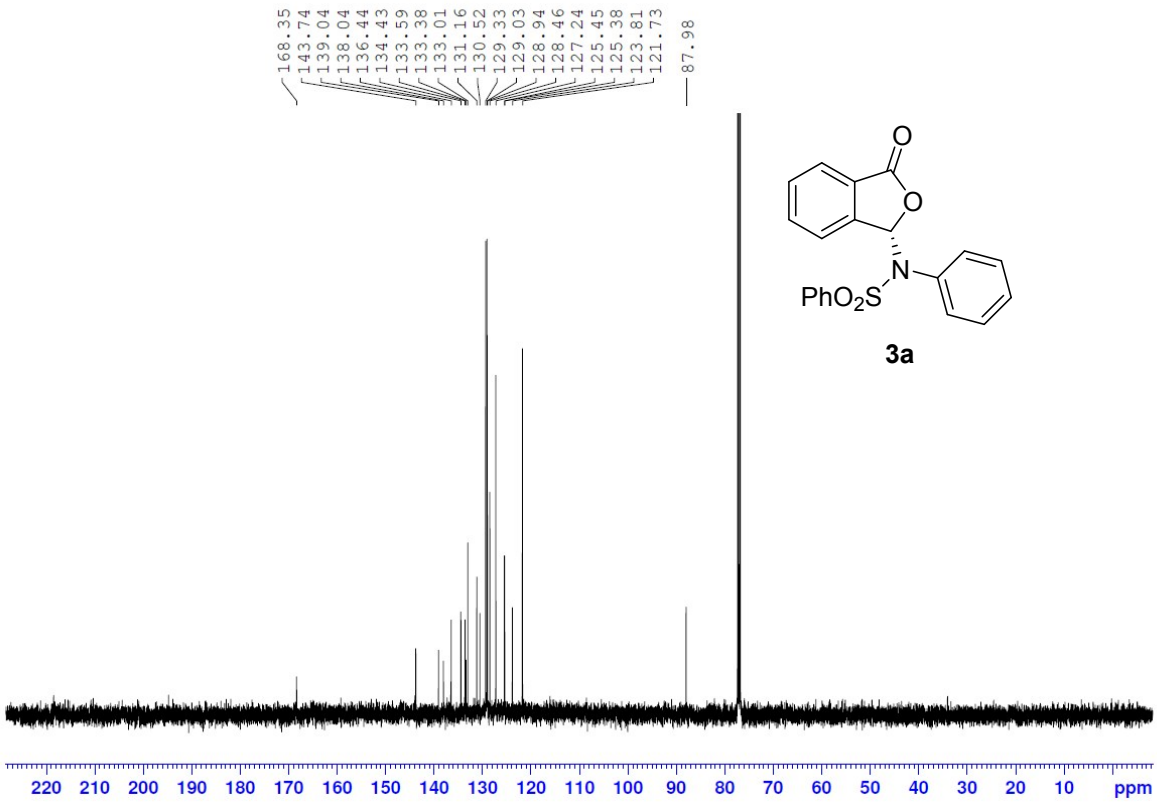

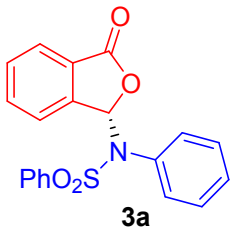

3a

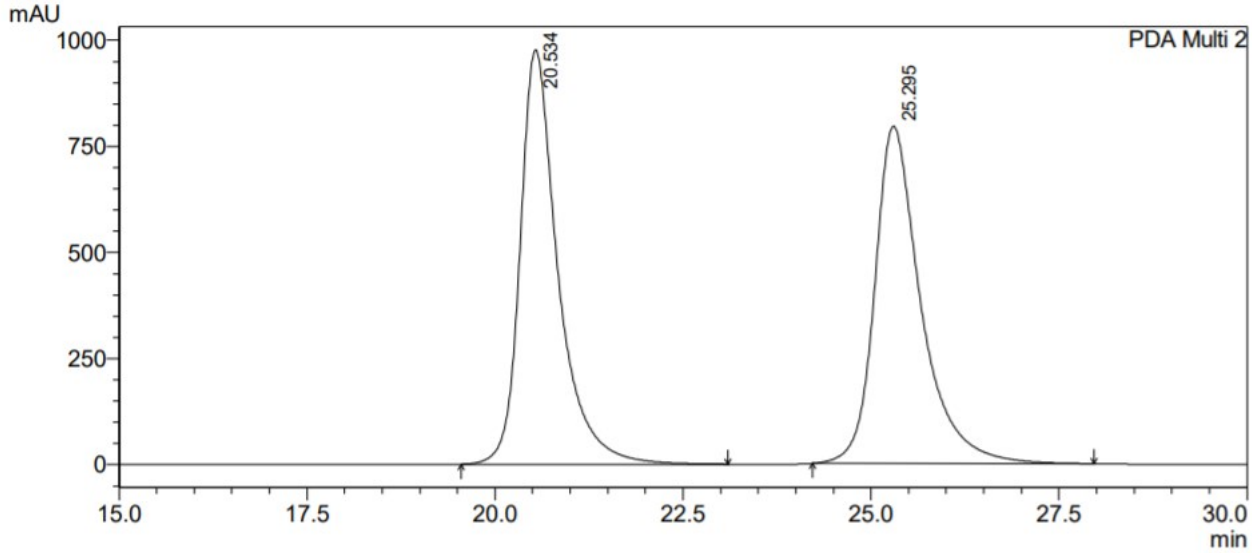

PDA Ch2 220nm 4nm

Peak#	Ret. Time	Area	Height	Area %	Height %
1	20.534	34279183	976143	50.208	55.124
2	25.295	33994556	794676	49.792	44.876
Total		68273739	1770820	100.000	100.000

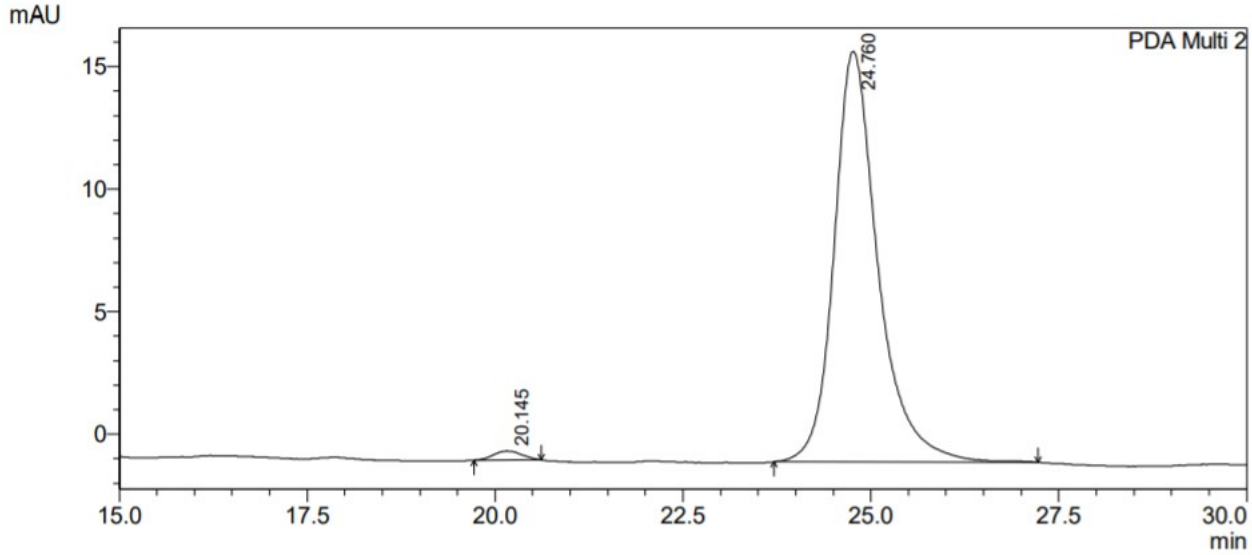

PDA Ch2 220nm 4nm

Peak#	Ret. Time	Area	Height	Area %	Height %
1	20.145	9609	368	1.385	2.150
2	24.760	684265	16755	98.615	97.850
Total		693875	17123	100.000	100.000

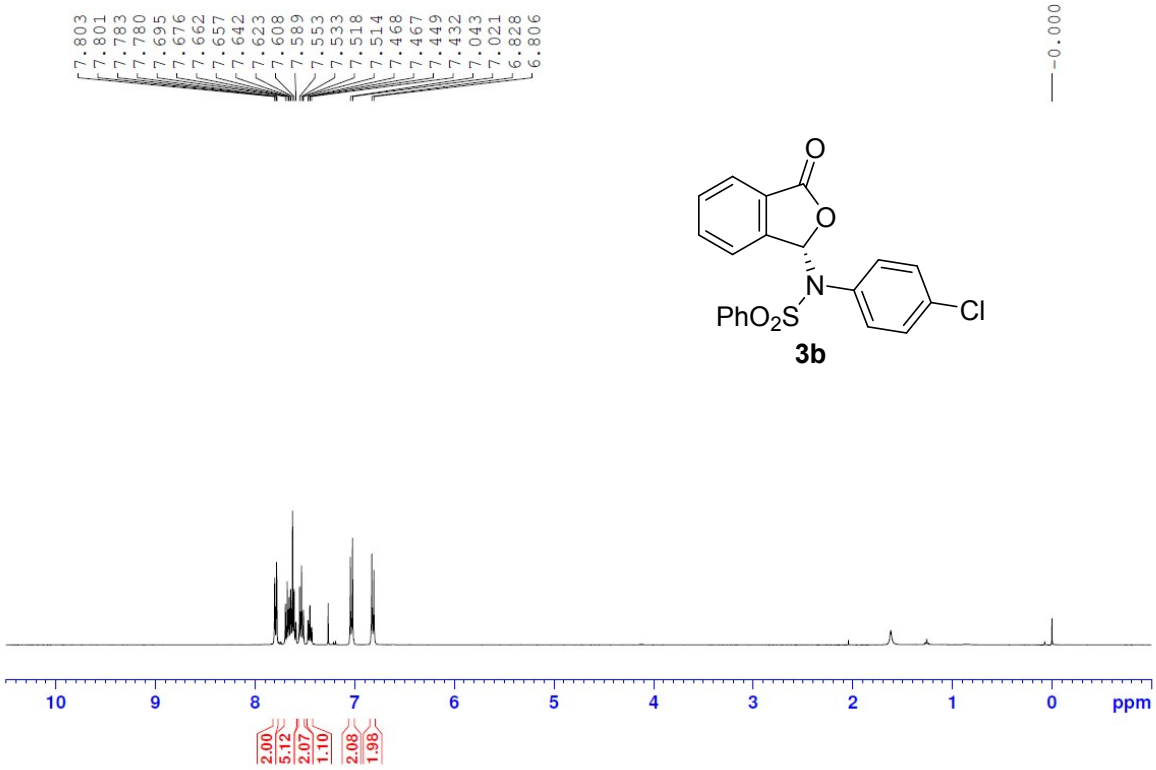
7.803
7.801
7.783
7.780
7.695
7.676
7.662
7.657
7.642
7.623
7.608
7.589
7.553
7.533
7.518
7.514
7.468
7.467
7.449
7.432
7.043
7.021
6.828
6.806
0.000
O
O
N
PhO2S
Cl
3b
10 9 8 7 6 5 4 3 2 1 0 ppm
2.00
5.12
2.07
1.10
2.08
1.98

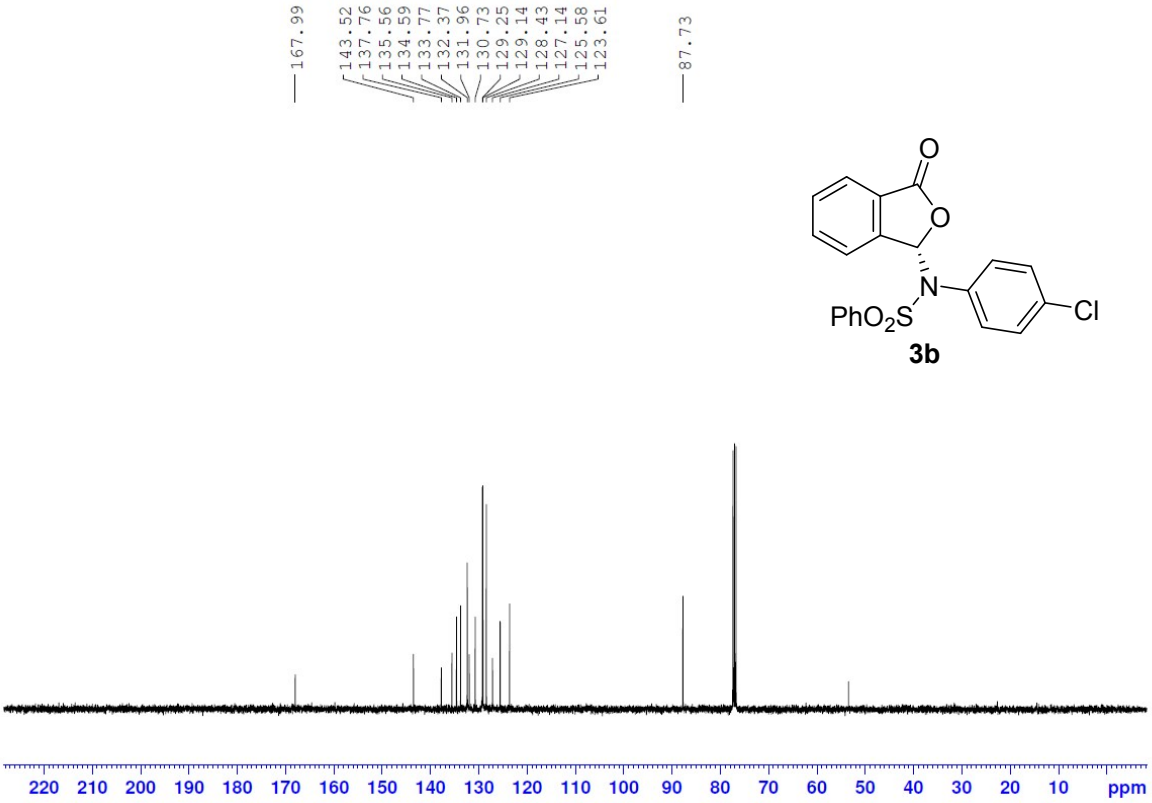
167.99
143.52
137.76
135.56
134.59
133.77
132.37
131.96
130.73
129.25
129.14
128.43
127.14
125.58
123.61
87.73
O
O
N
PhO2S
Cl
3b
220 210 200 190 180 170 160 150 140 130 120 110 100 90 80 70 60 50 40 30 20 10 ppm

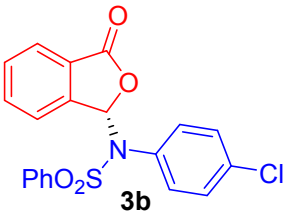

3b

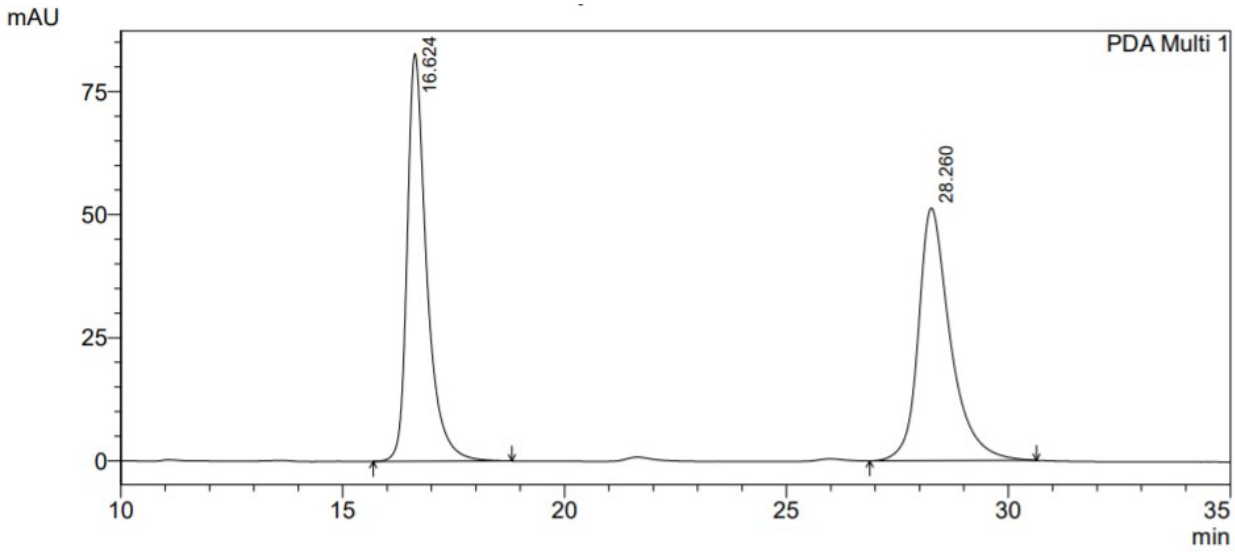

PDA Ch1 254nm 4nm

Peak#	Ret. Time	Area	Height	Area %	Height %
1	16.624	2530187	82788	49.567	61.721
2	28.260	2574374	51345	50.433	38.279
Total		5104561	134133	100.000	100.000

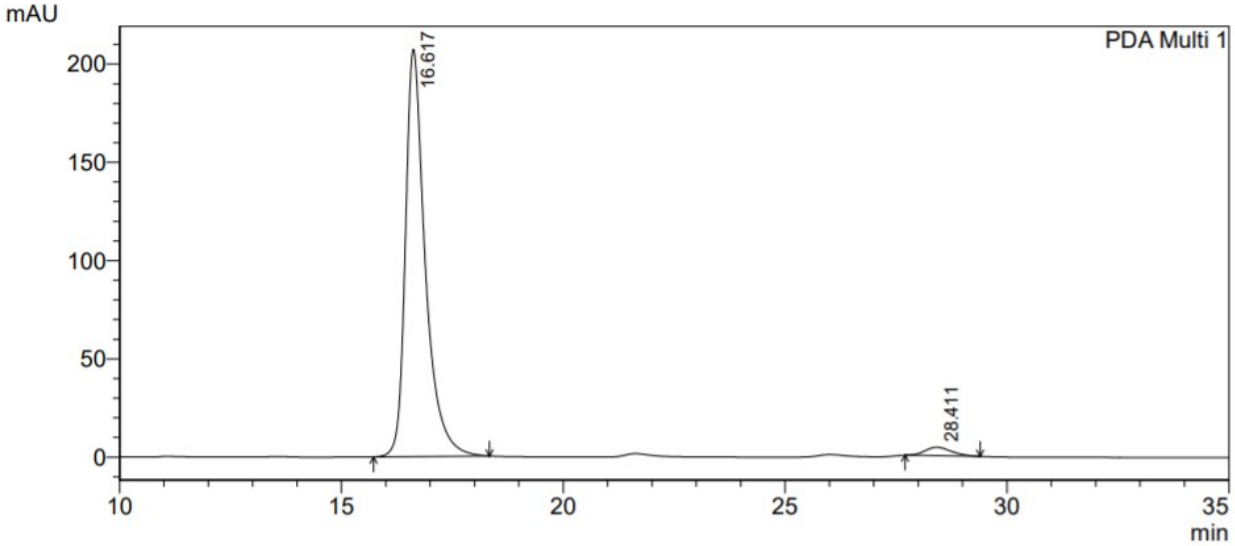

Peak#	Ret. Time	Area	Height	Area %	Height %
1	16.617	6454204	207284	97.292	97.967
2	28.411	179665	4302	2.708	2.033
Total		6633870	211586	100.000	100.000

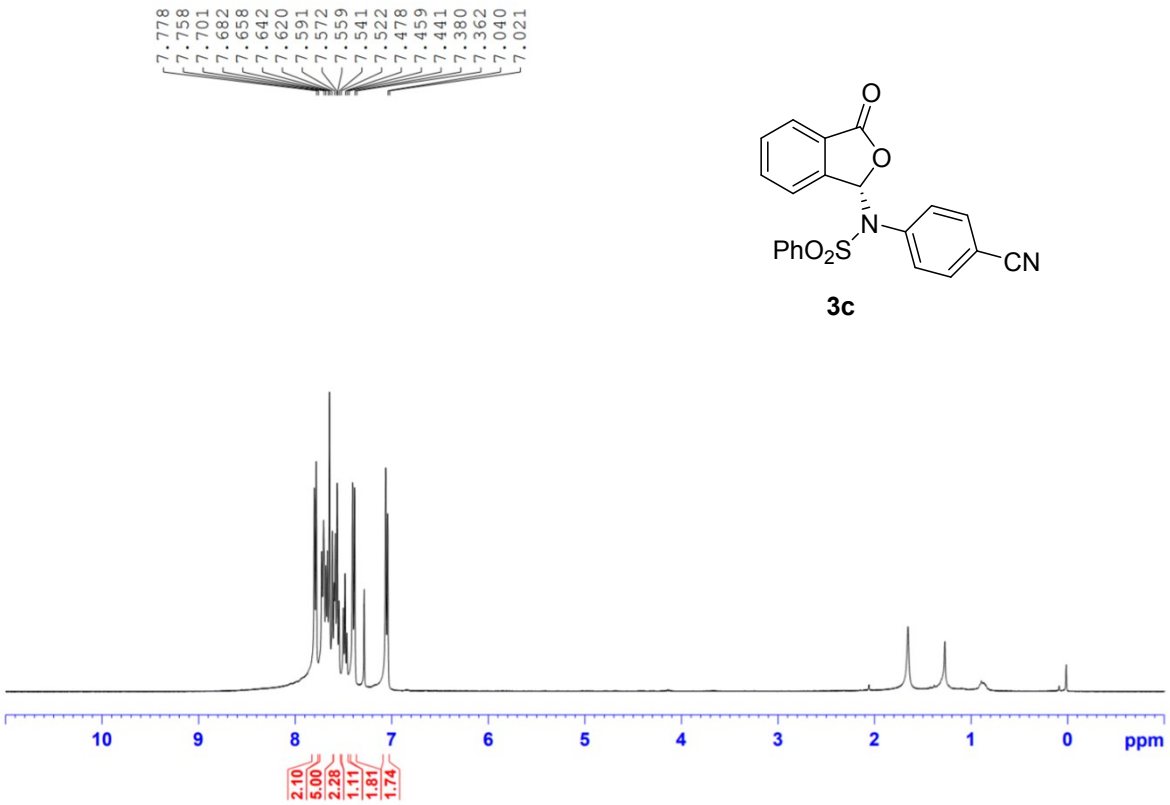
7.778
7.758
7.701
7.682
7.658
7.642
7.620
7.591
7.572
7.559
7.541
7.522
7.478
7.459
7.441
7.380
7.362
7.040
7.021
O
O
N
PhO2S
CN
3c
10
9
8
7
6
5
4
3
2
1
0
ppm
2.10
5.00
2.28
1.11
1.81
1.74

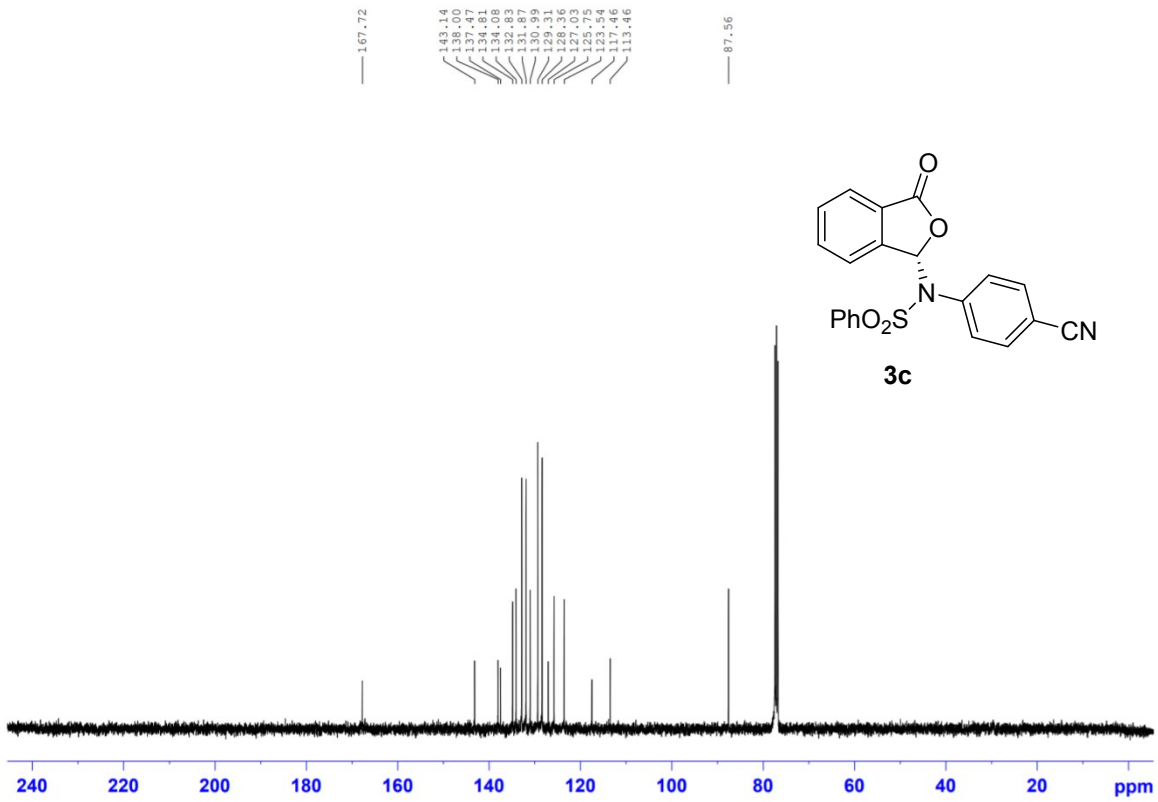
167.72
143.14
138.00
137.47
134.81
134.08
132.83
131.87
130.99
129.31
128.36
127.03
125.75
123.54
117.46
113.46
87.56
O
O
N
PhO2S
CN
3c
240
220
200
180
160
140
120
100
80
60
40
20
ppm

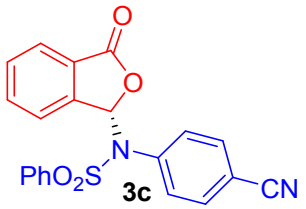

3c

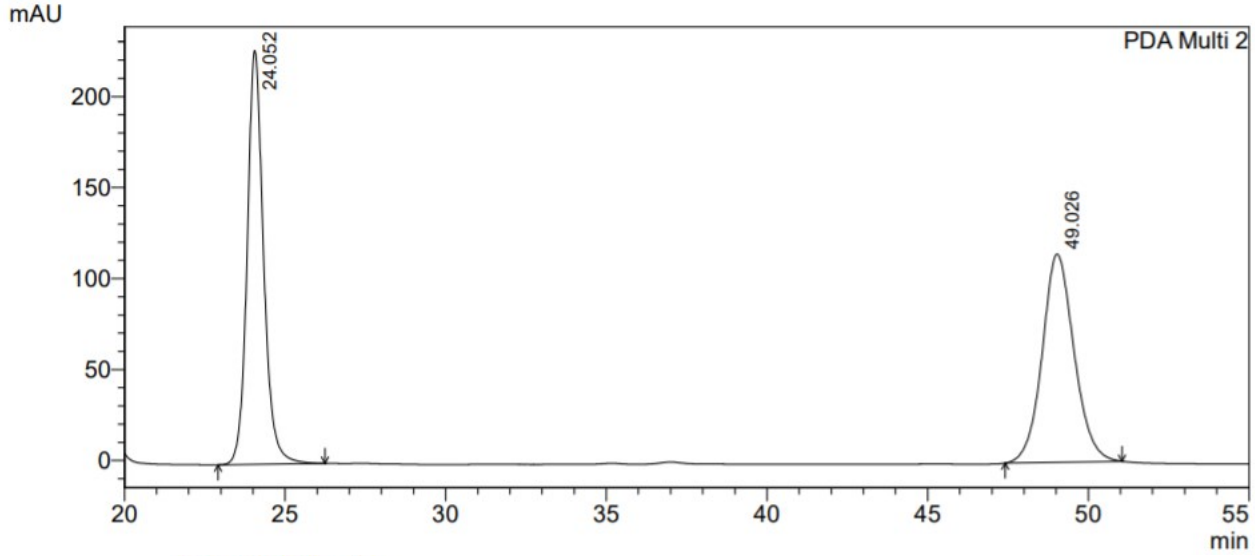

PDA Ch2 220nm 4nm

Peak#	Ret. Time	Area	Height	Area %	Height %
1	24.052	8084231	227340	50.567	66.525
2	49.026	7903020	114394	49.433	33.475
Total		15987251	341735	100.000	100.000

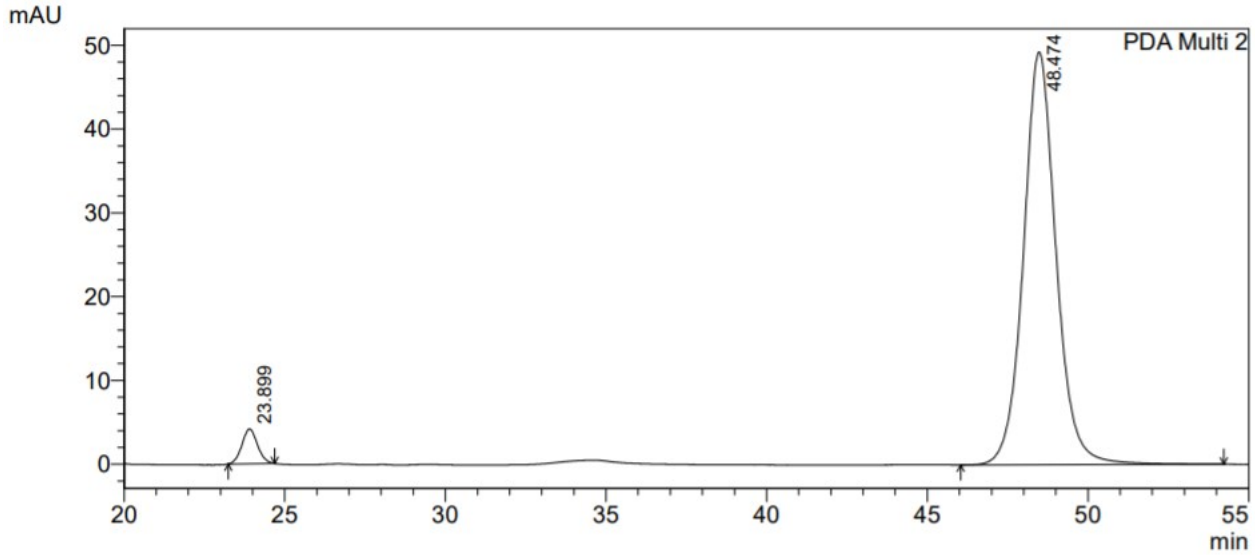

PDA Ch2 220nm 4nm

Peak#	Ret. Time	Area	Height	Area %	Height %
1	23.899	139966	4145	3.866	7.759
2	48.474	3480099	49279	96.134	92.241
Total		3620064	53424	100.000	100.000

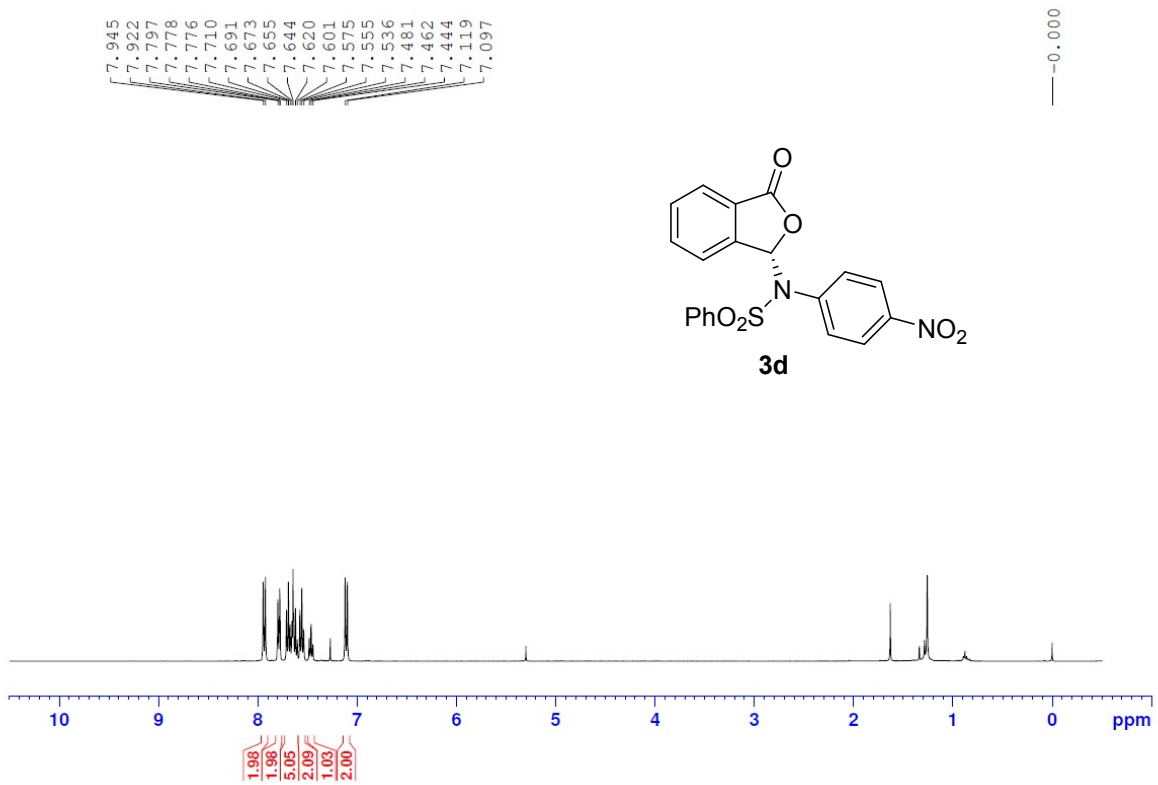
7.945
7.922
7.797
7.778
7.776
7.710
7.691
7.673
7.655
7.644
7.620
7.601
7.575
7.555
7.536
7.481
7.462
7.444
7.119
7.097
0.000
O
O
N
PhO2S
NO2
3d
10 9 8 7 6 5 4 3 2 1 0 ppm
1.98
1.98
5.05
2.09
1.03
2.00

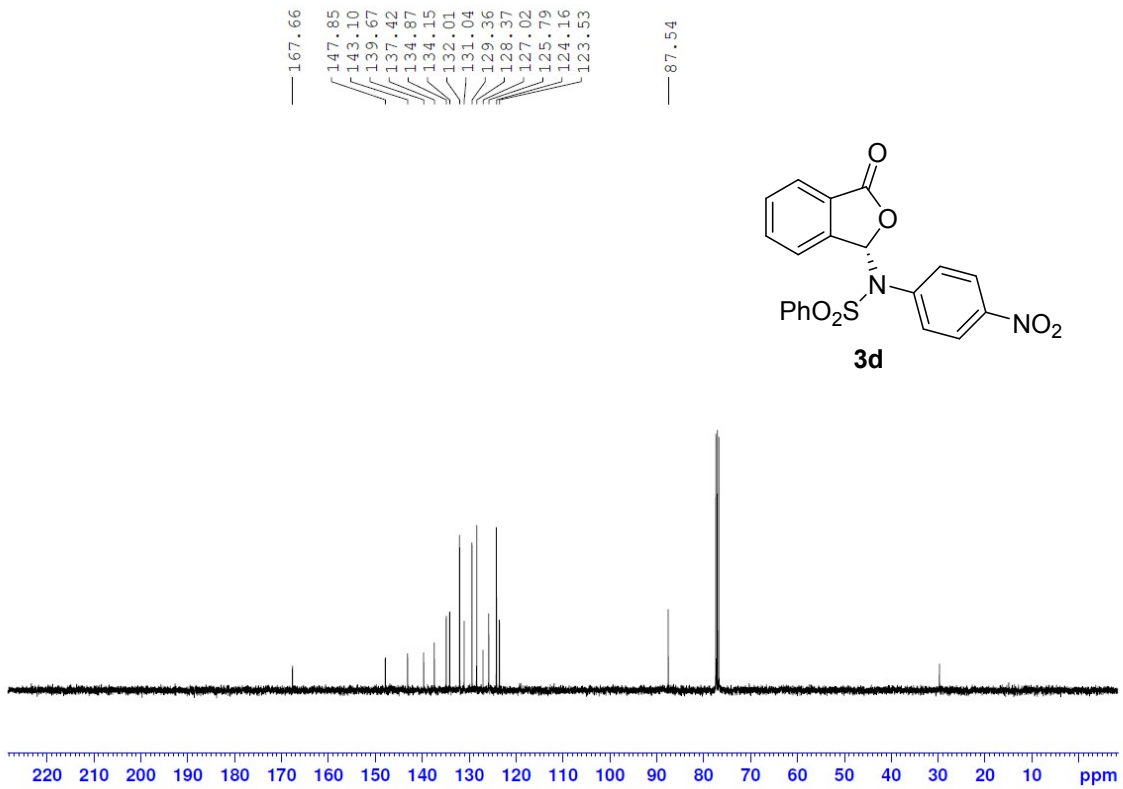
167.66
147.85
143.10
139.67
137.42
134.87
134.15
132.01
131.04
129.36
128.37
127.02
125.79
124.16
123.53
87.54
O
O
N
PhO2S
NO2
3d
220 210 200 190 180 170 160 150 140 130 120 110 100 90 80 70 60 50 40 30 20 10 ppm

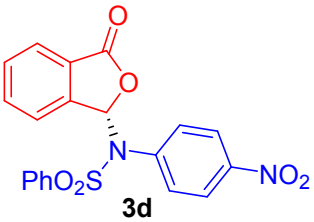

3d

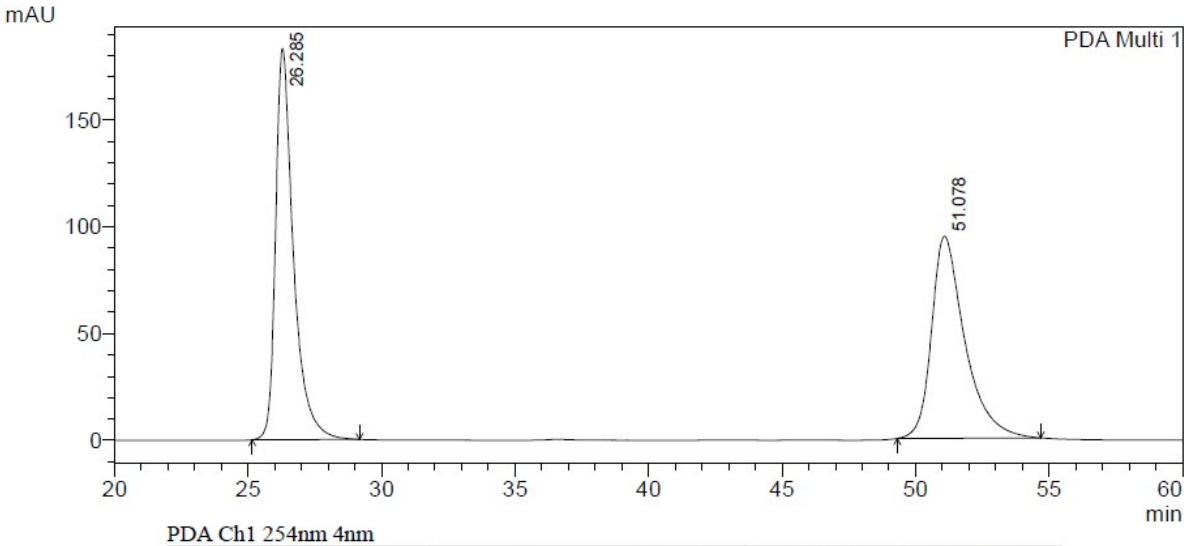

PDA Ch1 254nm 4nm

Peak#	Ret. Time	Area	Height	Area %	Height %
1	26.285	8528715	183022	50.971	65.939
2	51.078	8203753	94541	49.029	34.061
Total		16732468	277563	100.000	100.000

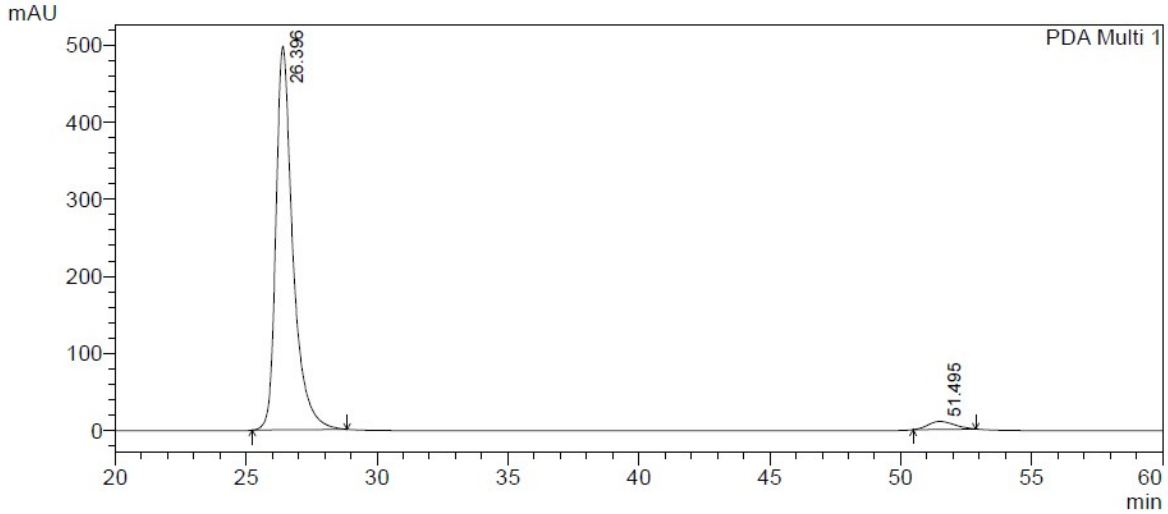

PDA Ch1 254nm 4nm

Peak#	Ret. Time	Area	Height	Area %	Height %
1	26.396	22432327	497710	96.884	97.946
2	51.495	721531	10437	3.116	2.054
Total		23153859	508147	100.000	100.000

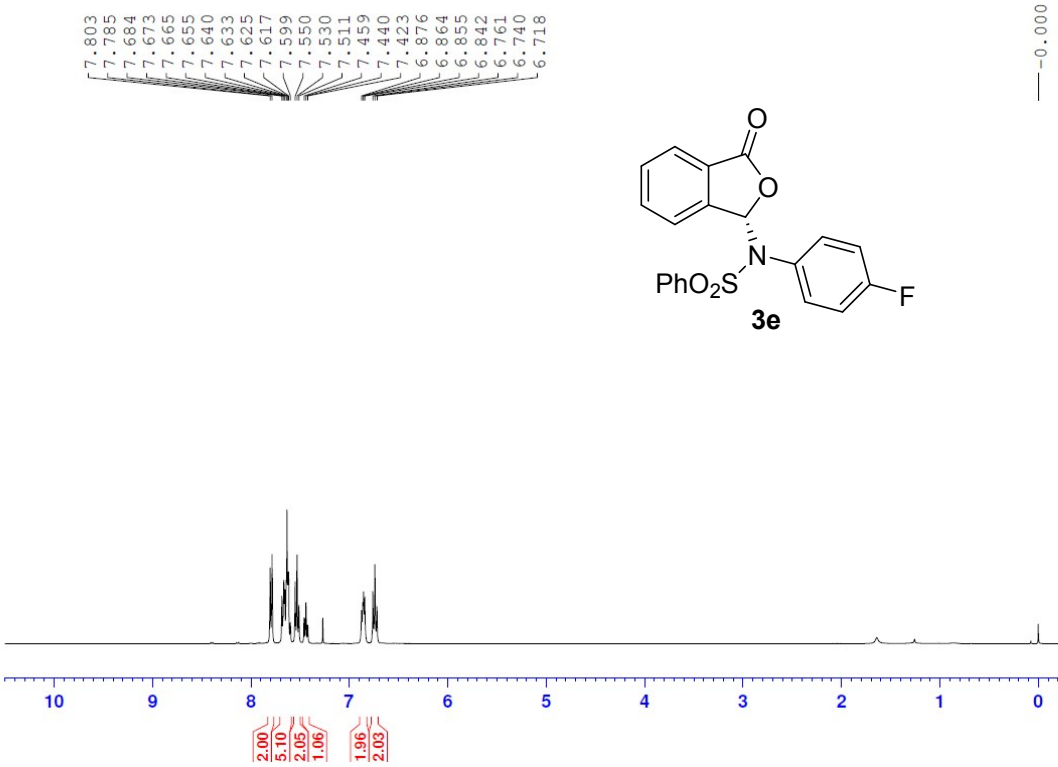
7.803
7.785
7.684
7.673
7.665
7.655
7.640
7.633
7.625
7.617
7.599
7.550
7.530
7.511
7.459
7.440
7.423
6.876
6.864
6.855
6.842
6.761
6.740
6.718
0.000
O
O
N
PhO2S
F
3e
10
9
8
7
6
5
4
3
2
1
0
ppm
2.00
5.10
2.05
1.06
1.96
2.03

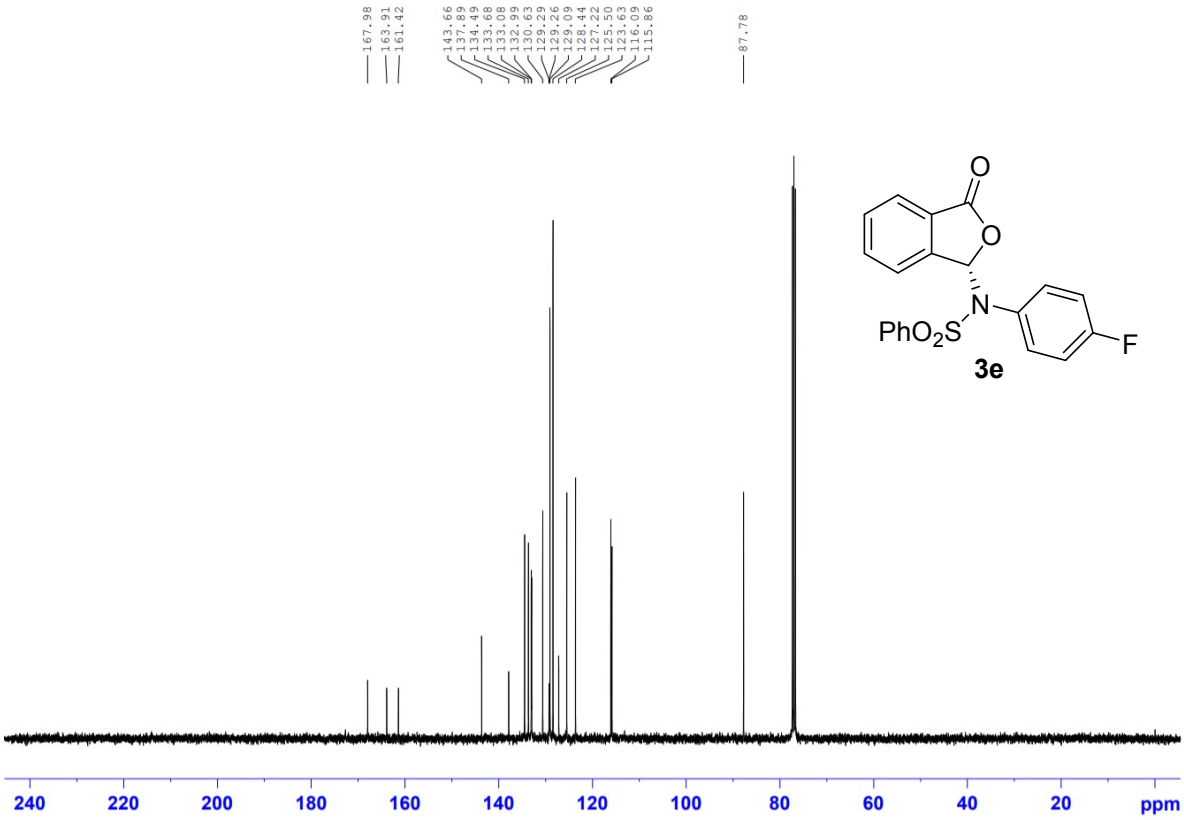
167.98
163.91
161.42
143.66
137.89
134.49
133.68
133.08
132.99
130.63
129.29
129.26
129.09
128.44
127.22
125.52
123.63
116.09
115.86
87.78
O
O
N
PhO2S
F
3e
240
220
200
180
160
140
120
100
80
60
40
20
ppm

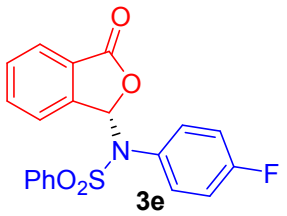

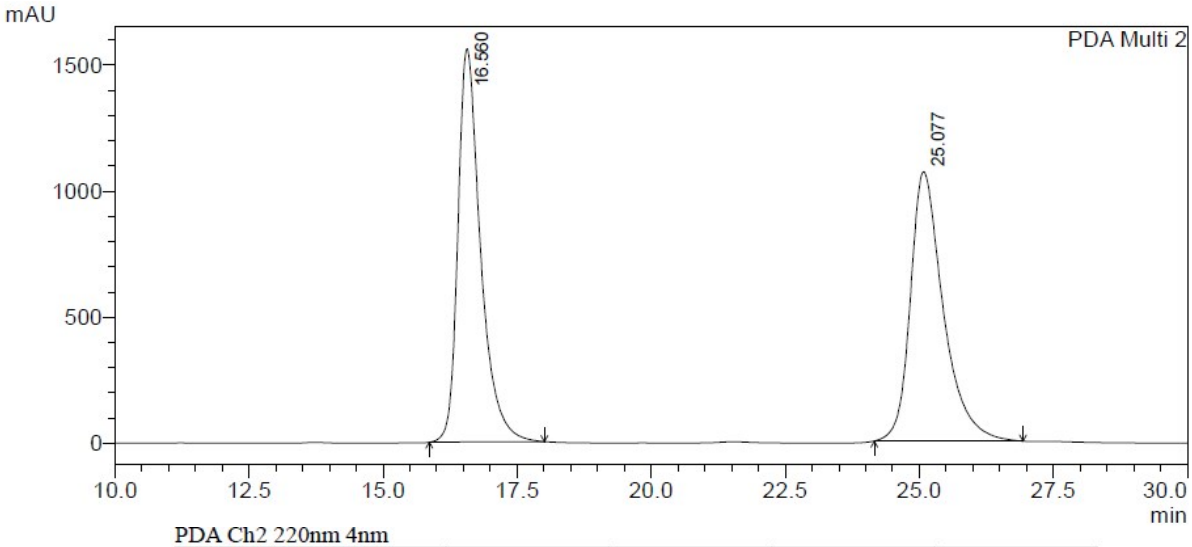

PDA Ch2 220nm 4nm

Peak#	Ret. Time	Area	Height	Area %	Height %
1	16.560	45918117	1560914	50.125	59.365
2	25.077	45688558	1068418	49.875	40.635
Total		91606675	2629331	100.000	100.000

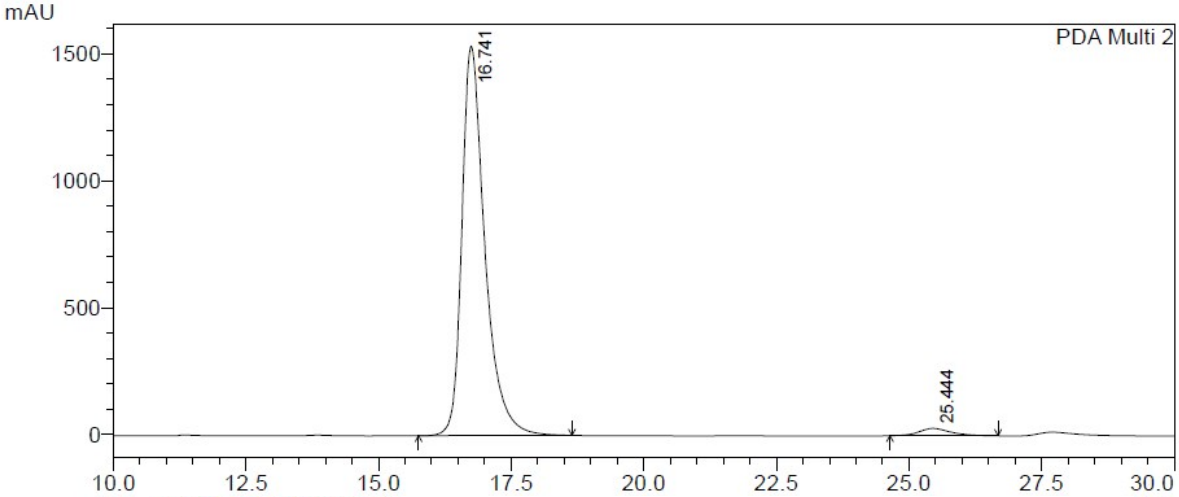

PDA Ch2 220nm 4nm

Peak#	Ret. Time	Area	Height	Area %	Height %
1	16.741	46248226	1534630	97.542	98.186
2	25.444	1165278	28345	2.458	1.814
Total		47413504	1562975	100.000	100.000

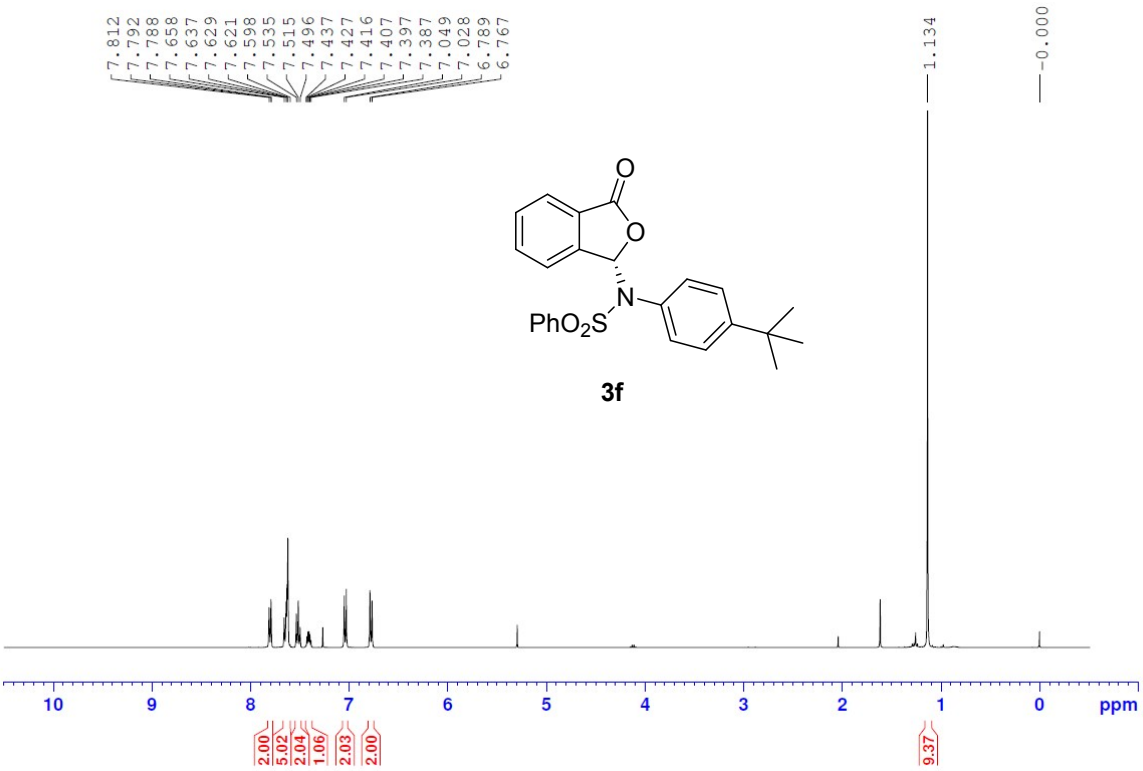
7.812
7.792
7.788
7.658
7.637
7.629
7.621
7.598
7.535
7.515
7.496
7.437
7.427
7.416
7.407
7.397
7.387
7.049
7.028
6.789
6.767
1.134
0.000
O
O
N
PhO2S
3f
10 9 8 7 6 5 4 3 2 1 0 ppm
2.00
5.02
2.04
1.06
2.03
2.00
9.37

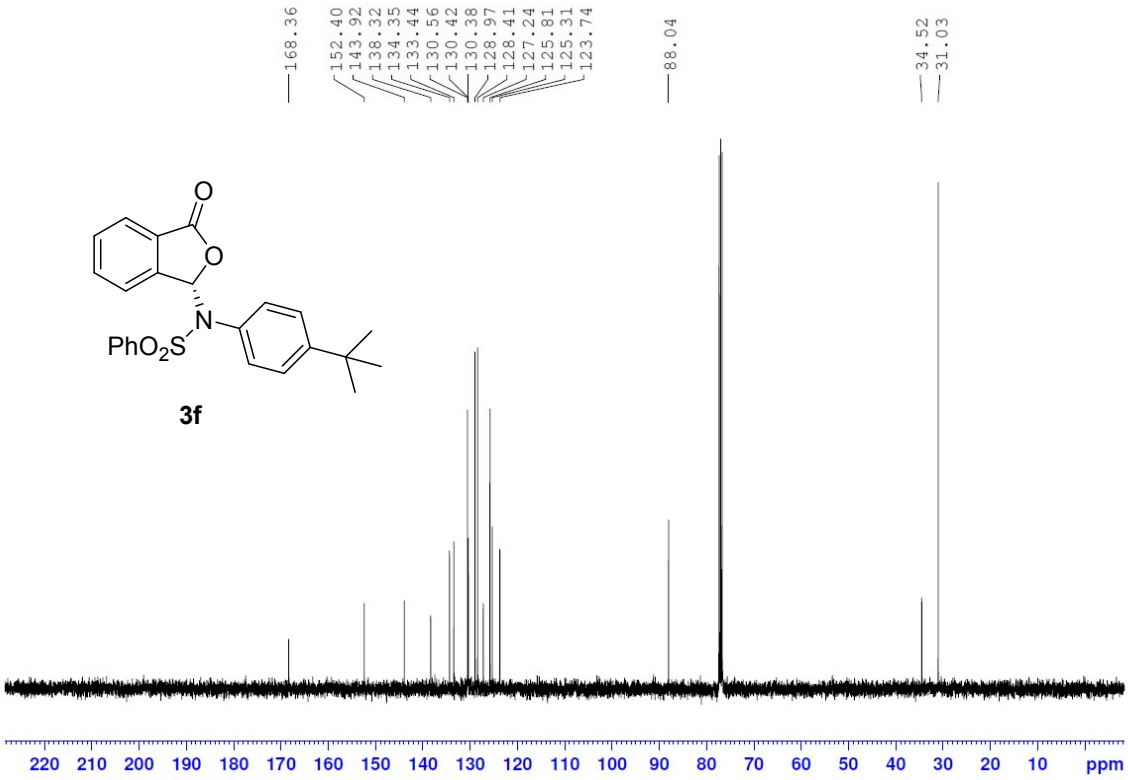
168.36
152.40
143.92
138.32
134.35
133.44
130.56
130.42
130.38
128.97
128.41
127.24
125.81
125.31
123.74
88.04
34.52
31.03
O
O
N
PhO2S
3f
220 210 200 190 180 170 160 150 140 130 120 110 100 90 80 70 60 50 40 30 20 10 ppm

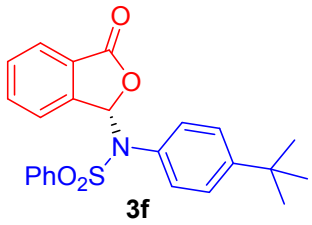

3f

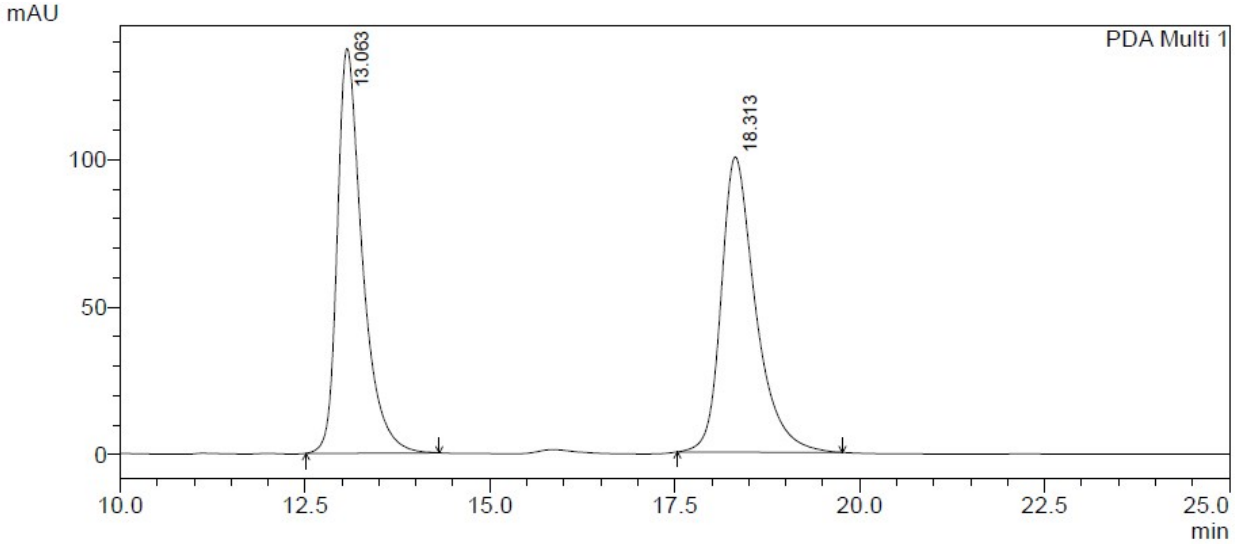

Peak#	Ret. Time	Area	Height	Area %	Height %
1	13.063	3237282	137239	49.931	57.838
2	18.313	3246188	100042	50.069	42.162
Total		6483469	237281	100.000	100.000

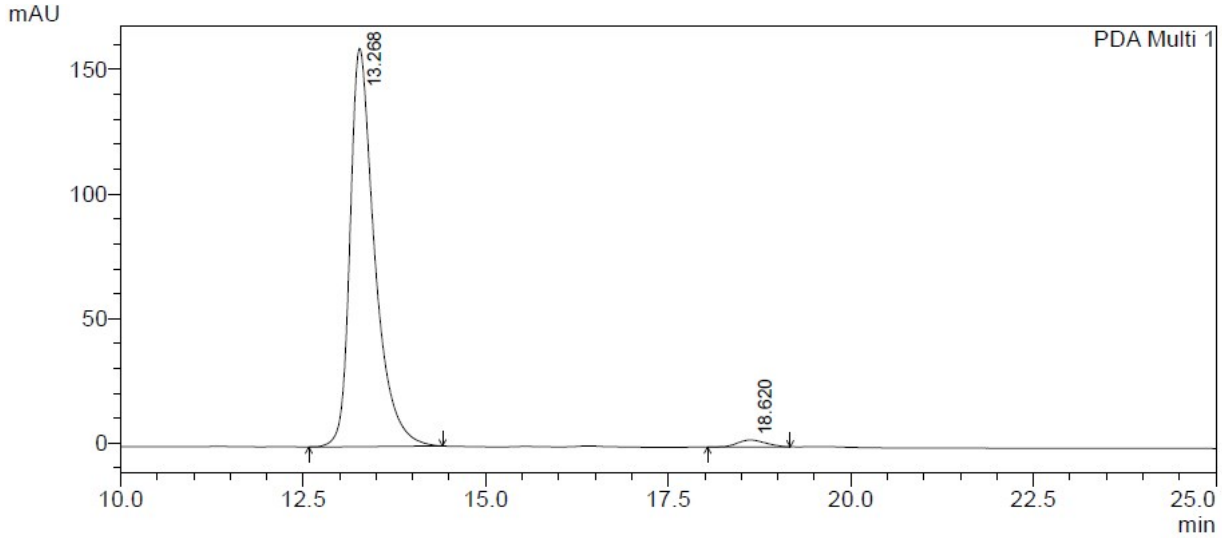

PDA Ch1 254nm 4nm

Peak#	Ret. Time	Area	Height	Area %	Height %
1	13.268	3749538	159847	98.019	98.273
2	18.620	75765	2809	1.981	1.727
Total		3825303	162656	100.000	100.000

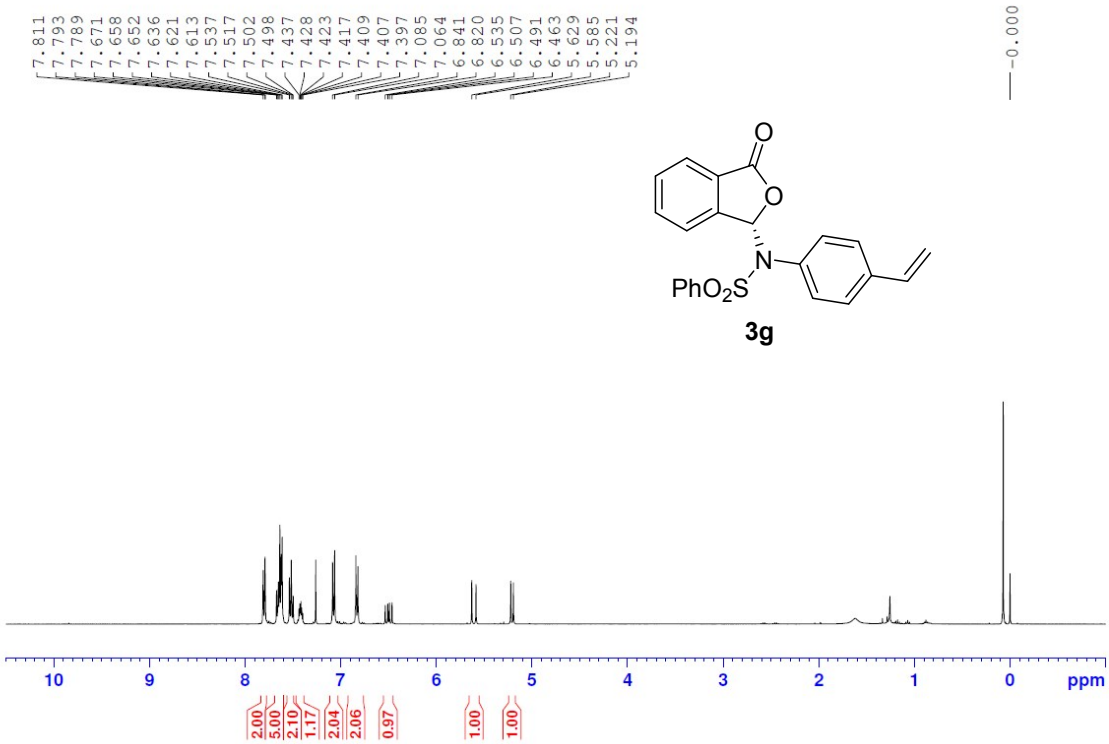
7.811
7.793
7.789
7.671
7.658
7.652
7.636
7.621
7.613
7.537
7.517
7.502
7.498
7.437
7.428
7.423
7.417
7.409
7.407
7.397
7.085
7.064
6.841
6.820
6.535
6.507
6.491
6.463
5.629
5.585
5.221
5.194
0.000
O
O
N
PhO2S
3g
10
9
8
7
6
5
4
3
2
1
0
ppm
2.00
5.00
2.10
1.17
2.04
2.06
0.97
1.00
1.00

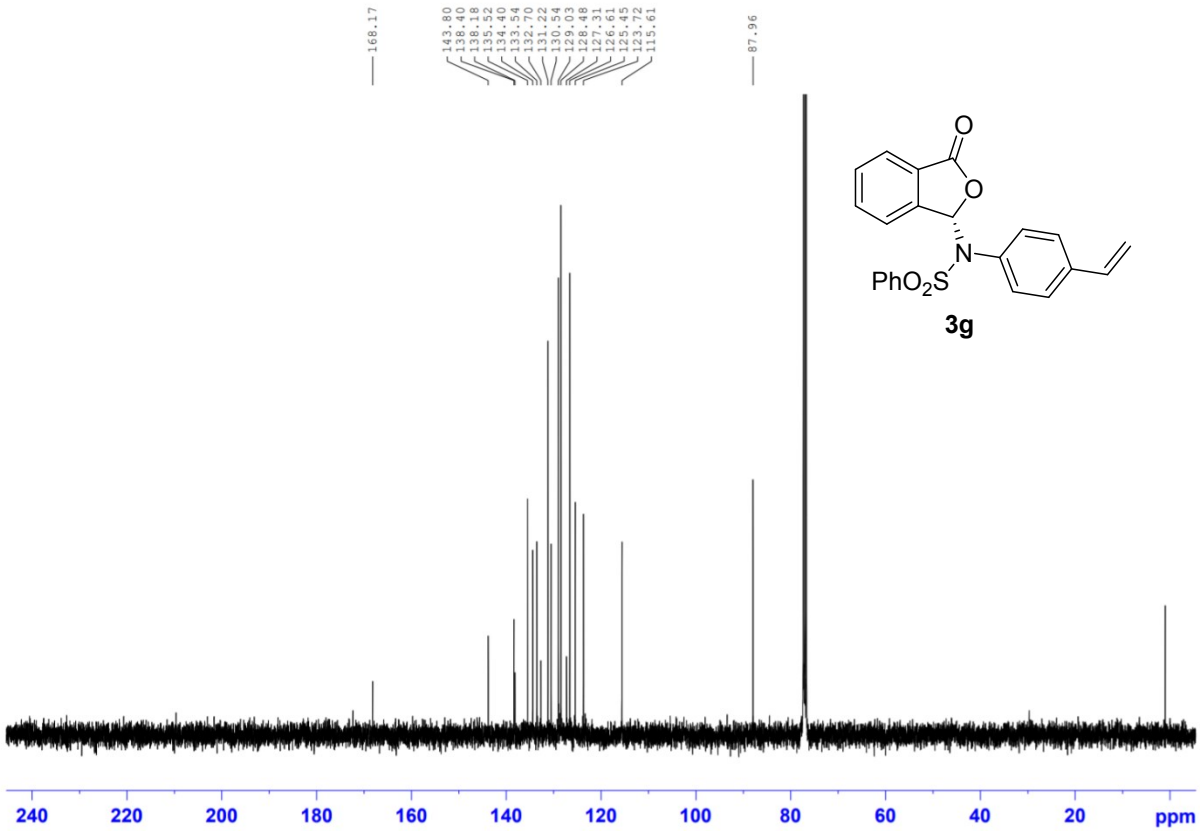
168.17
143.80
138.40
138.18
135.52
134.40
133.54
132.70
131.22
130.54
129.03
128.48
127.31
126.61
125.45
123.72
115.61
87.96
O
O
N
PhO2S
3g
240
220
200
180
160
140
120
100
80
60
40
20
ppm

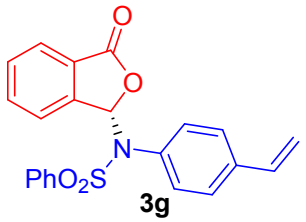

3g

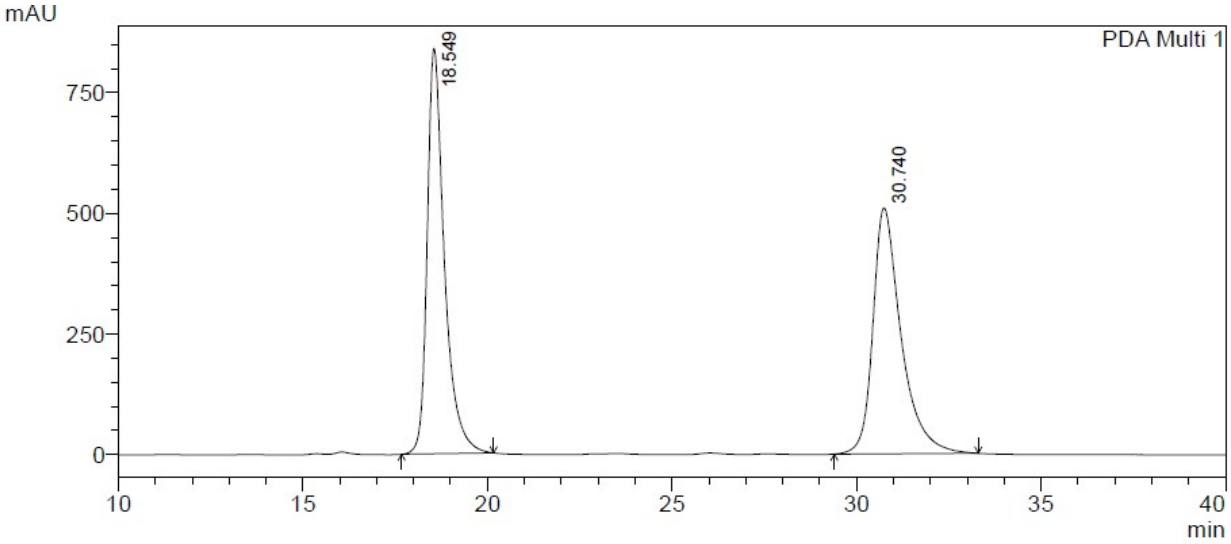

PDA Ch1 254nm 4nm

Peak#	Ret. Time	Area	Height	Area %	Height %
1	18.549	27218384	840070	50.144	62.241
2	30.740	27061806	509638	49.856	37.759
Total		54280190	1349708	100.000	100.000

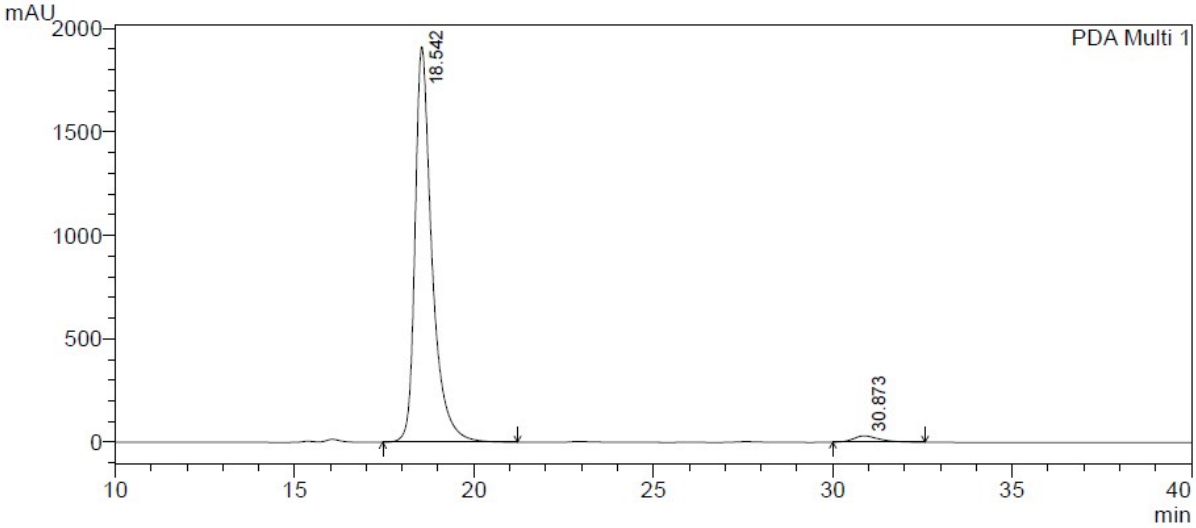

PDA Ch1 254nm 4nm

Peak#	Ret. Time	Area	Height	Area %	Height %
1	18.542	62771907	1912238	97.627	98.438
2	30.873	1525459	30340	2.373	1.562
Total		64297366	1942578	100.000	100.000

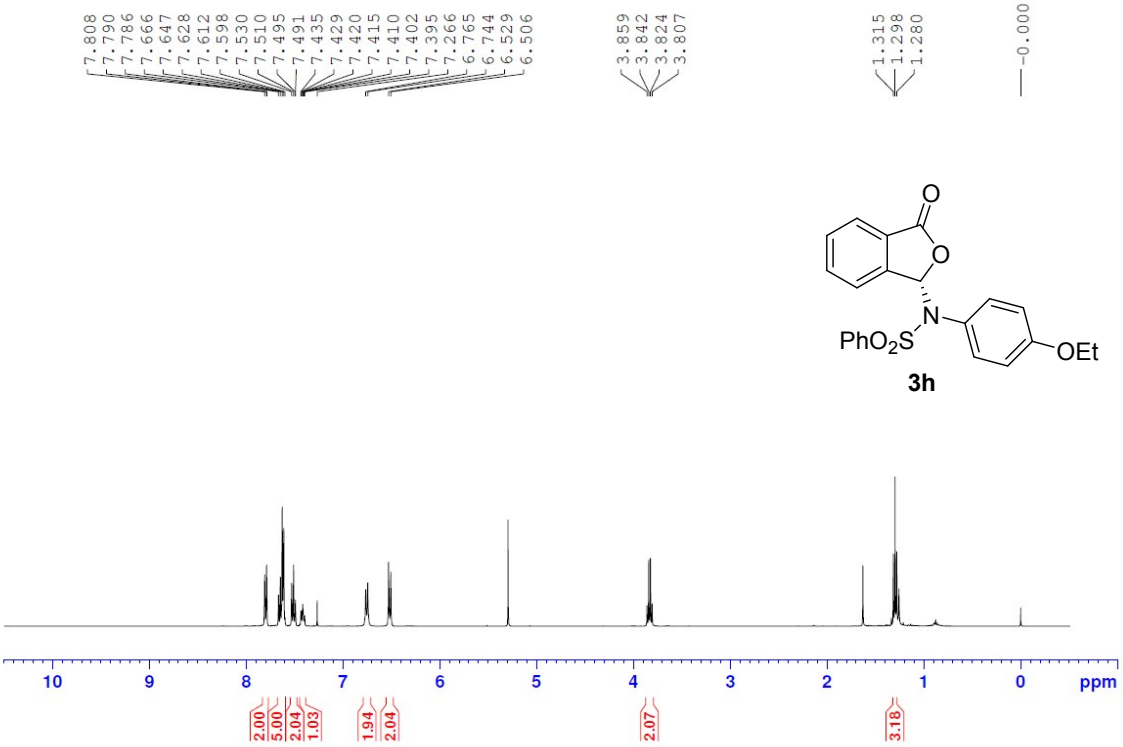
7.808
7.790
7.786
7.666
7.647
7.628
7.612
7.598
7.530
7.510
7.495
7.491
7.435
7.429
7.420
7.415
7.410
7.402
7.395
7.266
6.765
6.744
6.529
6.506
3.859
3.842
3.824
3.807
1.315
1.298
1.280
-0.000
O
O
N
PhO2S
OEt
3h
10
9
8
7
6
5
4
3
2
1
0
ppm
2.00
5.00
2.04
1.03
1.94
2.04
2.07
3.18

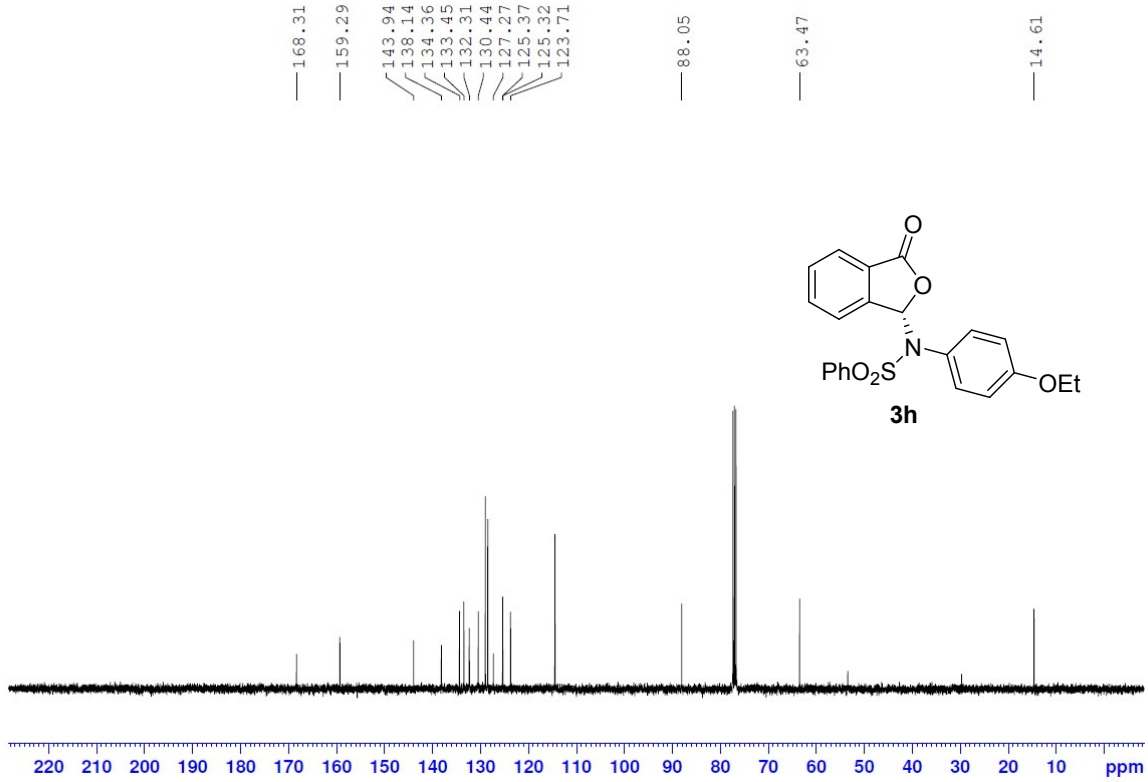
168.31
159.29
143.94
138.14
134.36
133.45
132.31
130.44
127.27
125.37
125.32
123.71
88.05
63.47
14.61
O
O
N
PhO2S
OEt
3h
220
210
200
190
180
170
160
150
140
130
120
110
100
90
80
70
60
50
40
30
20
10
ppm

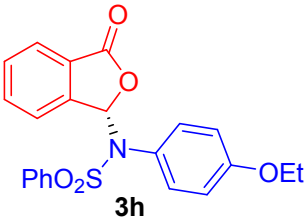

3h

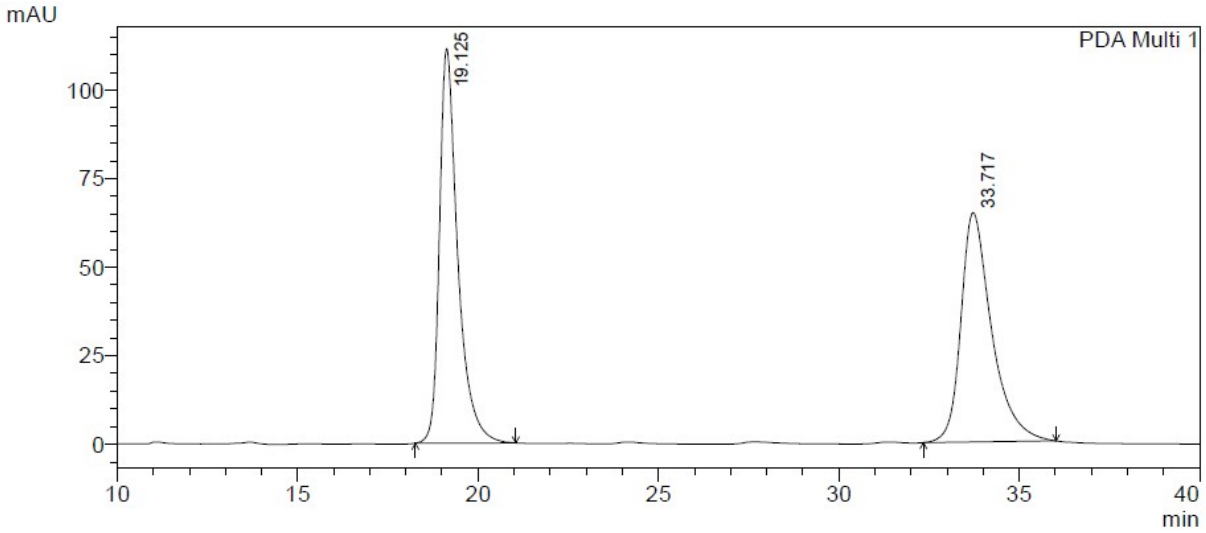

Peak#	Ret. Time	Area	Height	Area %	Height %
1	19.125	3937052	111404	50.609	63.229
2	33.717	3842249	64787	49.391	36.771
Total		7779300	176192	100.000	100.000

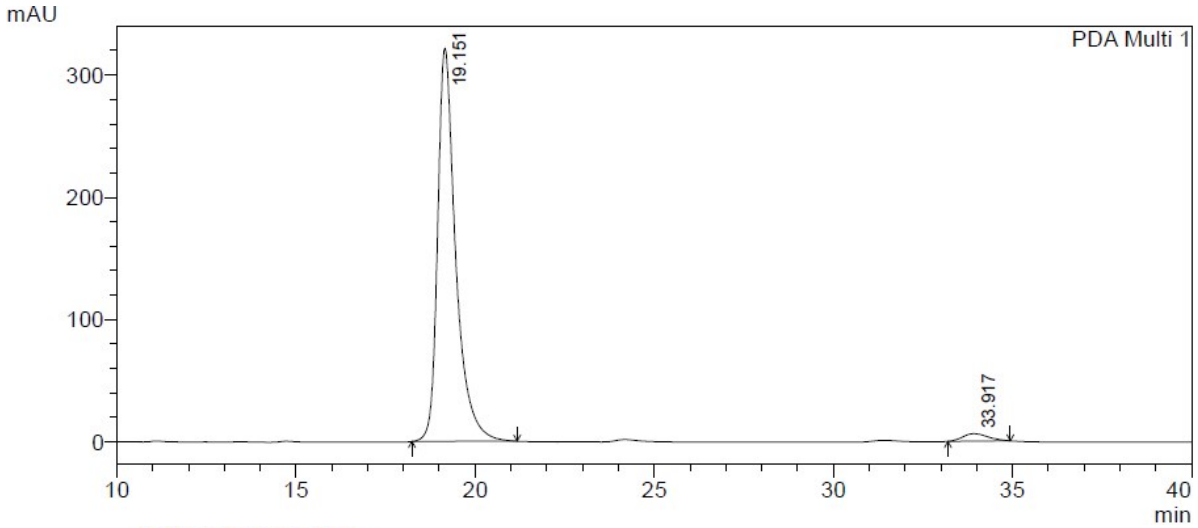

PDA Ch1 254nm 4nm

Peak#	Ret. Time	Area	Height	Area %	Height %
1	19.151	11309325	321760	97.409	98.118
2	33.917	300834	6172	2.591	1.882
Total		11610159	327933	100.000	100.000

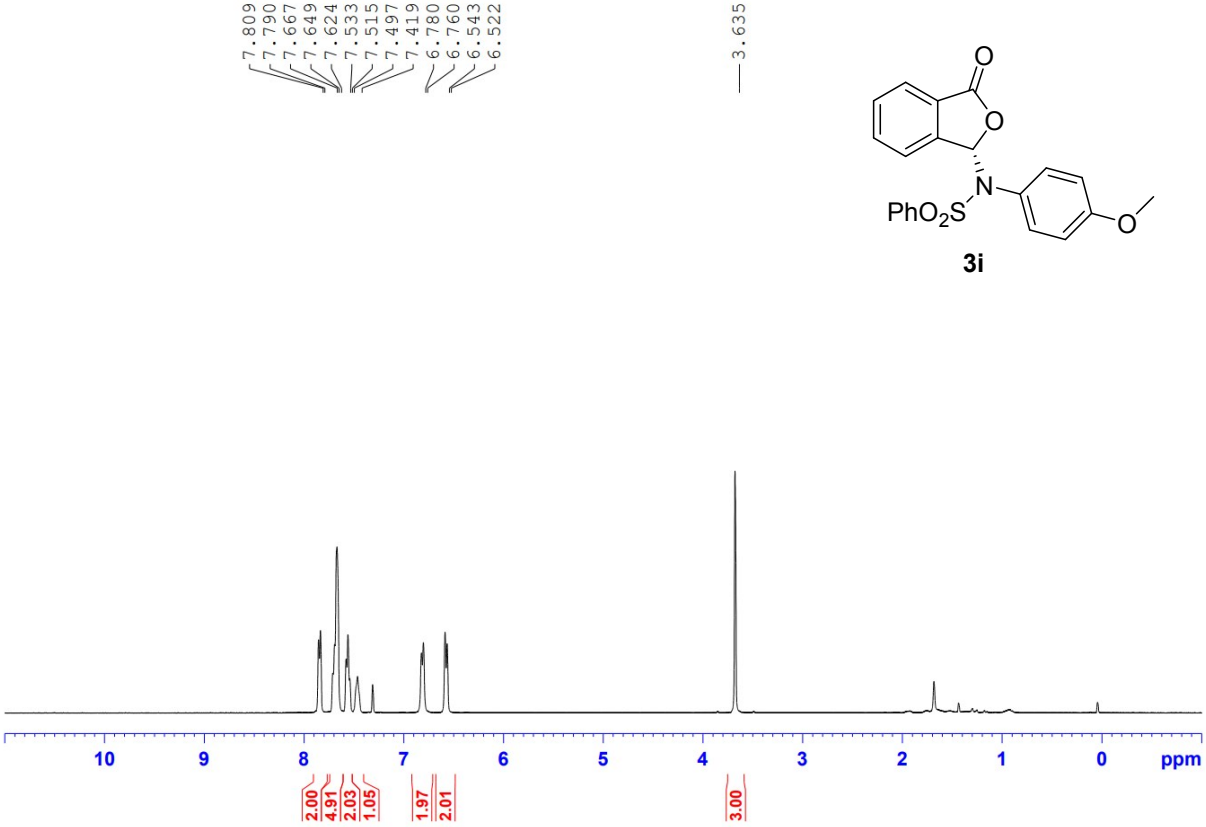
7.809
7.790
7.667
7.649
7.624
7.533
7.515
7.497
7.419
6.780
6.760
6.543
6.522
3.635
O
O
N
PhO2S
O
3i
10
9
8
7
6
5
4
3
2
1
0
ppm
2.00
4.91
2.03
1.05
1.97
2.01
3.00

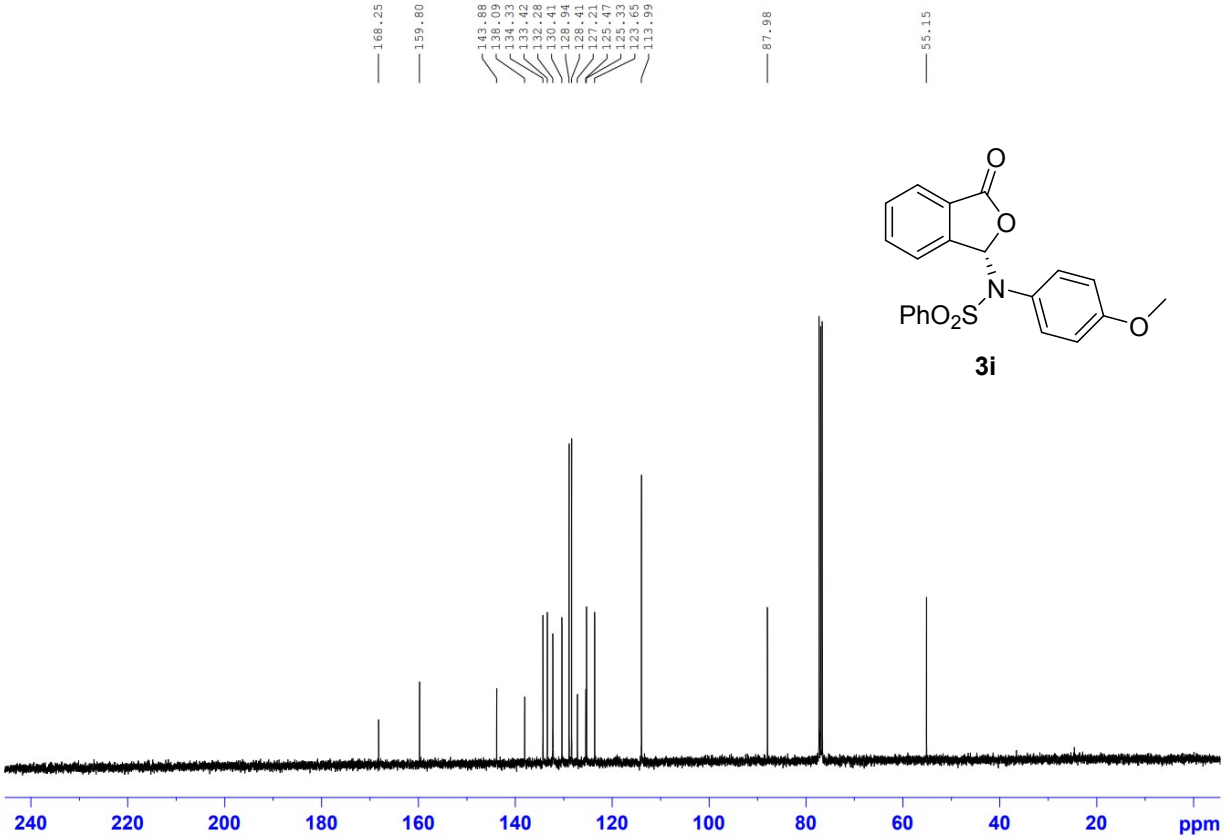
168.25
159.80
143.88
138.09
134.33
133.42
132.28
130.41
128.94
128.41
127.21
125.47
125.33
123.65
113.99
87.98
55.15
O
O
N
PhO2S
O
3i
240
220
200
180
160
140
120
100
80
60
40
20
ppm

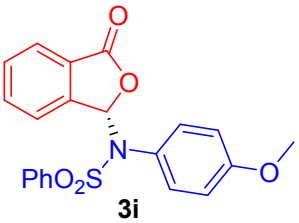

3i

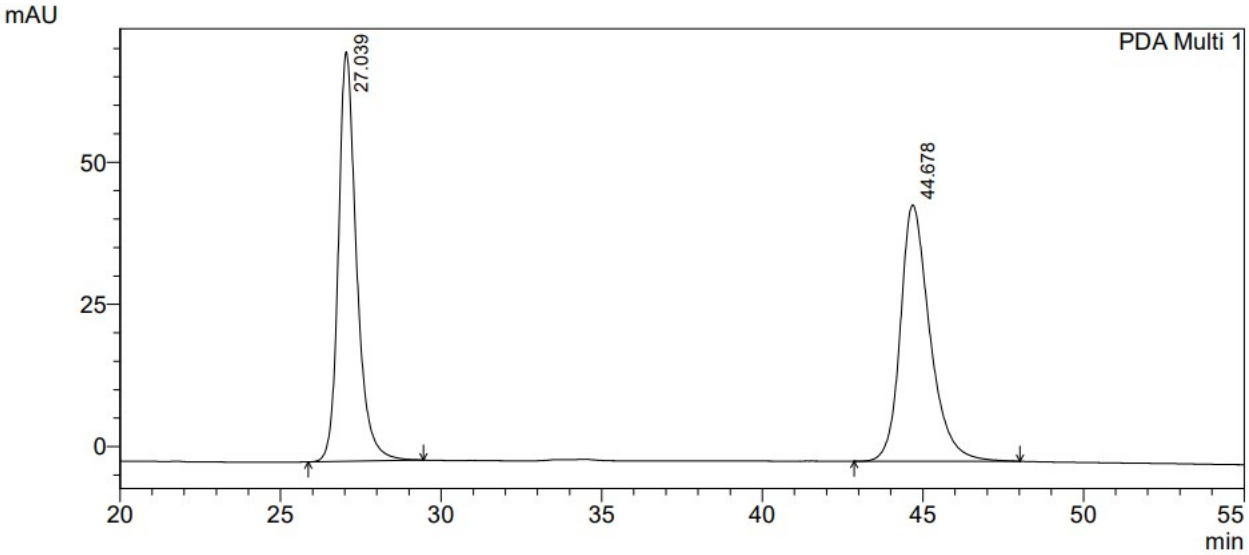

PDA Ch1 254nm 4nm

Peak#	Ret. Time	Area	Height	Area %	Height %
1	27.039	2832166	71997	49.549	61.491
2	44.678	2883686	45088	50.451	38.509
Total		5715851	117086	100.000	100.000

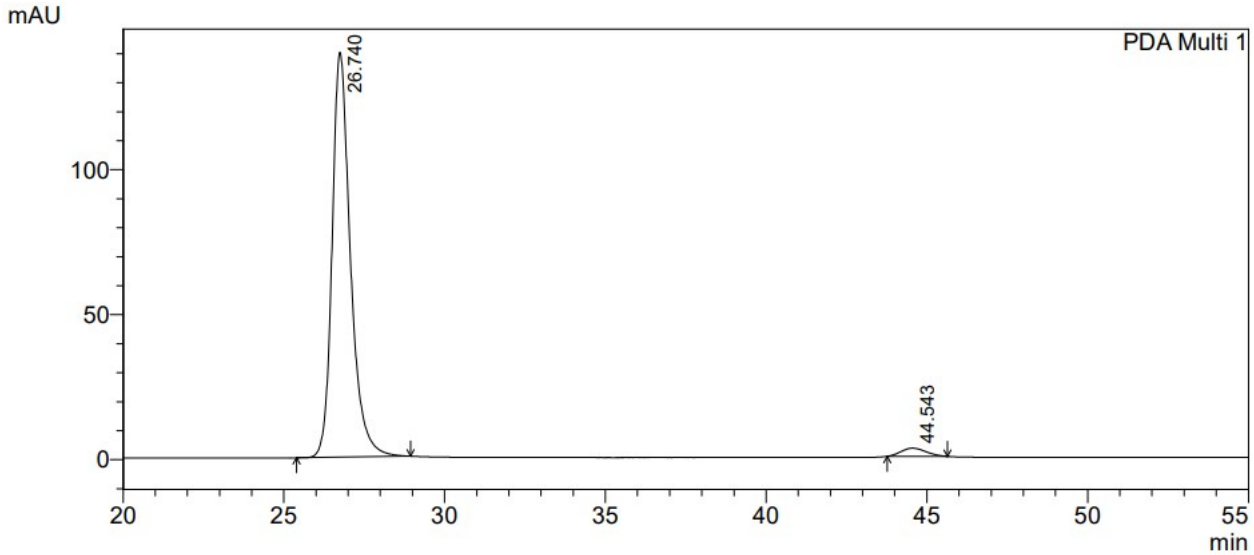

PDA Ch1 254nm 4nm

Peak#	Ret. Time	Area	Height	Area %	Height %
1	26.740	5535074	139672	97.332	98.020
2	44.543	151722	2821	2.668	1.980
Total		5686795	142493	100.000	100.000

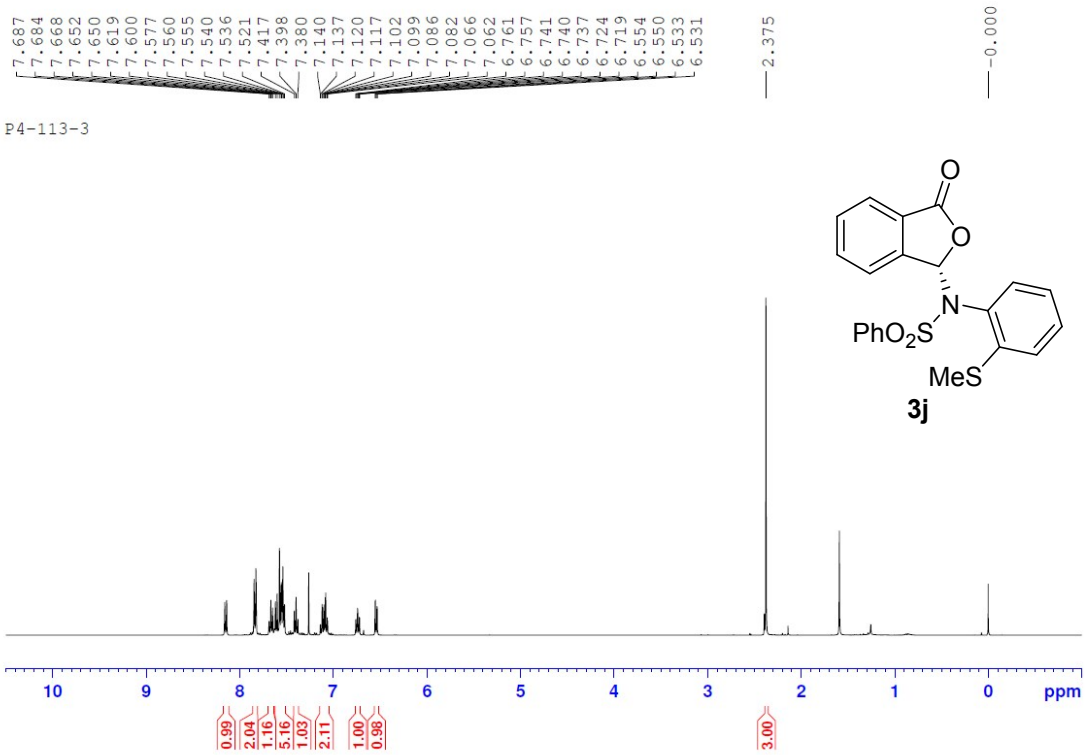
7.687
7.684
7.668
7.652
7.650
7.619
7.600
7.577
7.560
7.555
7.540
7.536
7.521
7.417
7.398
7.380
7.140
7.137
7.120
7.117
7.102
7.099
7.086
7.082
7.066
7.062
6.761
6.757
6.741
6.740
6.737
6.724
6.719
6.554
6.550
6.533
6.531
2.375
-0.000
P4-113-3
O
O
N
PhO2S
MeS
3j
10
9
8
7
6
5
4
3
2
1
0
ppm
0.99
2.04
1.16
5.16
1.03
2.11
1.00
0.98
3.00

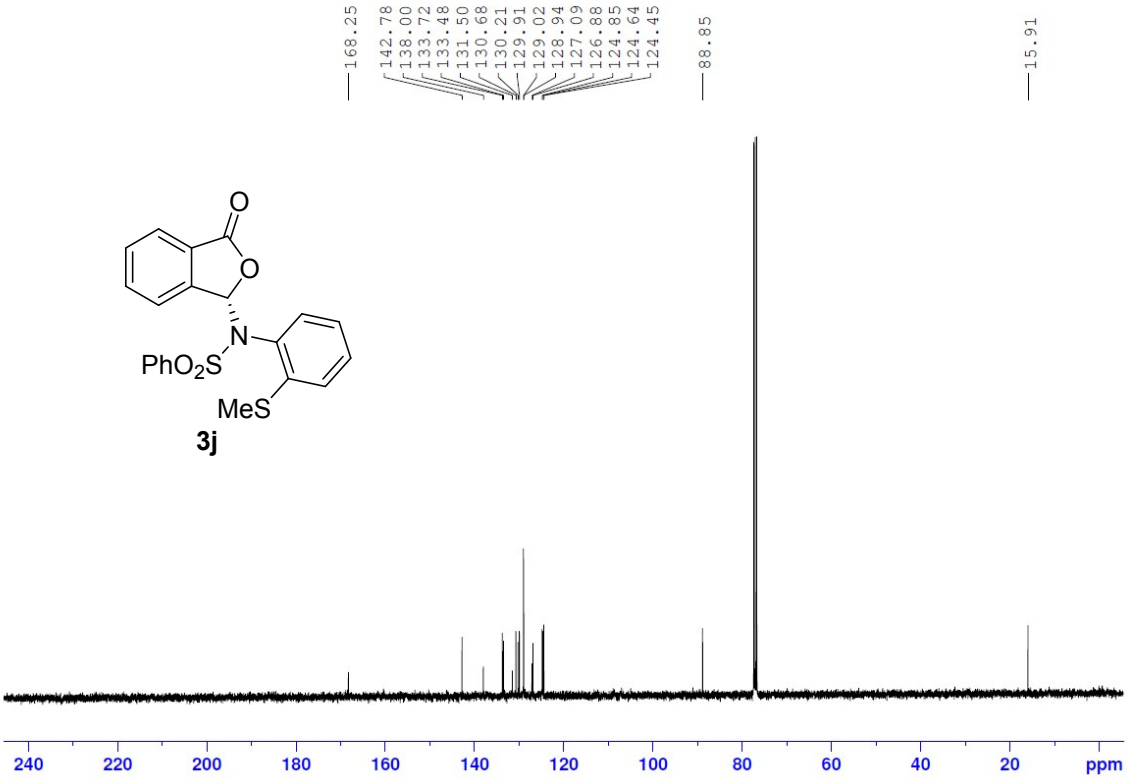
168.25
142.78
138.00
133.72
133.48
131.50
130.68
130.21
129.91
129.02
128.94
127.09
126.88
124.85
124.64
124.45
88.85
15.91
O
O
N
PhO2S
MeS
3j
240
220
200
180
160
140
120
100
80
60
40
20
ppm

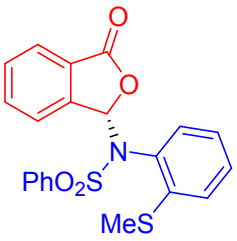

3j

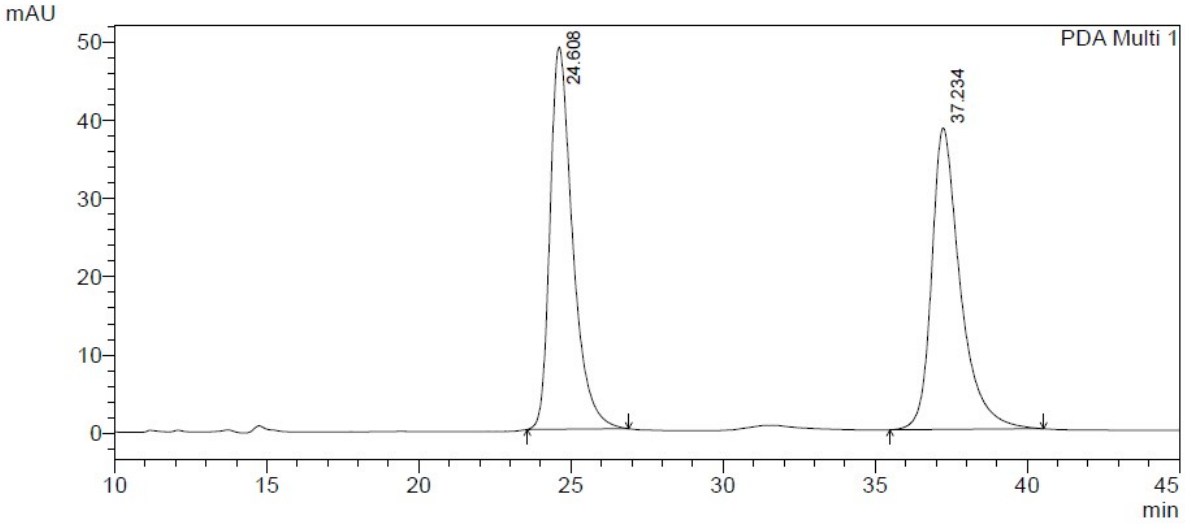

PDA Ch1 254nm 4nm

Peak#	Ret. Time	Area	Height	Area %	Height %
1	24.608	2523680	48785	49.998	55.909
2	37.234	2523847	38474	50.002	44.091
Total		5047528	87259	100.000	100.000

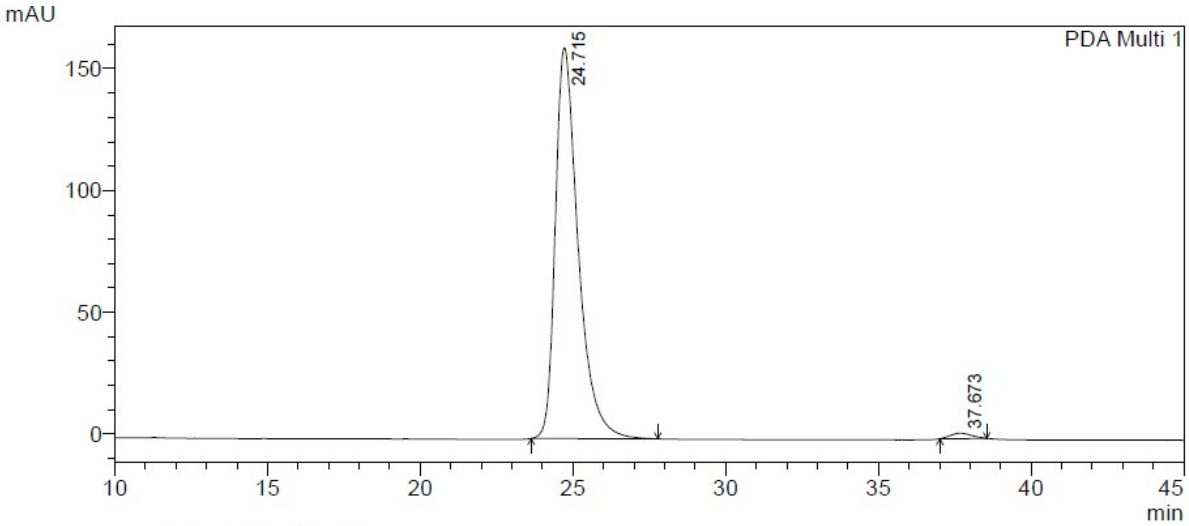

PDA Ch1 254nm 4nm

Peak#	Ret. Time	Area	Height	Area %	Height %
1	24.715	8352372	160455	98.756	98.667
2	37.673	105192	2168	1.244	1.333
Total		8457564	162623	100.000	100.000

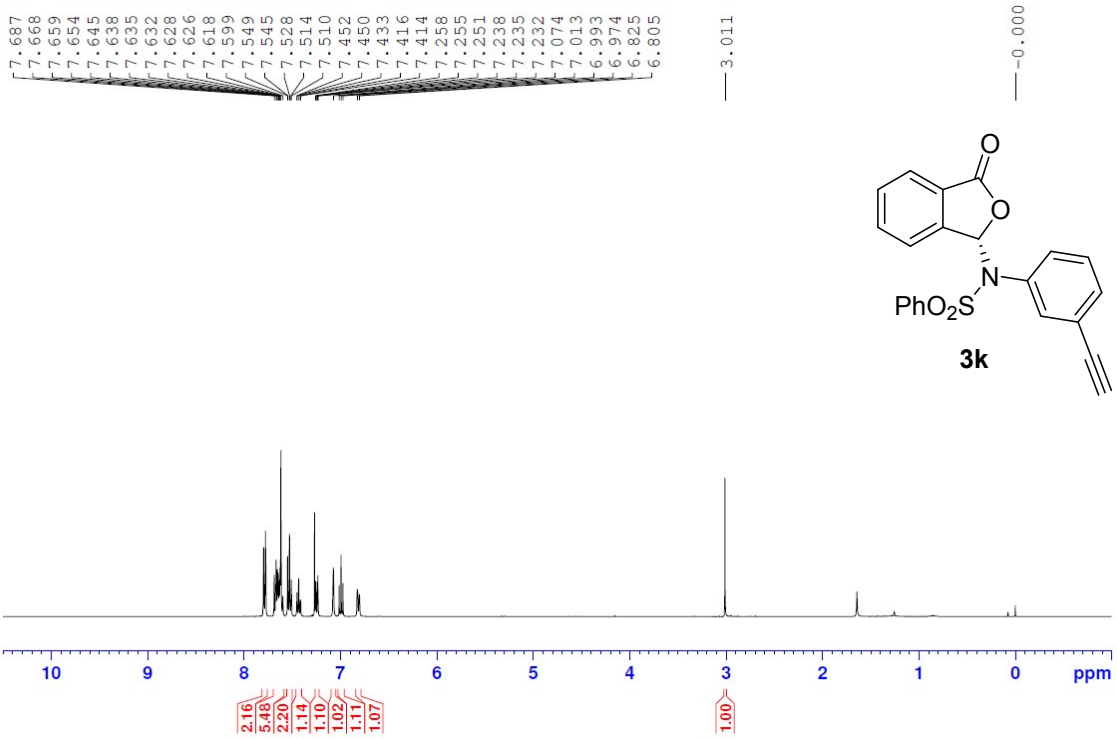
7.687
7.668
7.659
7.654
7.645
7.638
7.635
7.632
7.628
7.626
7.618
7.599
7.549
7.545
7.528
7.514
7.510
7.452
7.450
7.433
7.416
7.414
7.258
7.255
7.251
7.238
7.235
7.232
7.074
7.013
6.993
6.974
6.825
6.805
3.011
0.000
O
O
N
PhO2S
3k
10
9
8
7
6
5
4
3
2
1
0
ppm
2.16
5.48
2.20
1.14
1.10
1.02
1.11
1.07
1.00

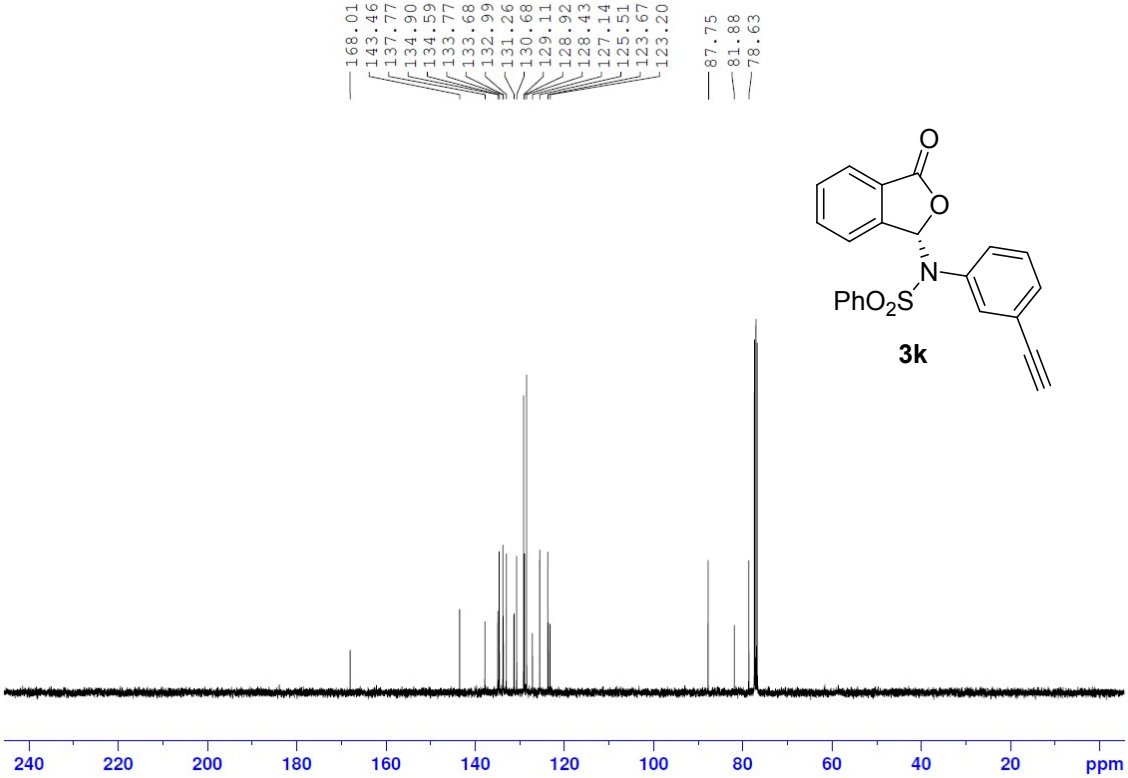
168.01
143.46
137.77
134.90
134.59
133.77
133.68
132.99
131.26
130.68
129.11
128.92
128.43
127.14
125.51
123.67
123.20
87.75
81.88
78.63
O
O
N
PhO2S
3k
240
220
200
180
160
140
120
100
80
60
40
20
ppm

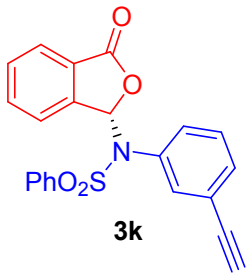

3k

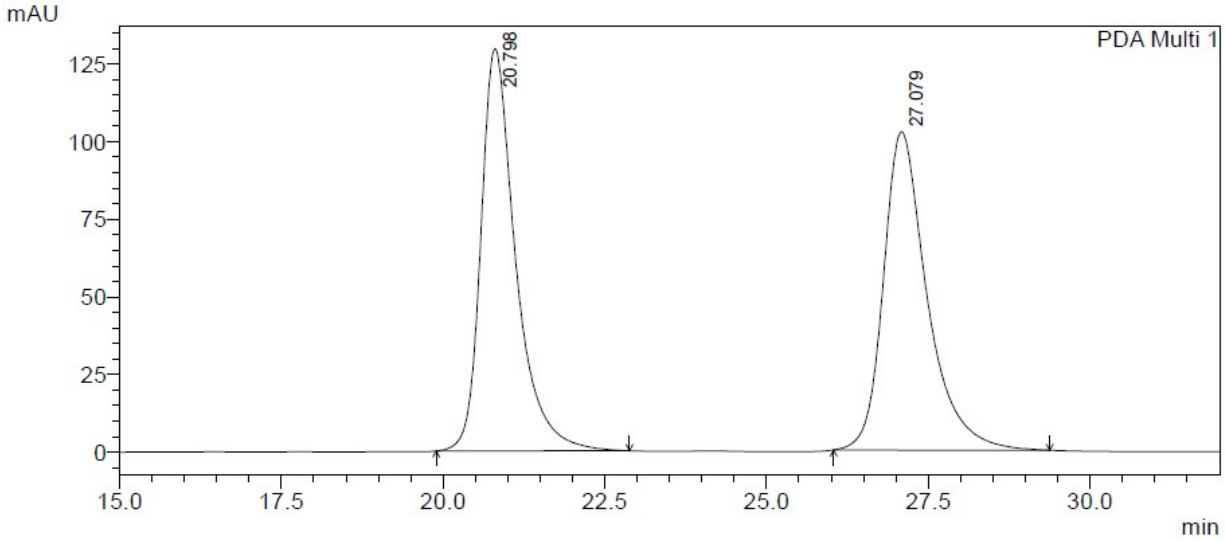

PDA Ch1 254nm 4nm

Peak#	Ret. Time	Area	Height	Area %	Height %
1	20.798	4842608	129561	50.079	55.826
2	27.079	4827310	102519	49.921	44.174
Total		9669918	232080	100.000	100.000

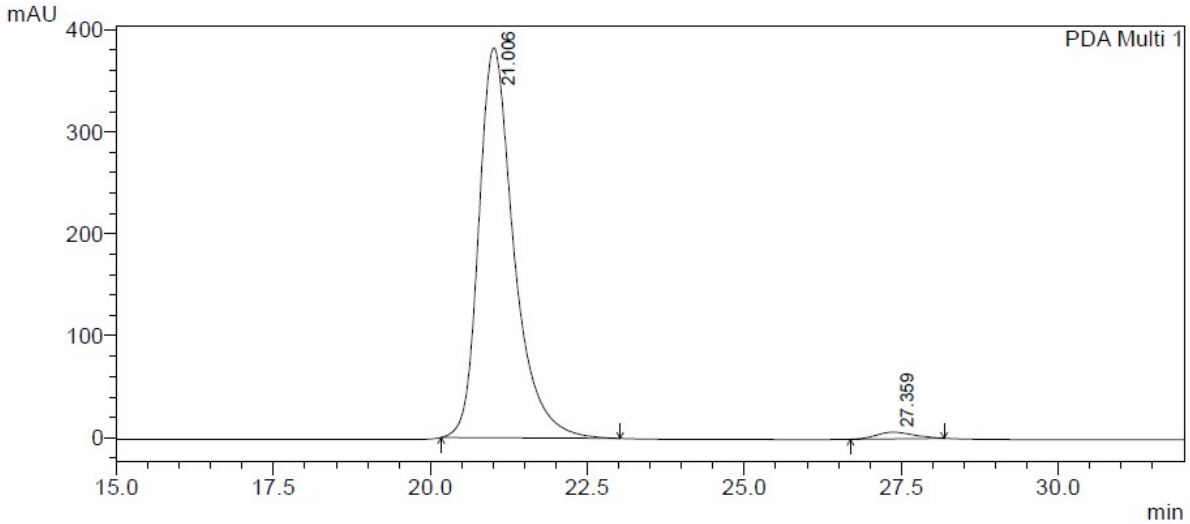

PDA Ch1 254nm 4nm

Peak#	Ret. Time	Area	Height	Area %	Height %
1	21.006	14878091	382323	98.256	98.362
2	27.359	264110	6368	1.744	1.638
Total		15142201	388690	100.000	100.000

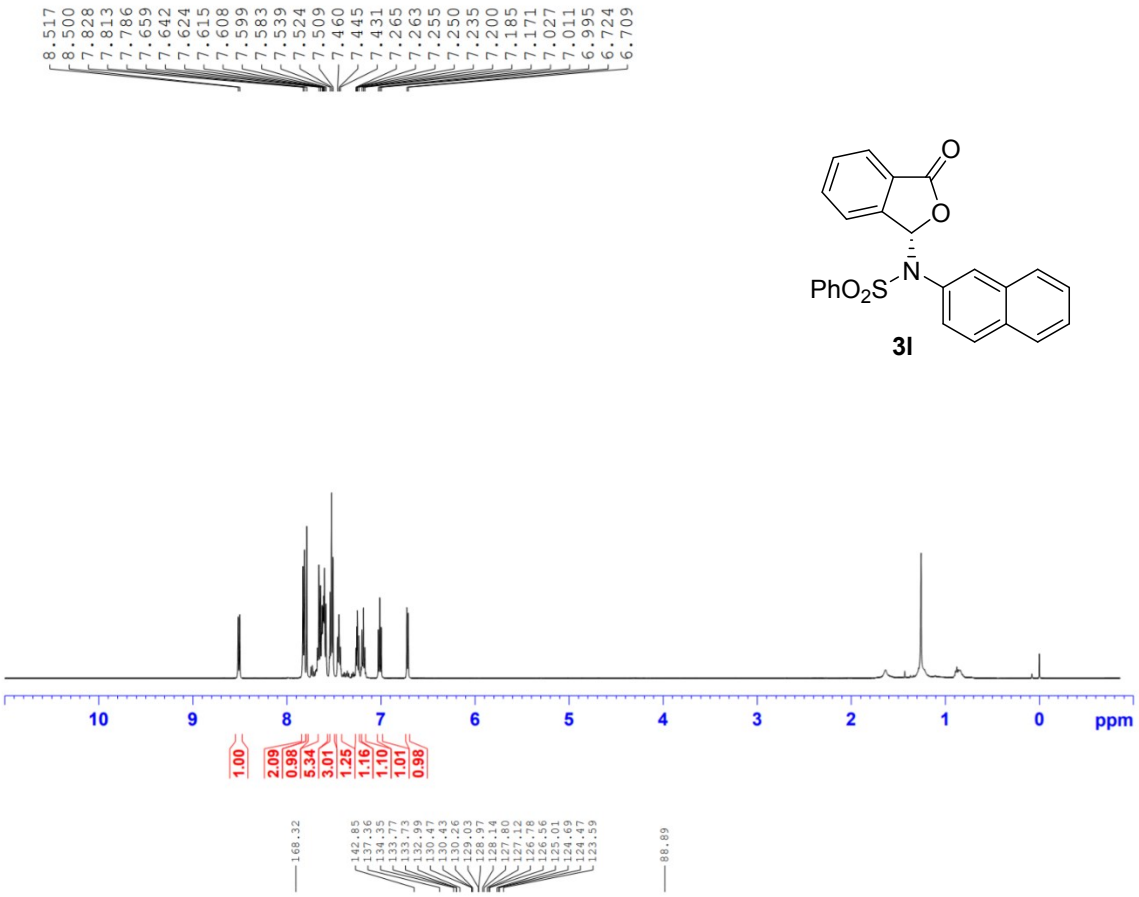
8.517
8.500
7.828
7.813
7.786
7.659
7.642
7.624
7.615
7.608
7.599
7.583
7.539
7.524
7.509
7.460
7.445
7.431
7.265
7.263
7.255
7.250
7.235
7.200
7.185
7.171
7.027
7.011
6.995
6.724
6.709
O
O
N
PhO2S
3l
10 9 8 7 6 5 4 3 2 1 0 ppm
1.00
2.09
0.98
5.34
3.01
1.25
1.16
1.10
1.01
0.98

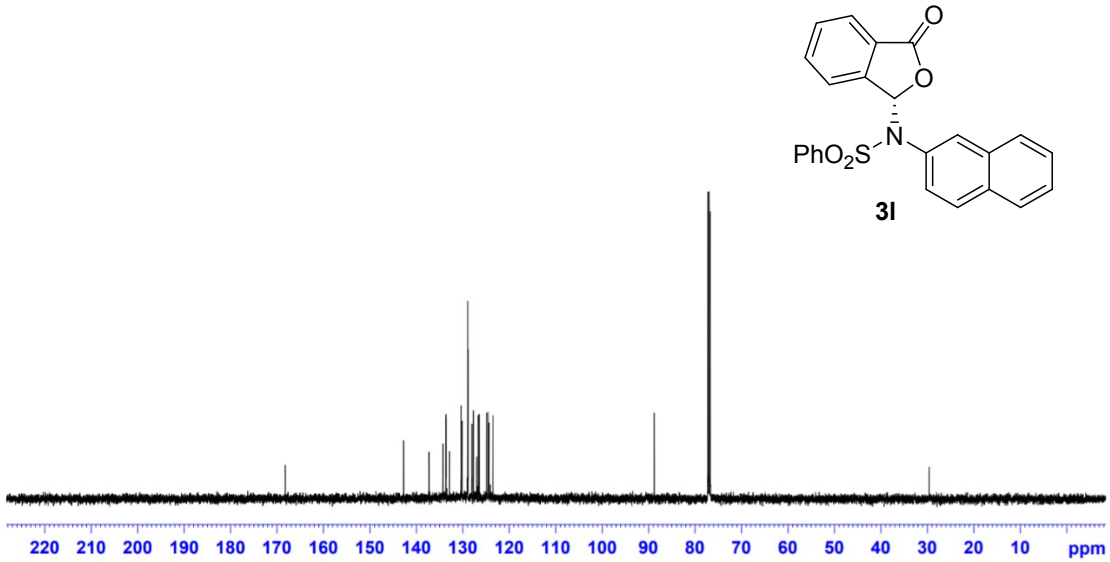
168.32
142.85
137.36
134.35
133.77
133.73
132.99
130.47
130.43
130.26
129.03
128.97
128.14
127.80
127.12
126.78
126.56
125.01
124.69
124.47
123.59
88.89
O
O
N
PhO2S
3l
220 210 200 190 180 170 160 150 140 130 120 110 100 90 80 70 60 50 40 30 20 10 ppm

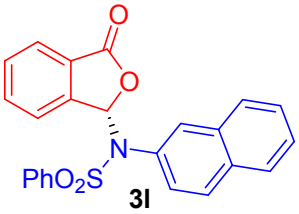

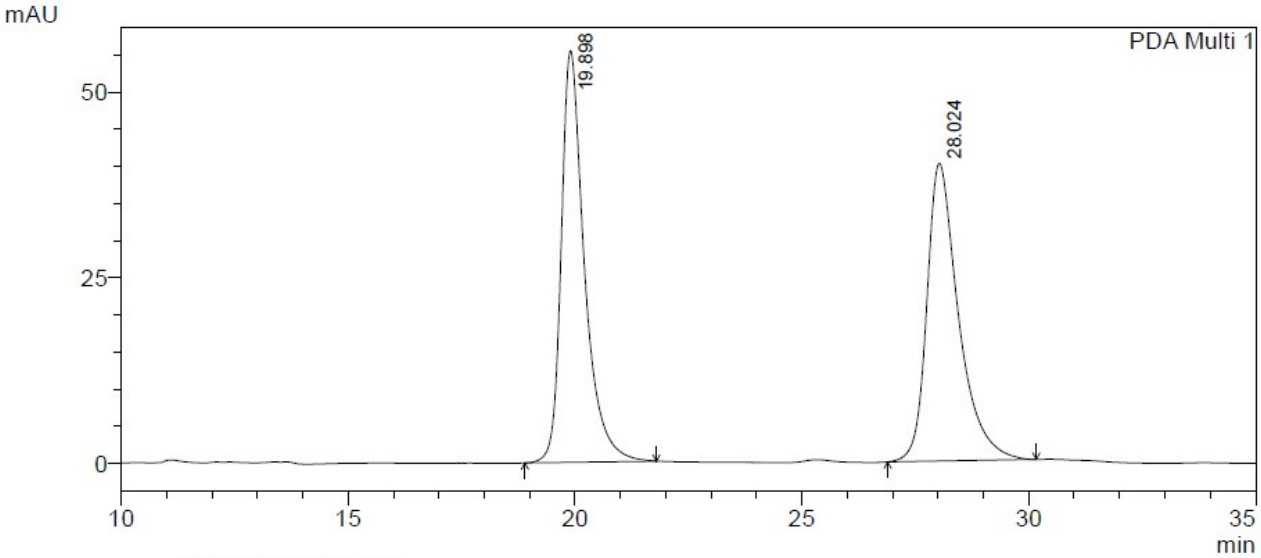

PDA Ch1 254nm 4nm

Peak#	Ret. Time	Area	Height	Area %	Height %
1	19.898	1963034	55402	50.272	58.047
2	28.024	1941758	40041	49.728	41.953
Total		3904792	95442	100.000	100.000

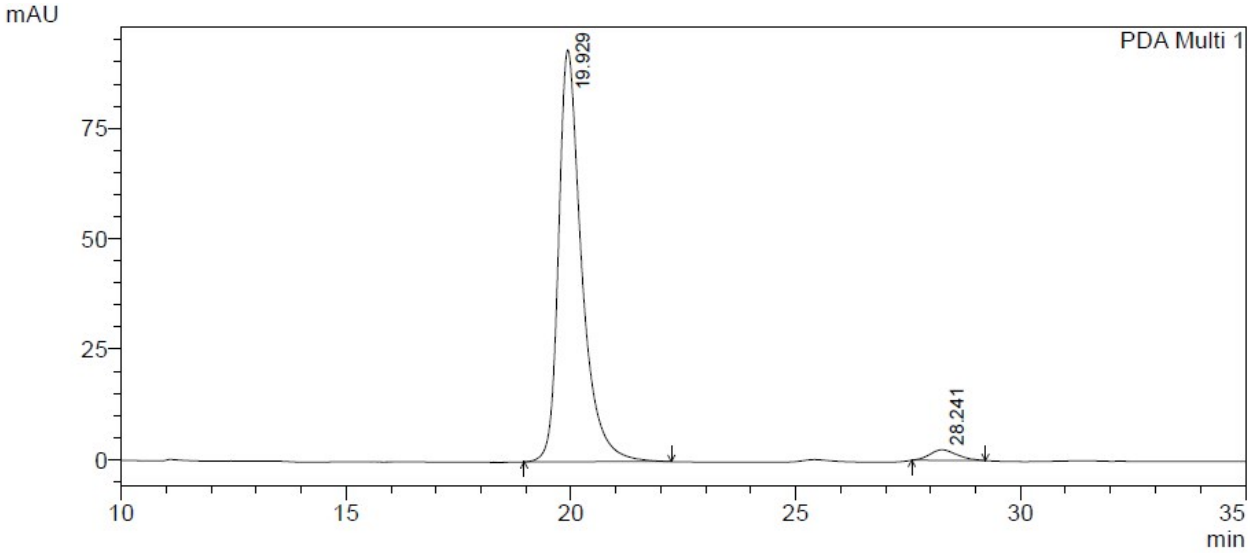

Peak#	Ret. Time	Area	Height	Area %	Height %
1	19.929	3334564	93211	97.023	97.504
2	28.241	102311	2386	2.977	2.496
Total		3436875	95597	100.000	100.000

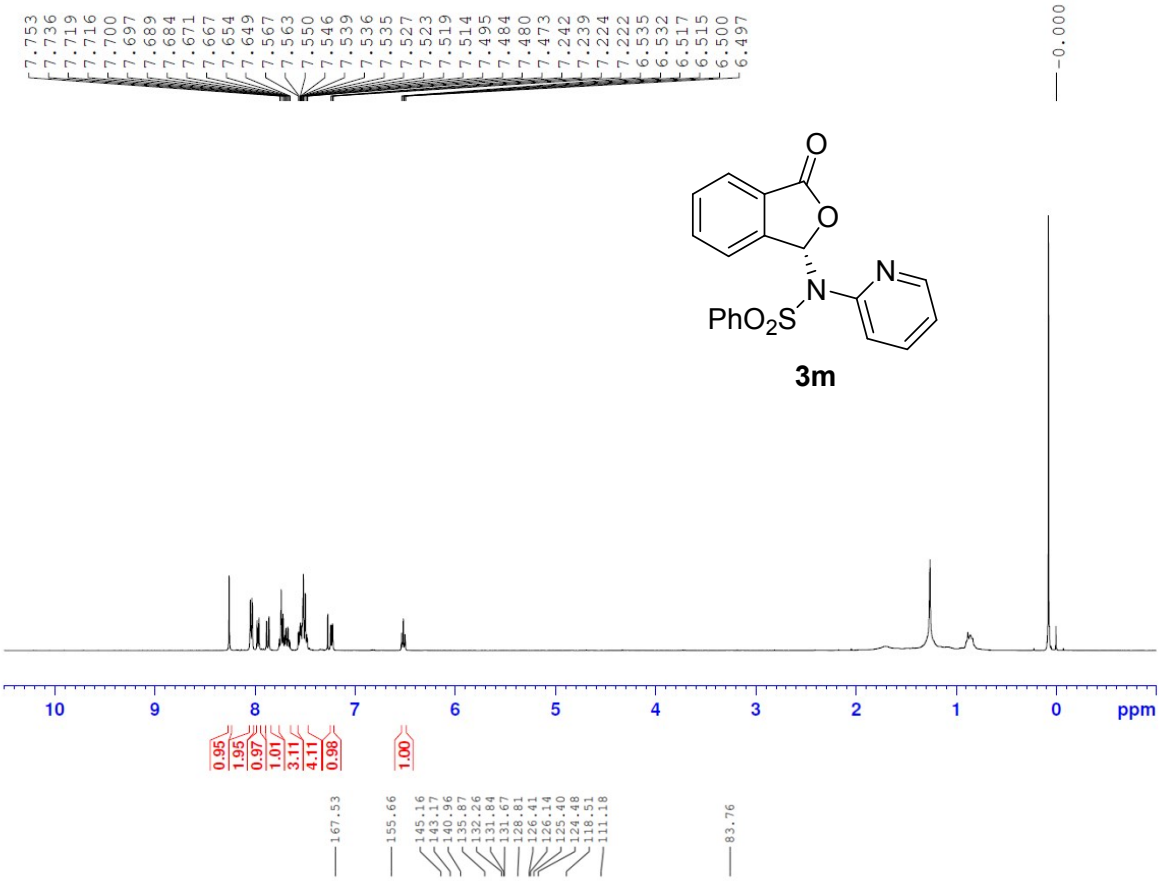
7.753
7.736
7.719
7.716
7.700
7.697
7.689
7.684
7.671
7.667
7.654
7.649
7.567
7.563
7.550
7.546
7.539
7.536
7.535
7.527
7.523
7.519
7.514
7.495
7.484
7.480
7.473
7.242
7.239
7.224
7.222
6.535
6.532
6.517
6.515
6.500
6.497
0.000
O
O
N
N
PhO2S
3m
10
9
8
7
6
5
4
3
2
1
0
ppm
0.95
1.95
0.97
1.01
3.11
4.11
0.98
1.00

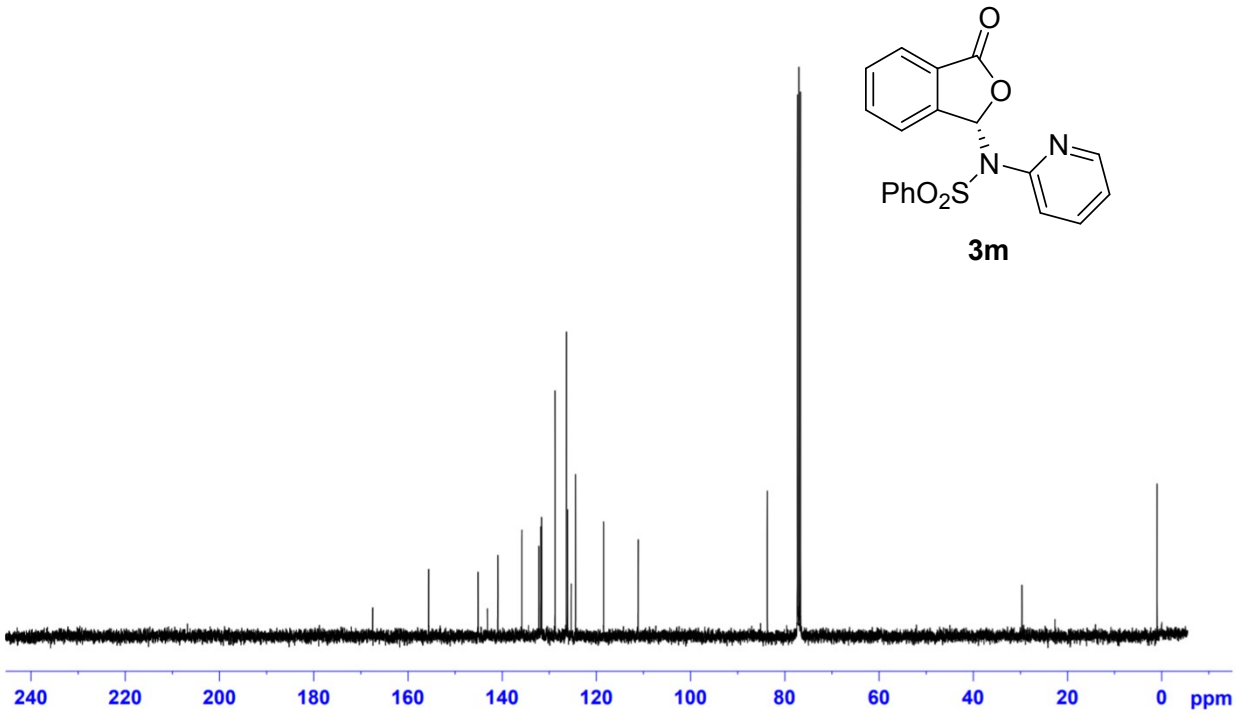
167.53
155.66
145.16
143.17
140.96
135.87
132.26
131.84
131.67
128.81
126.41
126.14
125.40
124.48
118.51
111.18
83.76
O
O
N
N
PhO2S
3m
240
220
200
180
160
140
120
100
80
60
40
20
0
ppm

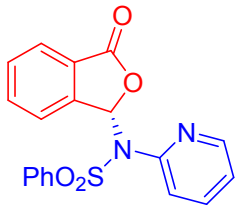

3m

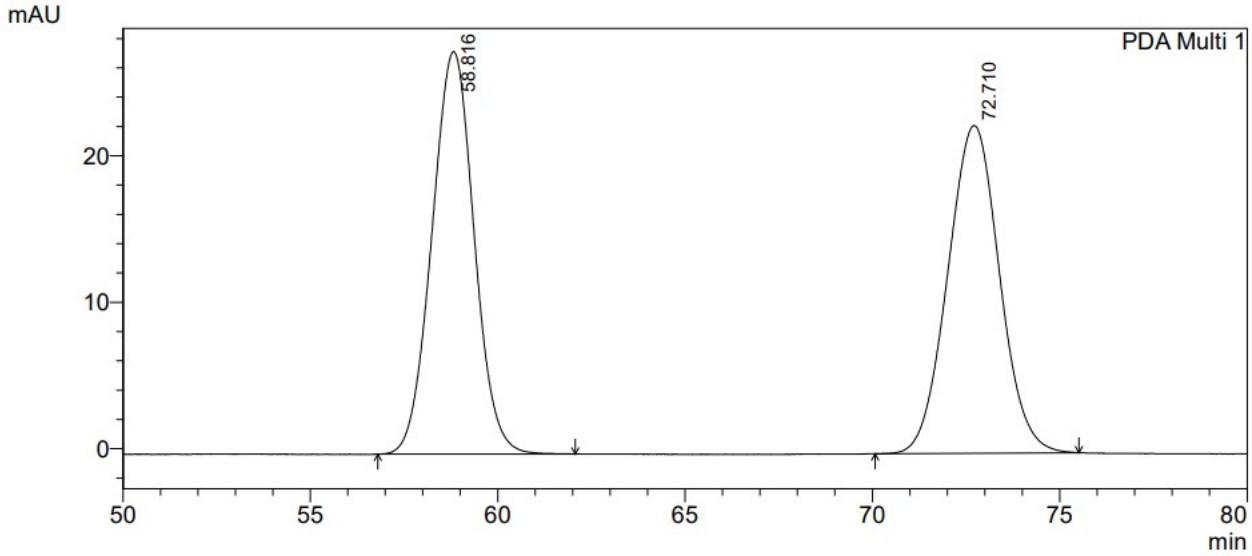

Peak#	Ret. Time	Area	Height	Area %	Height %
1	58.816	2152945	27477	50.066	55.113
2	72.710	2147232	22379	49.934	44.887
Total		4300177	49856	100.000	100.000

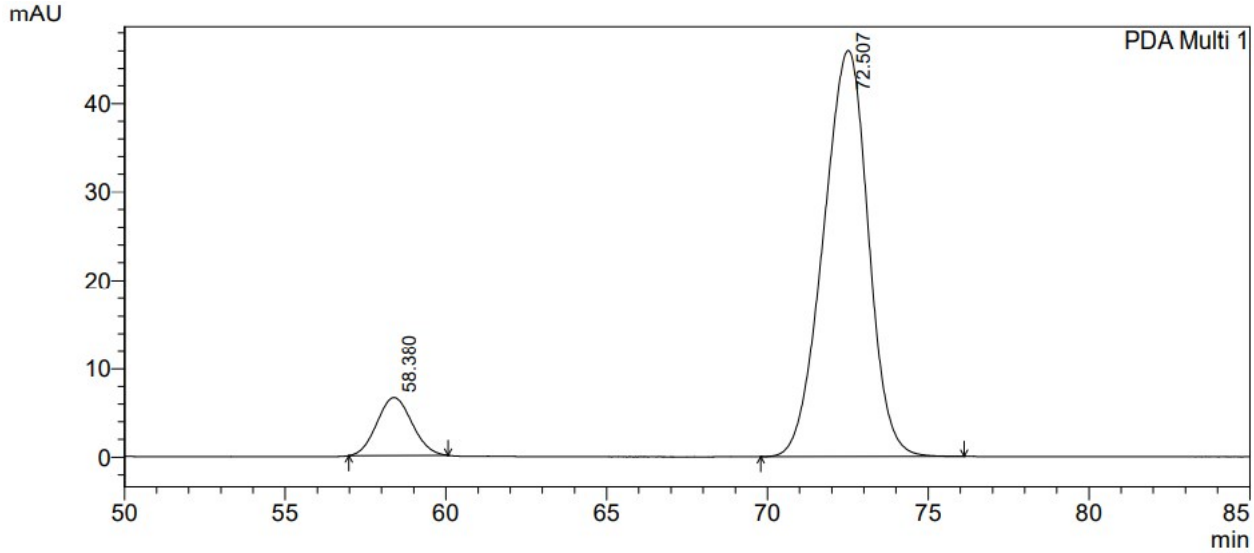

PDA Ch1 254nm 4nm

Peak#	Ret. Time	Area	Height	Area %	Height %
1	58.380	498557	6561	10.037	12.481
2	72.507	4468726	46004	89.963	87.519
Total		4967282	52565	100.000	100.000

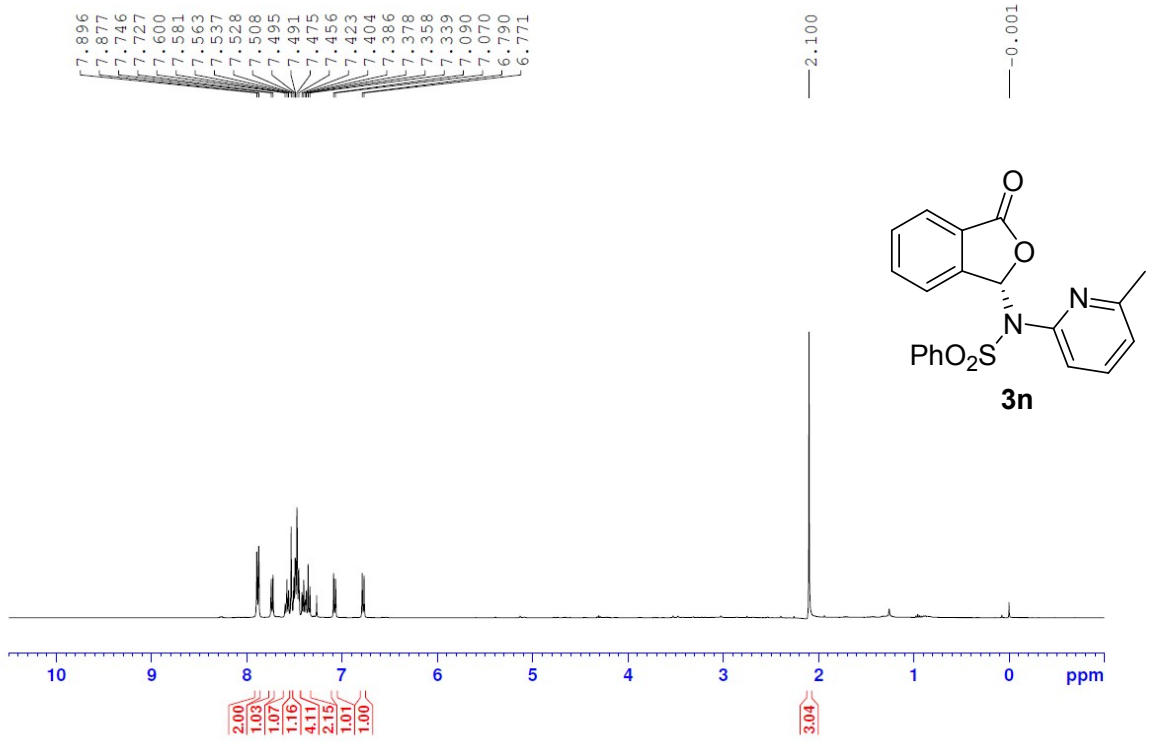
7.896
7.877
7.746
7.727
7.600
7.581
7.563
7.537
7.528
7.508
7.495
7.491
7.475
7.456
7.423
7.404
7.386
7.378
7.358
7.339
7.090
7.070
6.790
6.771
2.100
0.001
O
O
N
N
PhO2S
3n
10
9
8
7
6
5
4
3
2
1
0
ppm
2.00
1.03
1.07
1.16
4.11
2.15
1.01
1.00
3.04

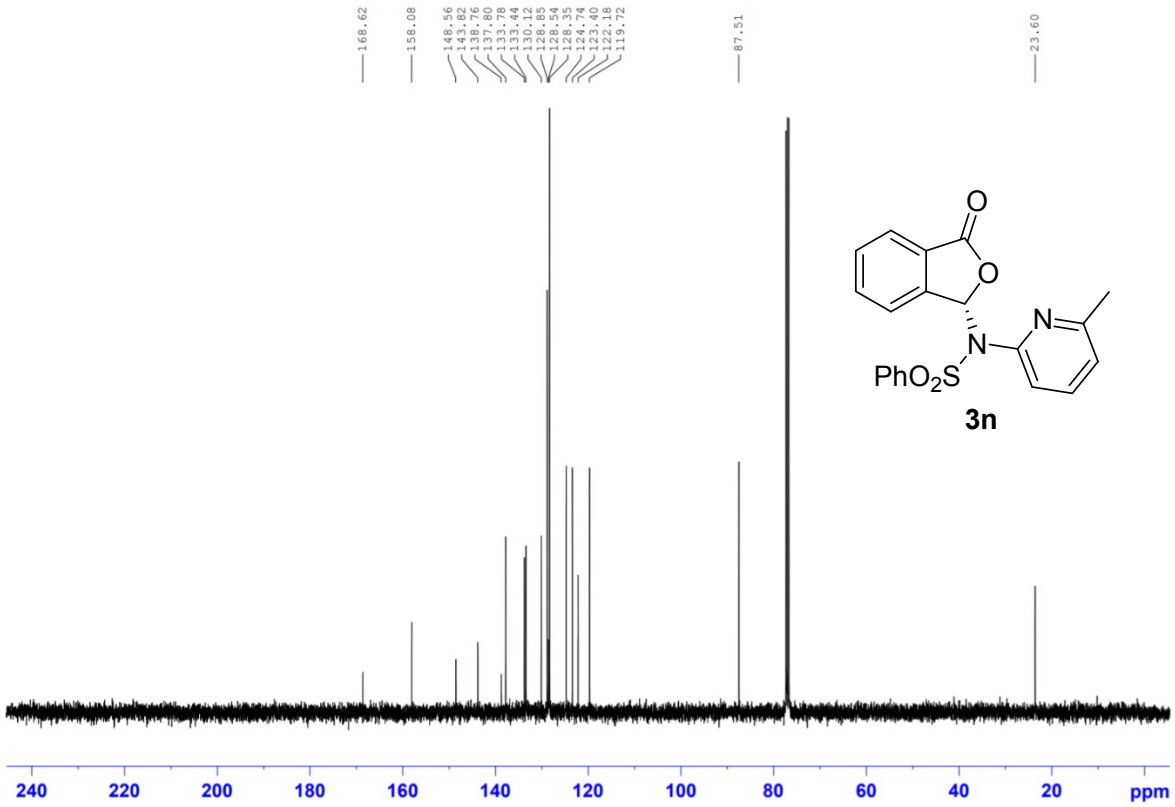
168.62
158.08
148.56
143.82
138.76
137.80
133.78
133.44
130.12
128.85
128.54
128.35
124.74
123.40
122.18
119.72
87.51
23.60
O
O
N
N
PhO2S
3n
240
220
200
180
160
140
120
100
80
60
40
20
ppm

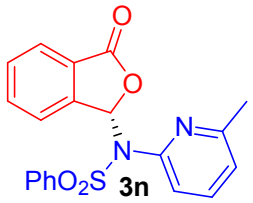

3n

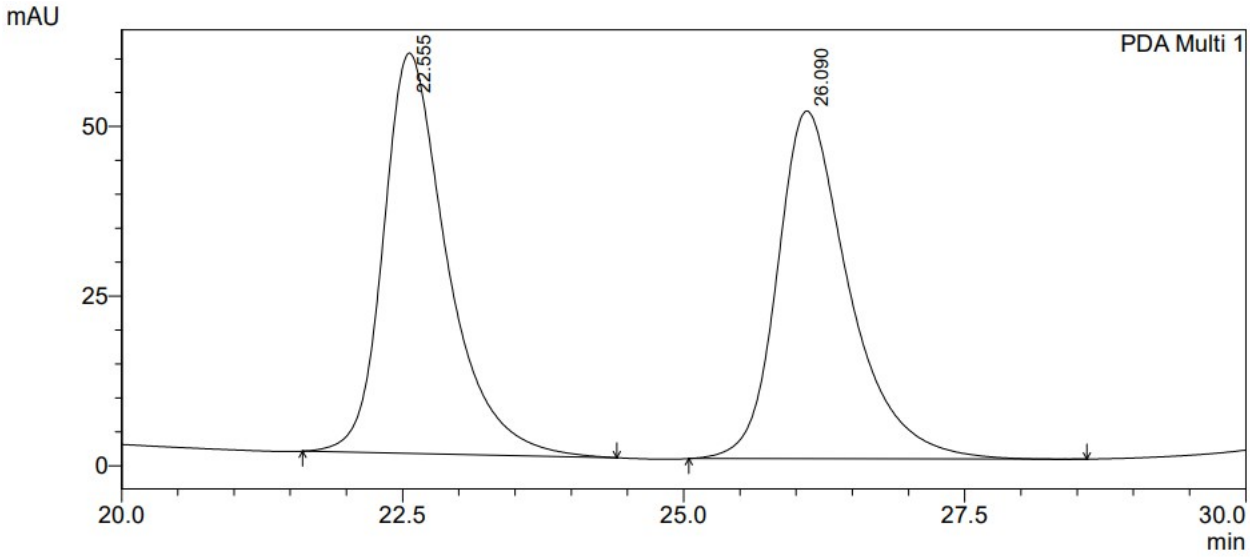

PDA Ch1 254nm 4nm

Peak#	Ret. Time	Area	Height	Area %	Height %
1	22.555	2337306	59056	50.550	53.552
2	26.090	2286408	51221	49.450	46.448
Total		4623713	110277	100.000	100.000

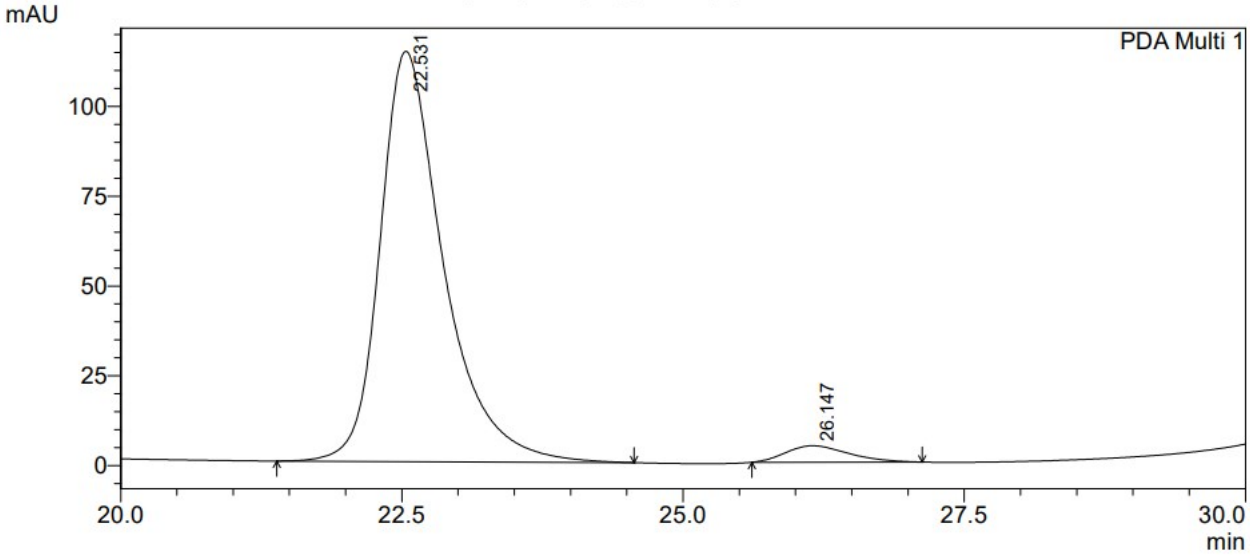

PDA Ch1 254nm 4nm

Peak#	Ret. Time	Area	Height	Area %	Height %
1	22.531	4495164	114192	96.200	96.136
2	26.147	177541	4589	3.800	3.864
Total		4672705	118782	100.000	100.000

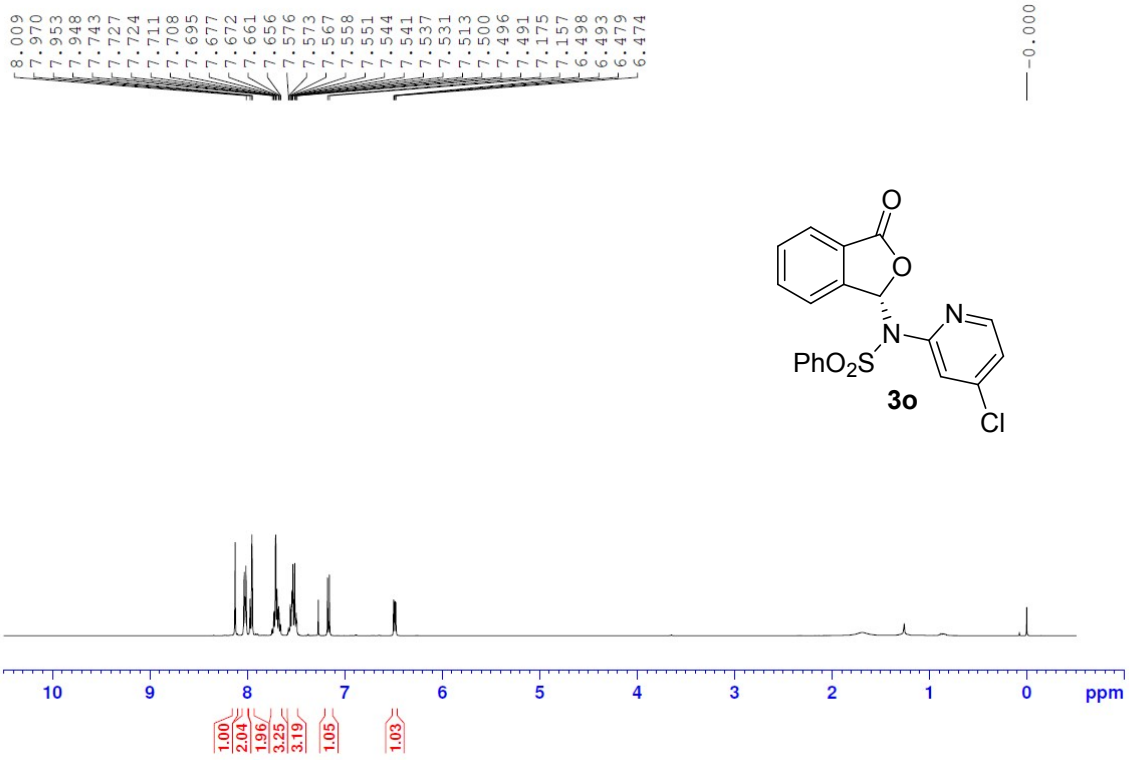
8.009
7.970
7.953
7.948
7.743
7.727
7.724
7.711
7.708
7.695
7.677
7.672
7.661
7.656
7.576
7.573
7.567
7.558
7.551
7.544
7.541
7.537
7.531
7.513
7.500
7.496
7.491
7.175
7.157
6.498
6.493
6.479
6.474
0.000
O
O
N
N
PhO2S
3o
Cl
10
9
8
7
6
5
4
3
2
1
0
ppm
1.00
2.04
1.96
3.25
3.19
1.05
1.03

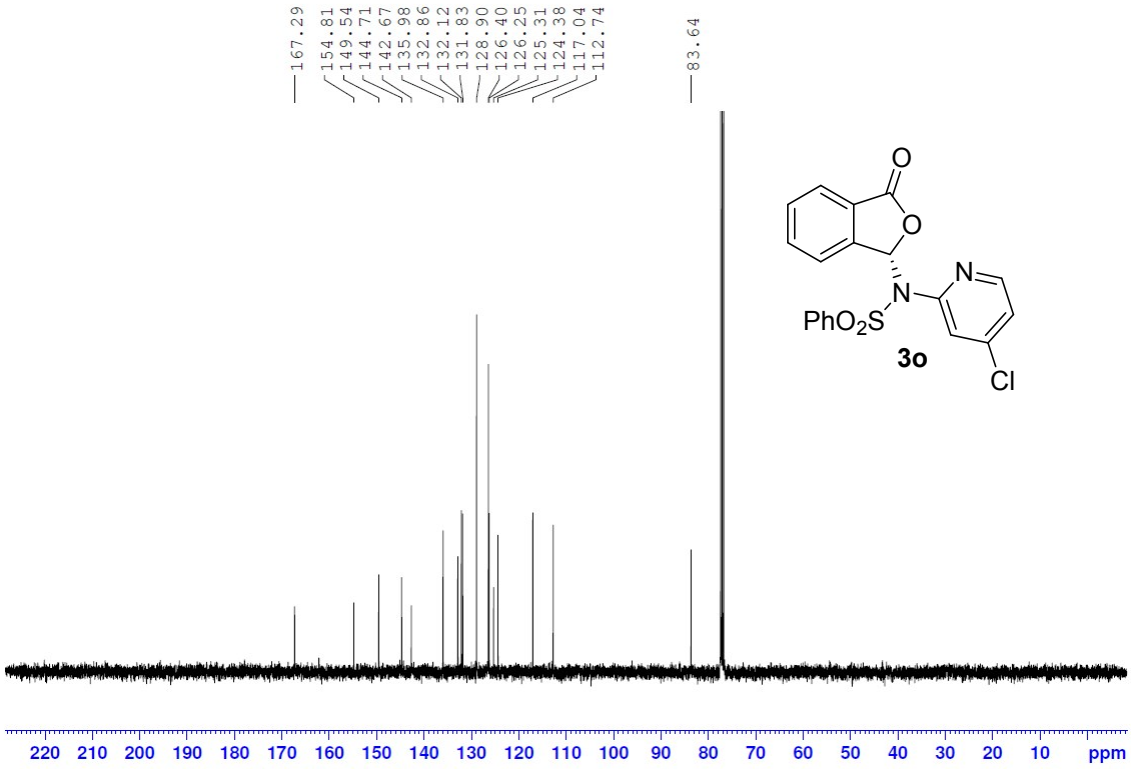
167.29
154.81
149.54
144.71
142.67
135.98
132.86
132.12
131.83
128.90
126.40
126.25
125.31
124.38
117.04
112.74
83.64
O
O
N
N
PhO2S
3o
Cl
220
210
200
190
180
170
160
150
140
130
120
110
100
90
80
70
60
50
40
30
20
10
ppm

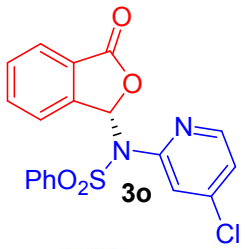

3o

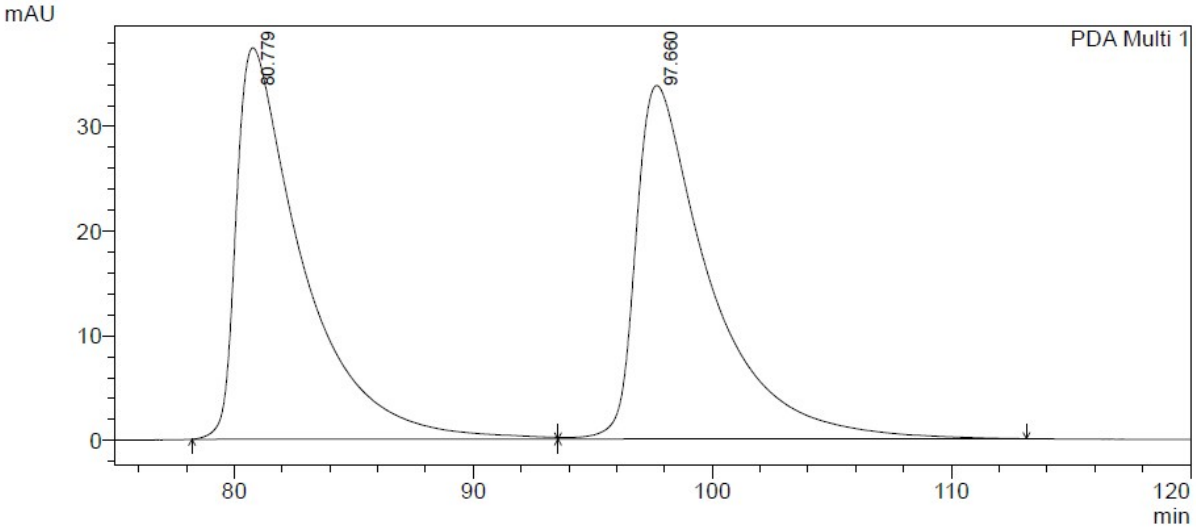

PDA Ch1 254nm 4nm

Peak#	Ret. Time	Area	Height	Area %	Height %
1	80.779	7216150	37388	49.767	52.549
2	97.660	7283696	33761	50.233	47.451
Total		14499847	71149	100.000	100.000

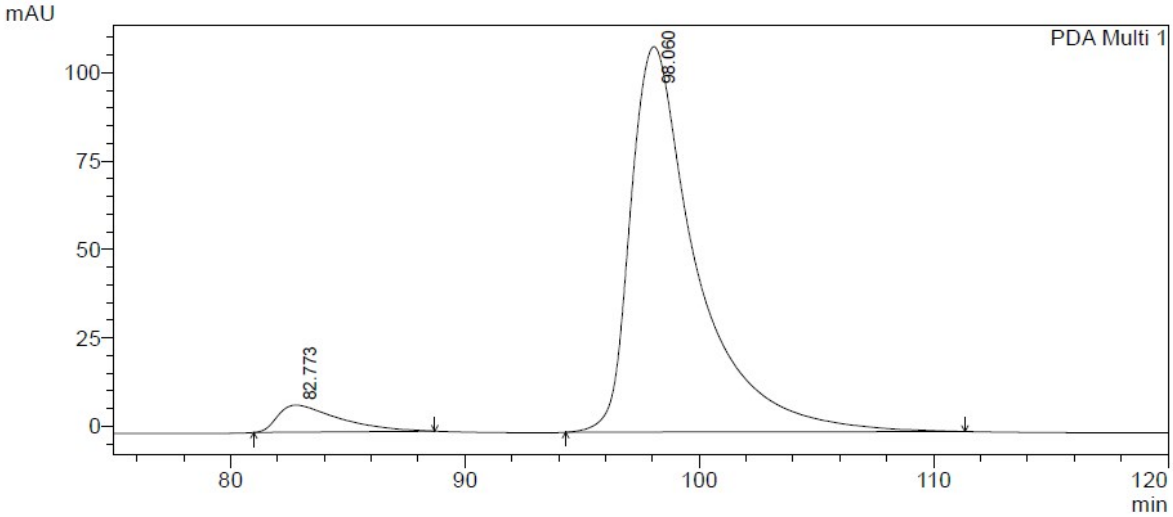

PDA Ch1 254nm 4nm

Peak#	Ret. Time	Area	Height	Area %	Height %
1	82.773	1389407	7657	6.086	6.562
2	98.060	21440231	109032	93.914	93.438
Total		22829638	116689	100.000	100.000

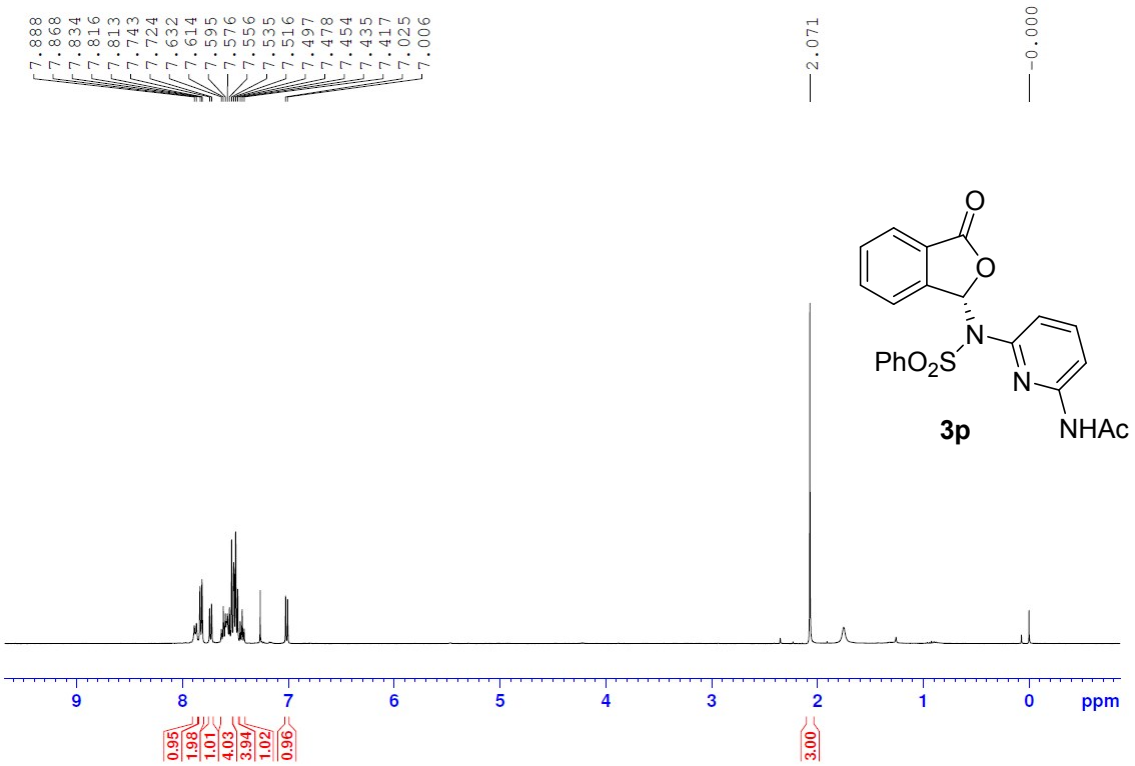
7.888
7.868
7.834
7.816
7.813
7.743
7.724
7.632
7.614
7.595
7.576
7.556
7.535
7.516
7.497
7.478
7.454
7.435
7.417
7.025
7.006
2.071
0.000
O
O
N
PhO2S
N
NHAc
3p
9
8
7
6
5
4
3
2
1
0
ppm
0.95
1.98
1.01
4.03
3.94
1.02
0.96
3.00

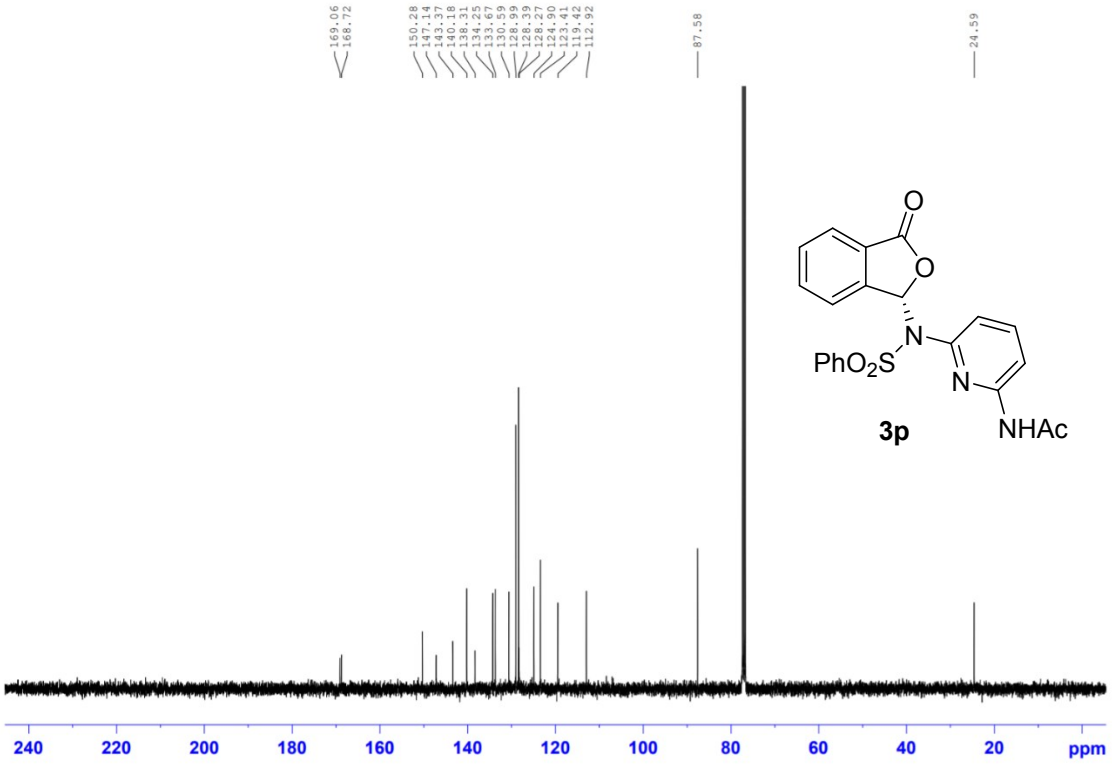
169.06
168.72
150.28
147.14
143.37
140.18
138.31
134.25
133.67
130.59
128.99
128.39
128.27
124.90
123.41
119.42
112.92
87.58
24.59
O
O
N
PhO2S
N
NHAc
3p
240
220
200
180
160
140
120
100
80
60
40
20
ppm

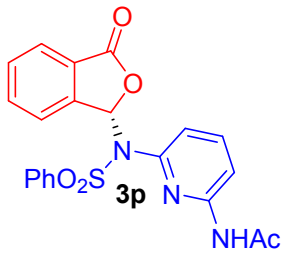

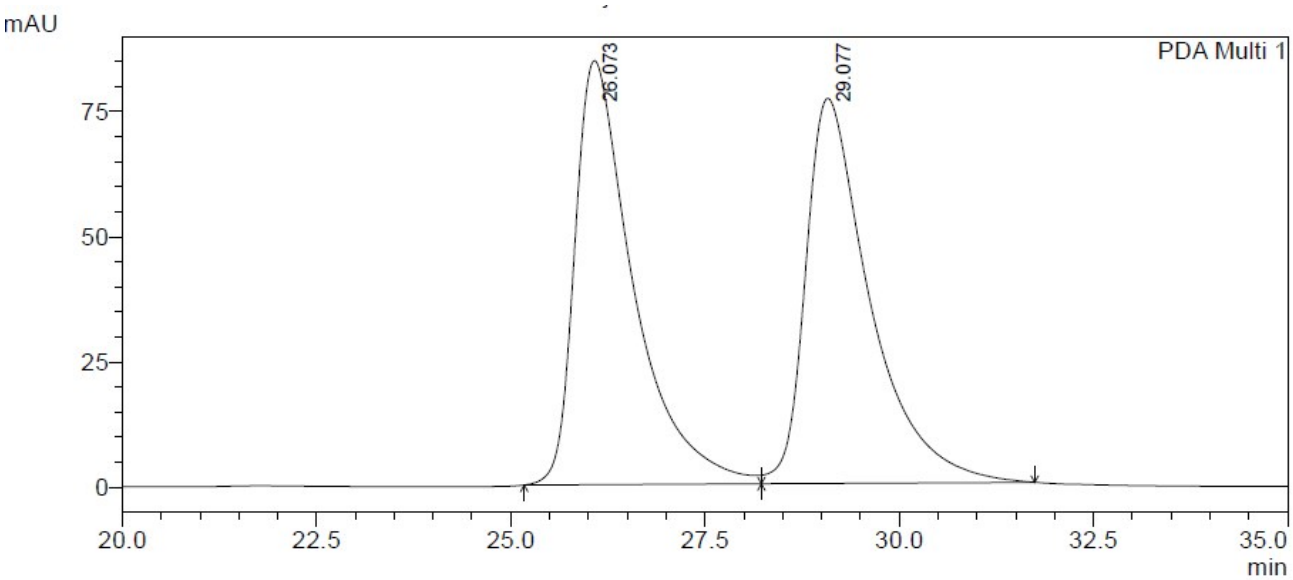

PDA Ch1 254nm 4nm

Peak#	Ret. Time	Area	Height	Area %	Height %
1	26.073	4449838	84649	50.119	52.410
2	29.077	4428661	76863	49.881	47.590
Total		8878498	161512	100.000	100.000

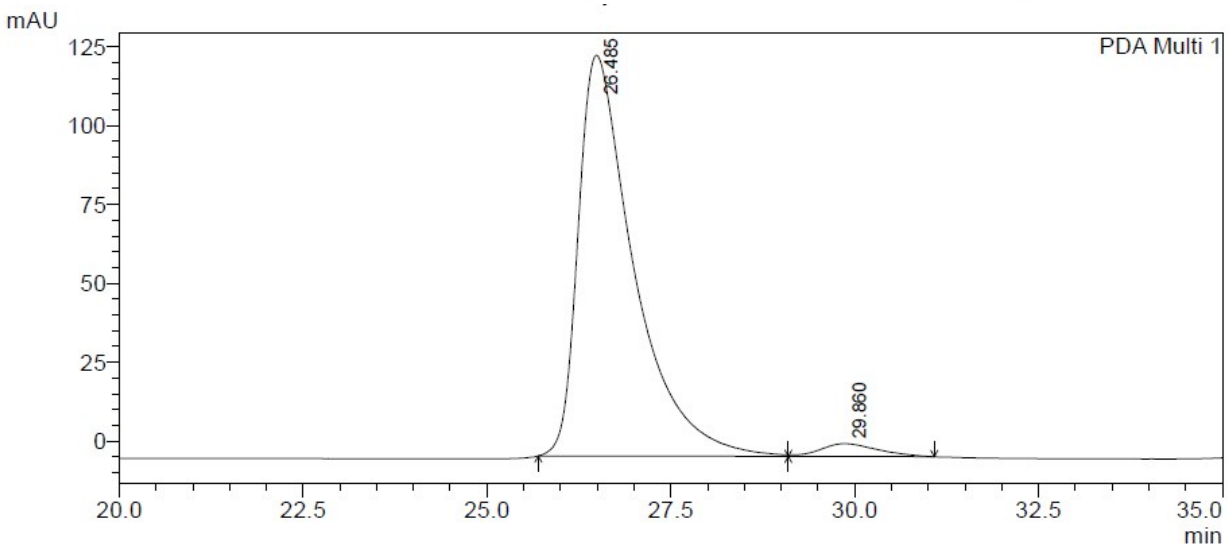

Peak#	Ret. Time	Area	Height	Area %	Height %
1	26.485	6676572	127027	96.803	96.912
2	29.860	220486	4048	3.197	3.088
Total		6897058	131075	100.000	100.000

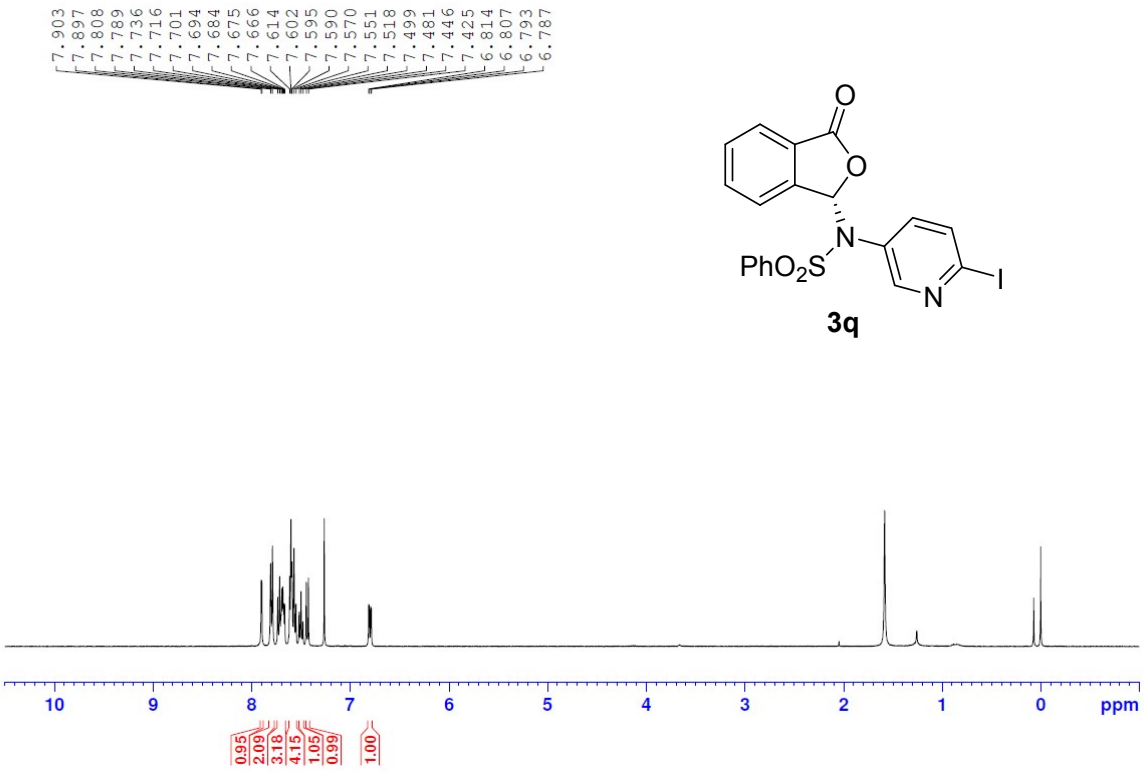
7.903
7.897
7.808
7.789
7.736
7.716
7.701
7.694
7.684
7.675
7.666
7.614
7.602
7.595
7.590
7.570
7.551
7.518
7.499
7.481
7.446
7.425
6.814
6.807
6.793
6.787
O
O
N
PhO2S
N
I
3q
10
9
8
7
6
5
4
3
2
1
0
ppm
0.95
2.09
3.18
4.15
1.05
0.99
1.00

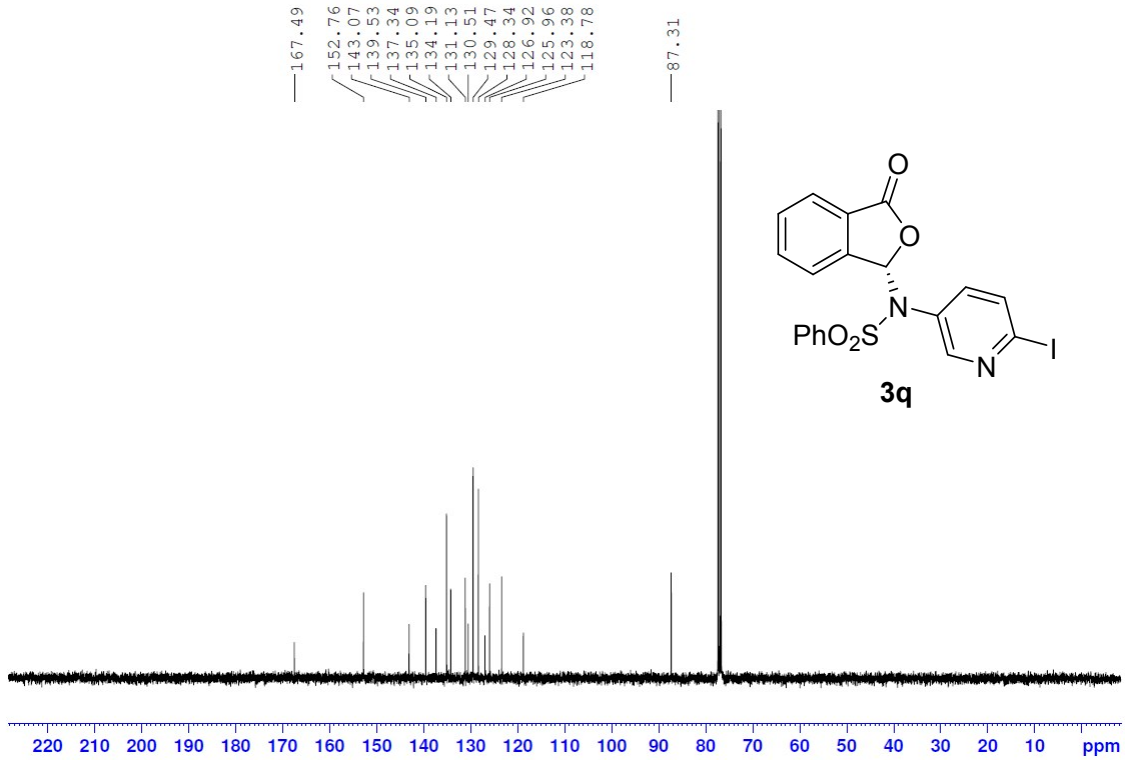
167.49
152.76
143.07
139.53
137.34
135.09
134.19
131.13
130.51
129.47
128.34
126.92
125.96
123.38
118.78
87.31
O
O
N
PhO2S
N
I
3q
220
210
200
190
180
170
160
150
140
130
120
110
100
90
80
70
60
50
40
30
20
10
ppm

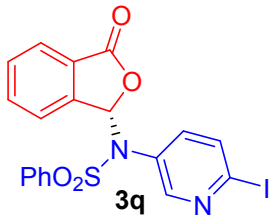

3q

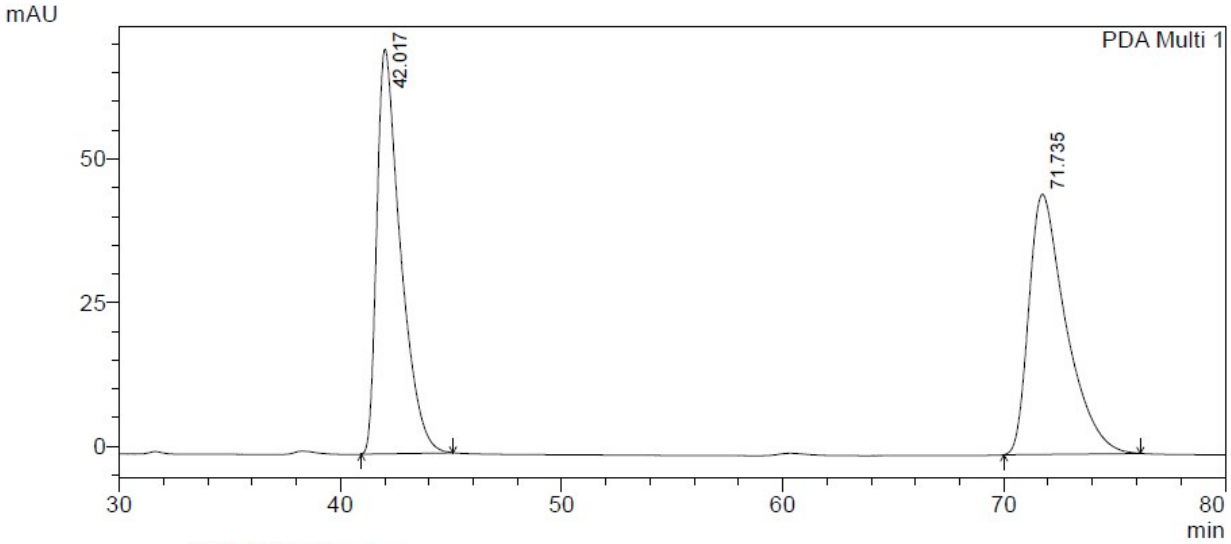

PDA Ch1 254nm 4nm

Peak#	Ret. Time	Area	Height	Area %	Height %
1	42.017	5246806	70356	49.905	60.876
2	71.735	5266719	45217	50.095	39.124
Total		10513526	115572	100.000	100.000

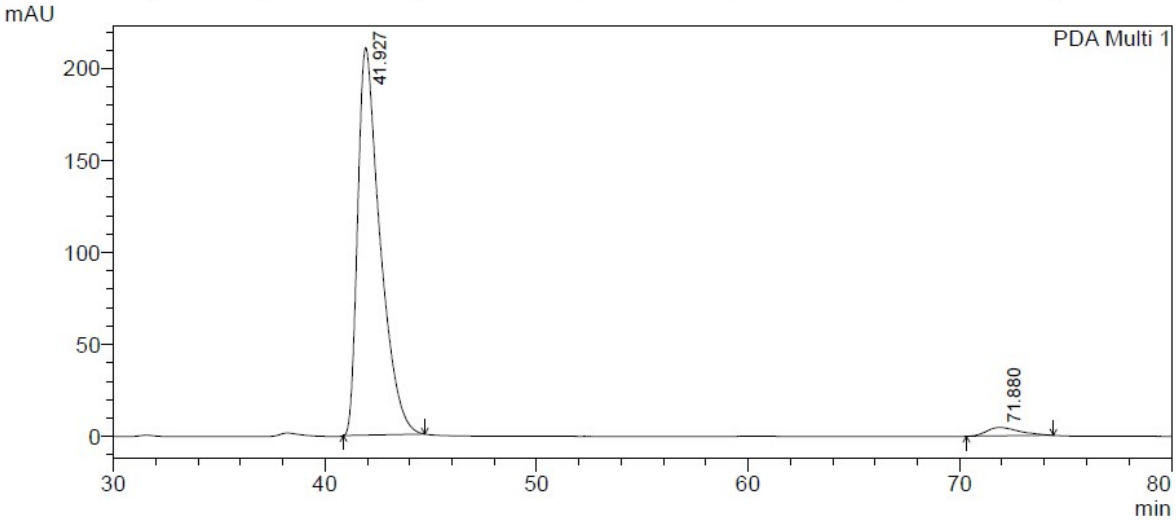

Peak#	Ret. Time	Area	Height	Area %	Height %
1	41.927	15523852	210887	96.882	97.834
2	71.880	499572	4669	3.118	2.166
Total		16023424	215556	100.000	100.000

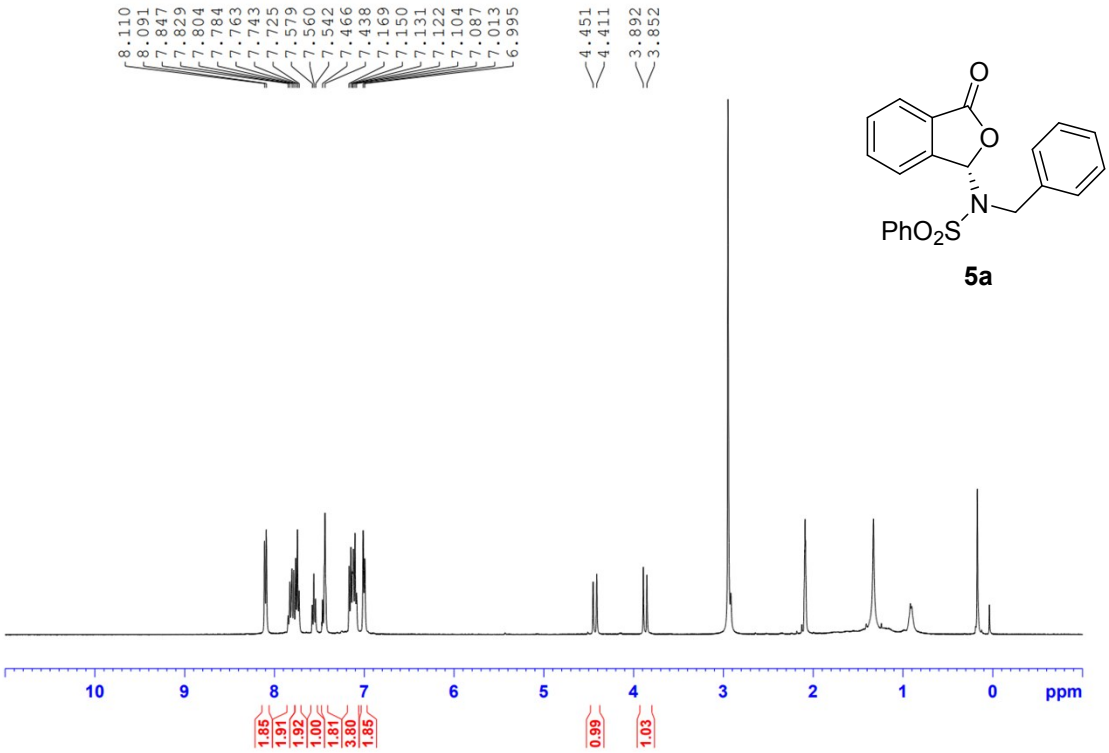
8.110
8.091
7.847
7.829
7.804
7.784
7.763
7.743
7.725
7.579
7.560
7.542
7.466
7.438
7.169
7.150
7.131
7.122
7.104
7.087
7.013
6.995
4.451
4.411
3.892
3.852
O
O
N
PhO2S
5a
10
9
8
7
6
5
4
3
2
1
0
ppm
1.85
1.91
1.92
1.00
1.81
3.80
1.85
0.99
1.03

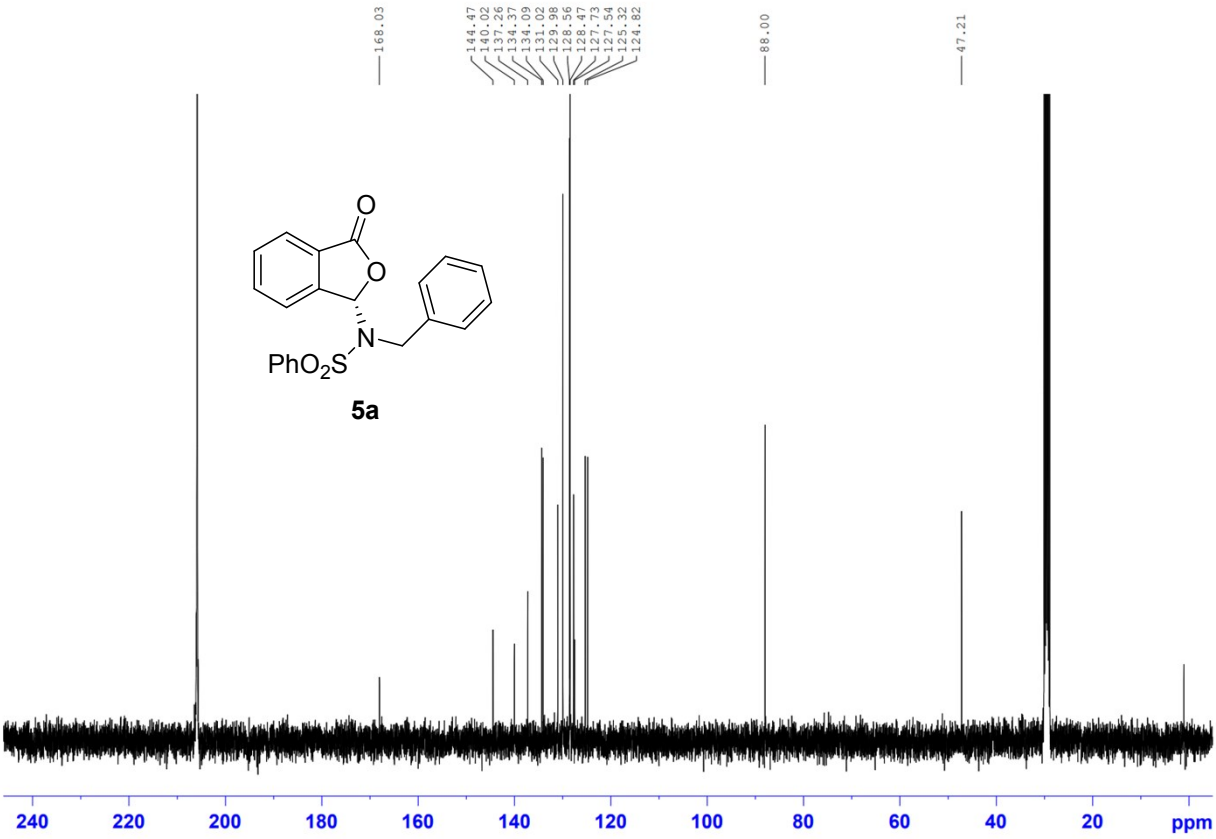
168.03
144.47
140.02
137.26
134.37
134.09
131.02
129.98
128.56
128.47
127.73
127.54
125.32
124.82
88.00
47.21
O
O
N
PhO2S
5a
240
220
200
180
160
140
120
100
80
60
40
20
ppm

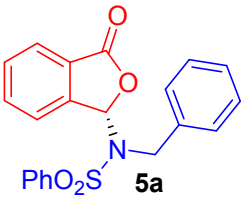

5a

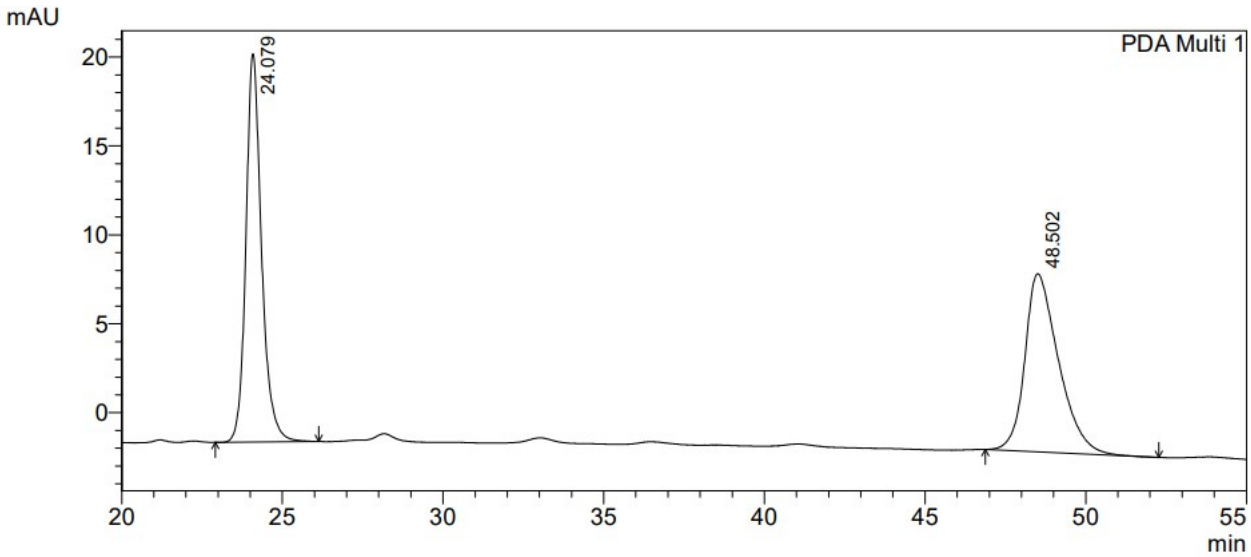

PDA Ch1 254nm 4nm

Peak#	Ret. Time	Area	Height	Area %	Height %
1	24.079	739459	21834	50.303	68.560
2	48.502	730542	10013	49.697	31.440
Total		1470000	31847	100.000	100.000

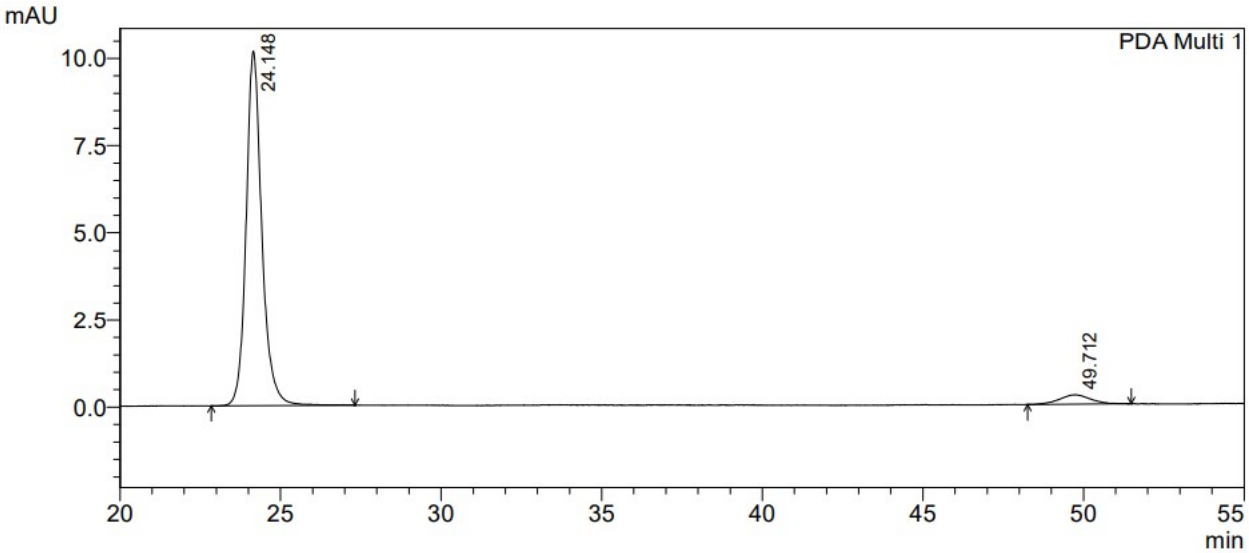

PDA Ch1 254nm 4nm

Peak#	Ret. Time	Area	Height	Area %	Height %
1	24.148	345959	10166	95.021	97.395
2	49.712	18127	272	4.979	2.605
Total		364086	10438	100.000	100.000

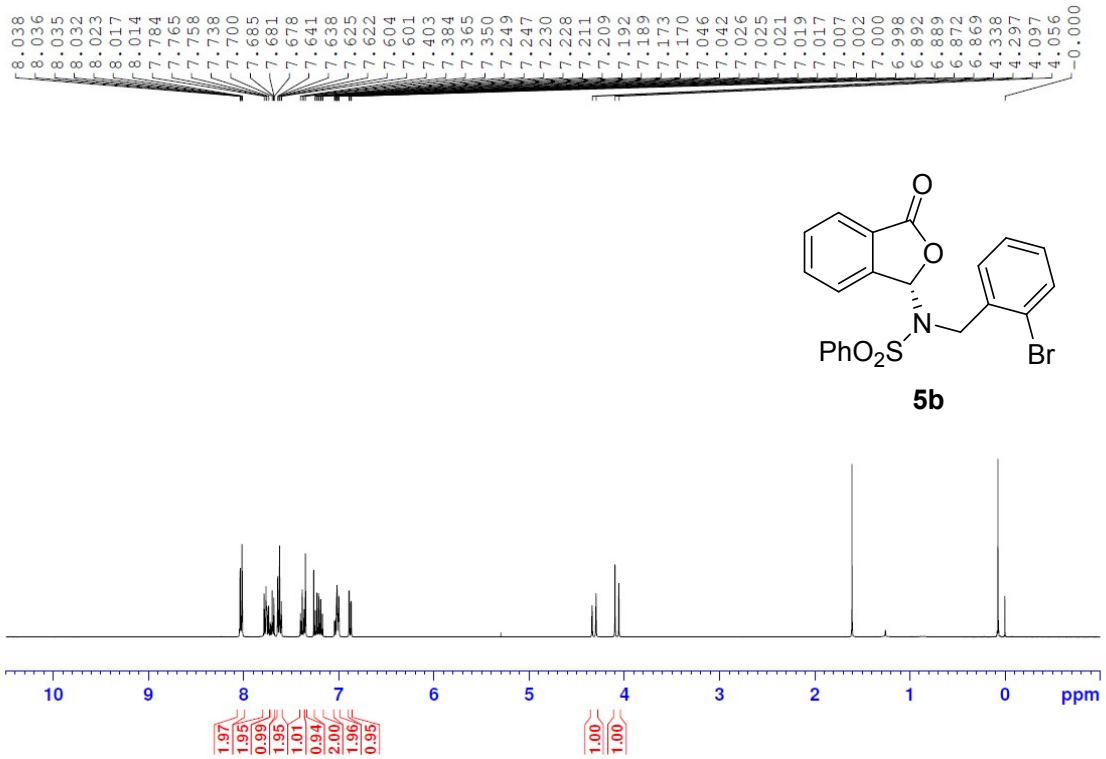
8.038
8.036
8.035
8.032
8.023
8.017
8.014
7.784
7.765
7.758
7.738
7.700
7.685
7.681
7.678
7.641
7.638
7.625
7.622
7.604
7.601
7.403
7.384
7.365
7.350
7.249
7.247
7.230
7.228
7.211
7.209
7.192
7.189
7.173
7.170
7.046
7.042
7.026
7.025
7.021
7.019
7.017
7.007
7.002
7.000
6.998
6.992
6.889
6.872
6.869
4.338
4.297
4.097
4.056
0.000
O
O
N
PhO2S
Br
5b
10
9
8
7
6
5
4
3
2
1
0
ppm
1.97
1.95
0.99
1.95
1.01
0.94
2.00
1.96
0.95
1.00
1.00

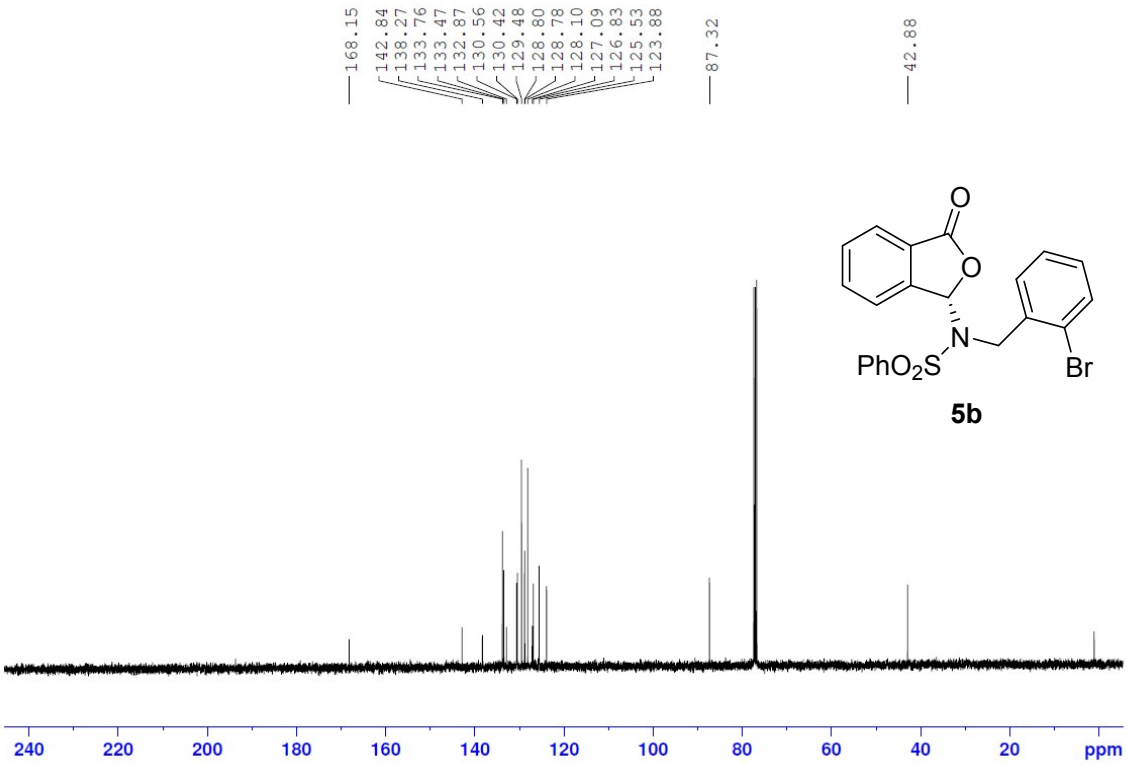
168.15
142.84
138.27
133.76
133.47
132.87
130.56
130.42
129.48
128.80
128.78
128.10
127.09
126.83
125.53
123.88
87.32
42.88
O
O
N
PhO2S
Br
5b
240
220
200
180
160
140
120
100
80
60
40
20
ppm

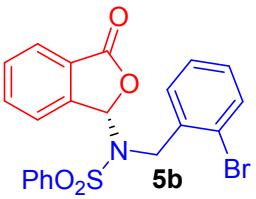
O
O
N
PhO2S
Br
5b

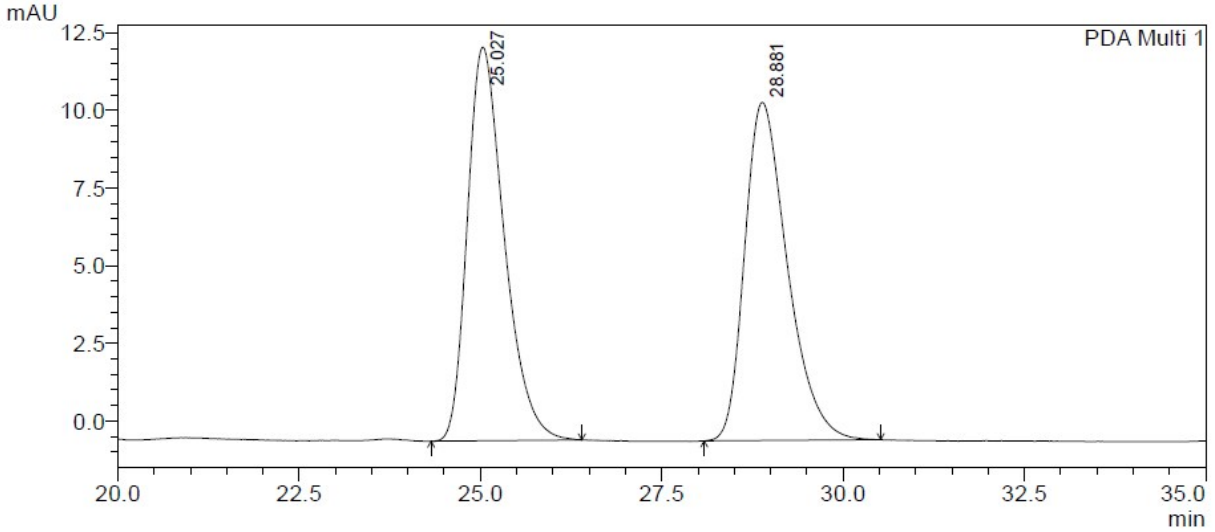

PDA Ch1 254nm 4nm

Peak#	Ret. Time	Area	Height	Area %	Height %
1	25.027	449029	12670	50.098	53.791
2	28.881	447270	10884	49.902	46.209
Total		896299	23553	100.000	100.000

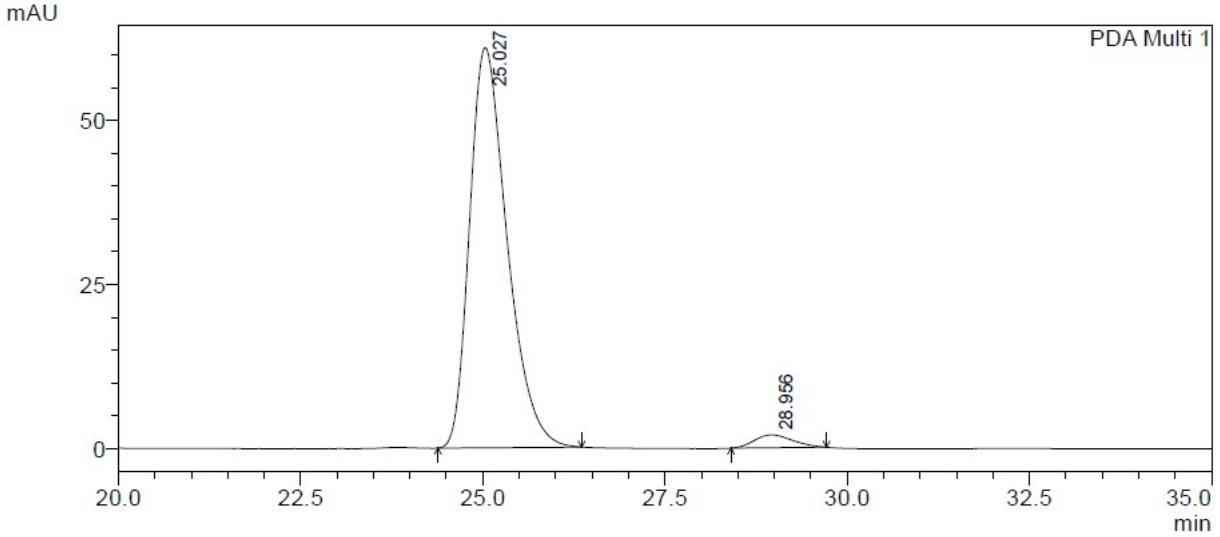

PDA Ch1 254nm 4nm

Peak#	Ret. Time	Area	Height	Area %	Height %
1	25.027	2183040	60982	96.805	96.866
2	28.956	72058	1973	3.195	3.134
Total		2255098	62955	100.000	100.000

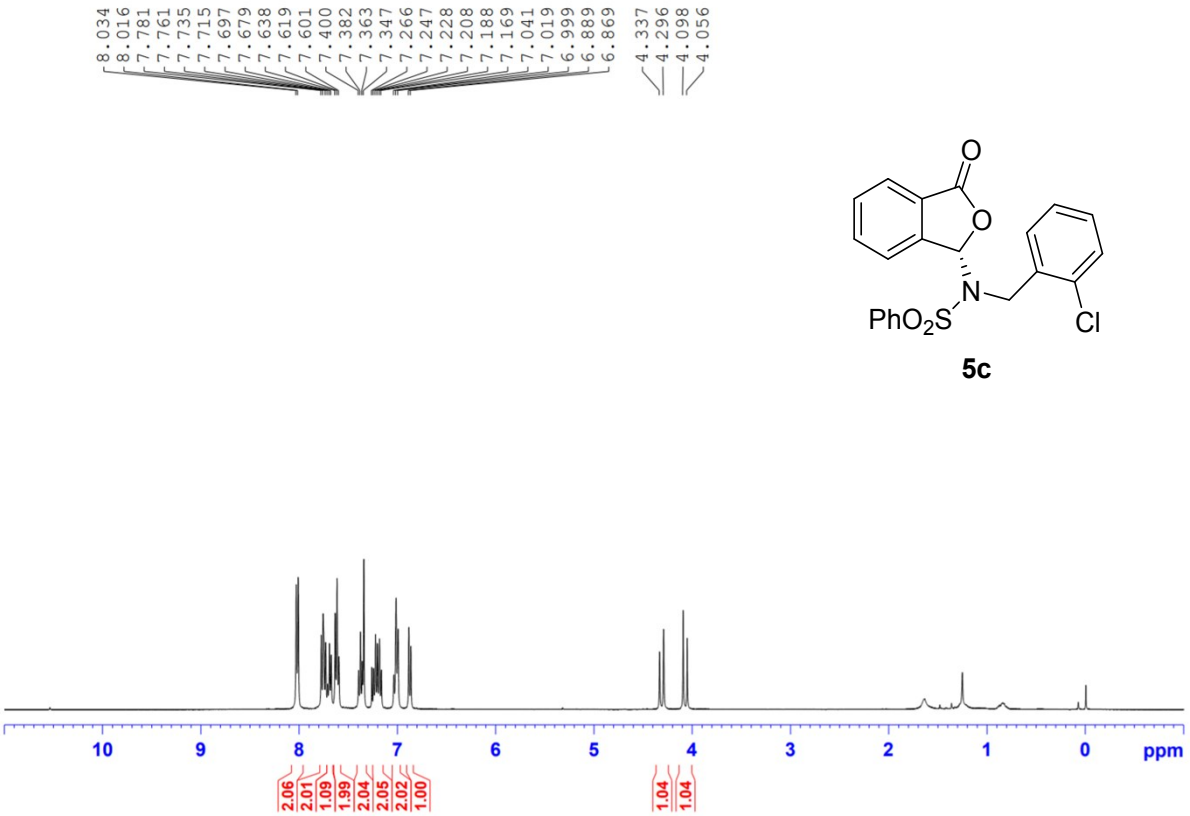
8.034
8.016
7.781
7.761
7.735
7.715
7.697
7.679
7.638
7.619
7.601
7.400
7.382
7.363
7.347
7.266
7.247
7.228
7.208
7.188
7.169
7.041
7.019
6.999
6.889
6.869
4.337
4.296
4.098
4.056
O
O
N
PhO2S
Cl
5c
10
9
8
7
6
5
4
3
2
1
0
ppm
2.06
2.01
1.09
1.99
2.04
2.05
2.02
1.00
1.04
1.04

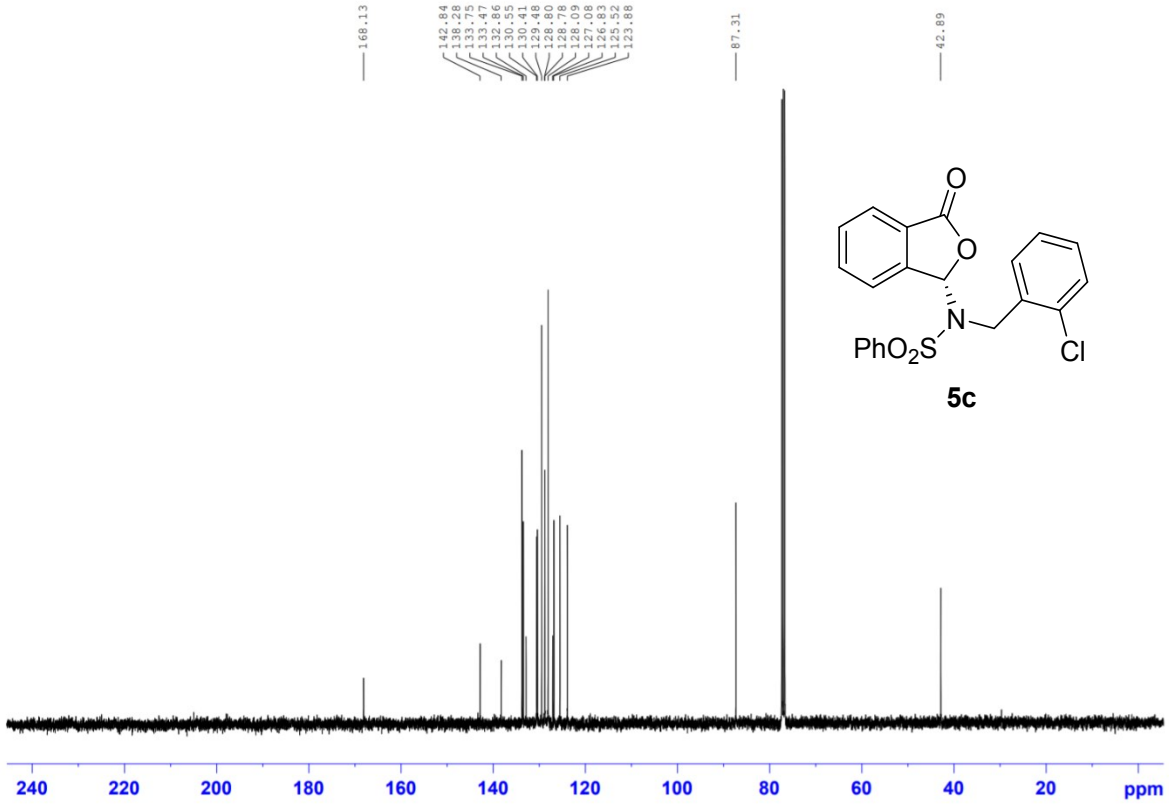
168.13
142.84
136.28
133.75
133.47
132.86
130.55
130.41
129.48
128.80
128.78
128.09
127.08
126.83
125.52
123.88
87.31
42.89
O
O
N
PhO2S
Cl
5c
240
220
200
180
160
140
120
100
80
60
40
20
ppm

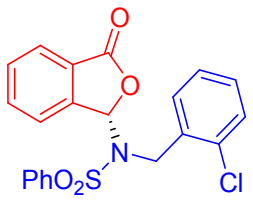
O
O
N
PhO2S
Cl

5c

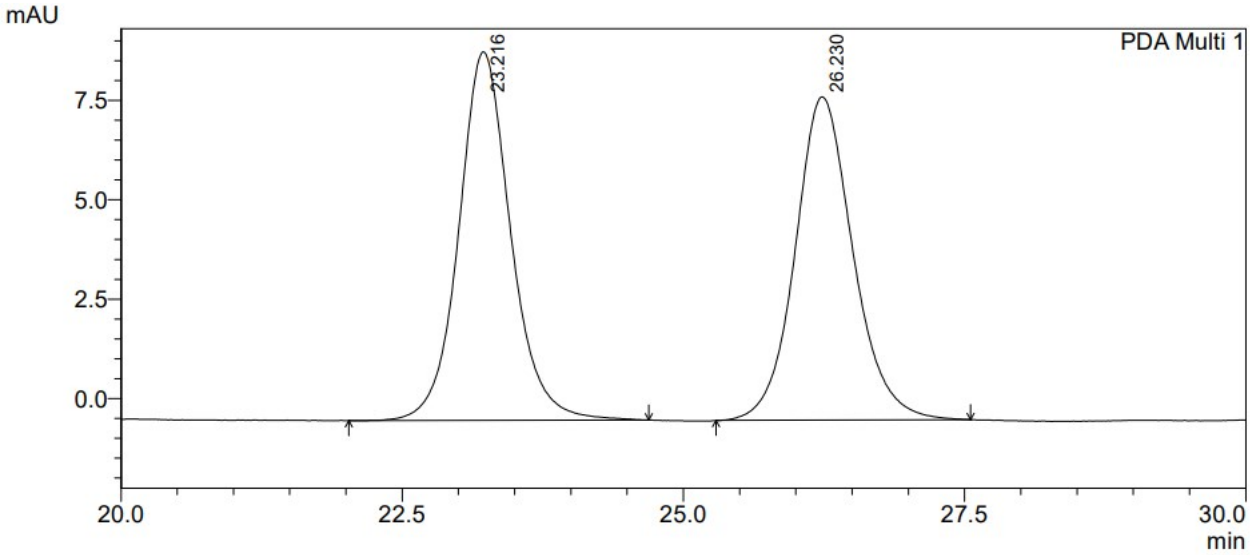

PDA Ch1 254nm 4nm

Peak#	Ret. Time	Area	Height	Area %	Height %
1	23.216	297631	9273	50.555	53.274
2	26.230	291098	8133	49.445	46.726
Total		588730	17406	100.000	100.000

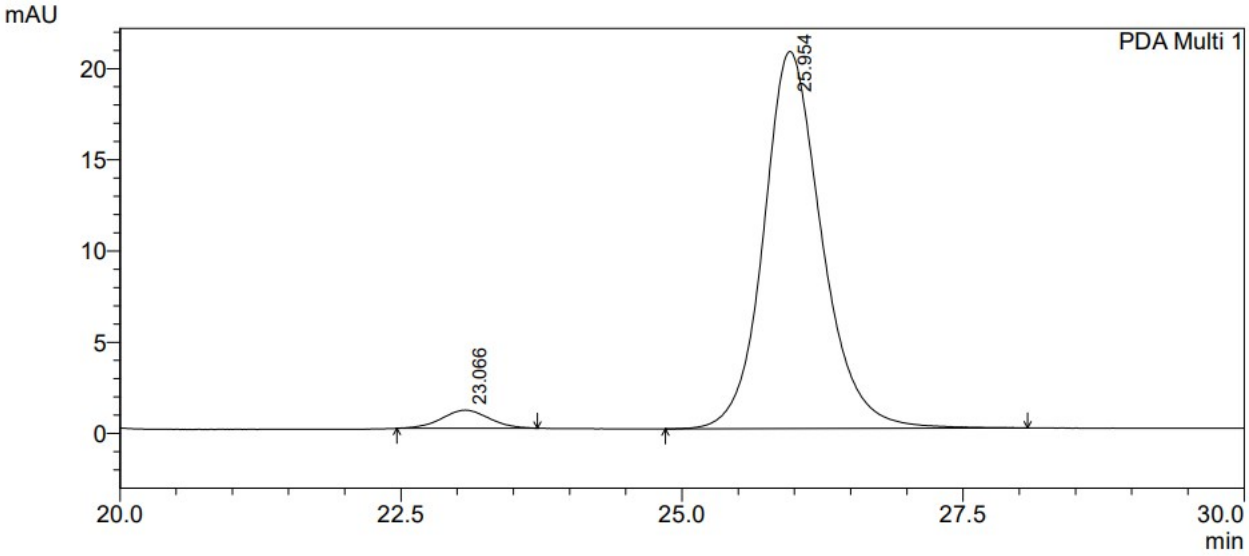

PDA Ch1 254nm 4nm

Peak#	Ret. Time	Area	Height	Area %	Height %
1	23.066	29072	992	3.756	4.582
2	25.954	744892	20669	96.244	95.418
Total		773965	21661	100.000	100.000

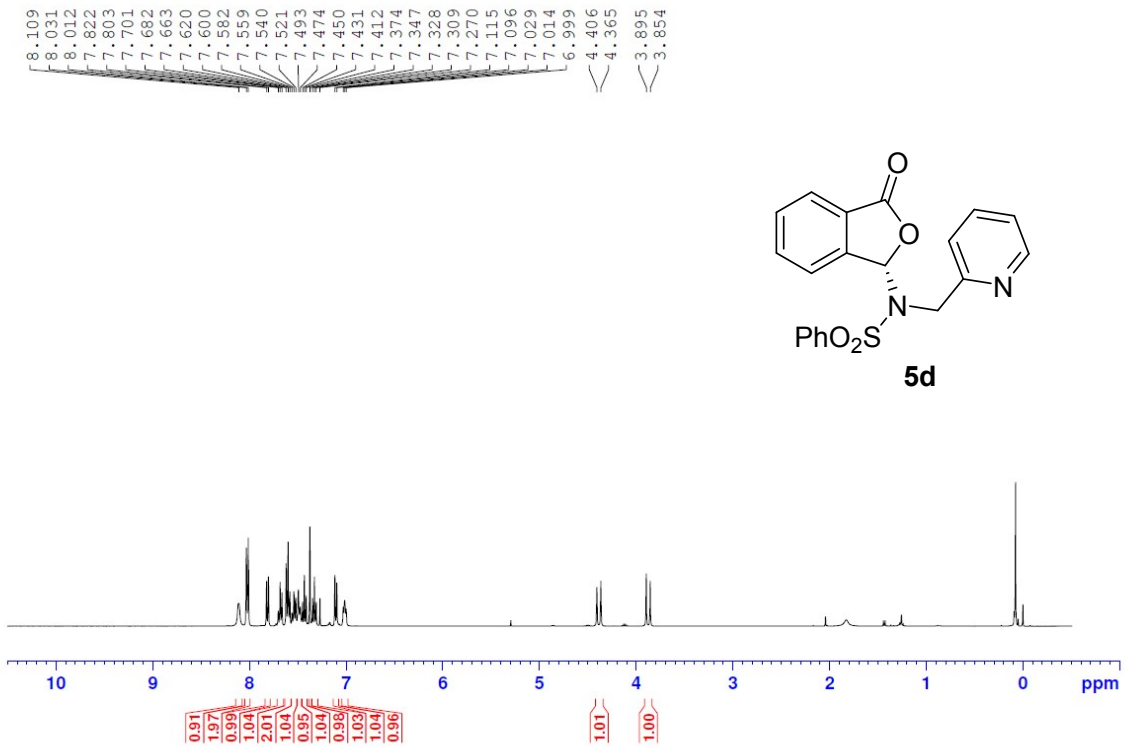
8.109
8.031
8.012
7.822
7.803
7.701
7.682
7.663
7.620
7.600
7.582
7.559
7.540
7.521
7.493
7.474
7.450
7.431
7.412
7.374
7.347
7.328
7.309
7.270
7.115
7.096
7.029
7.014
6.999
4.406
4.365
3.895
3.854
O
O
N
N
PhO2S
5d
10 9 8 7 6 5 4 3 2 1 0 ppm
0.91 1.97 0.99 1.04 2.01 1.04 0.95 1.04 0.98 1.03 1.04 0.96
1.01
1.00

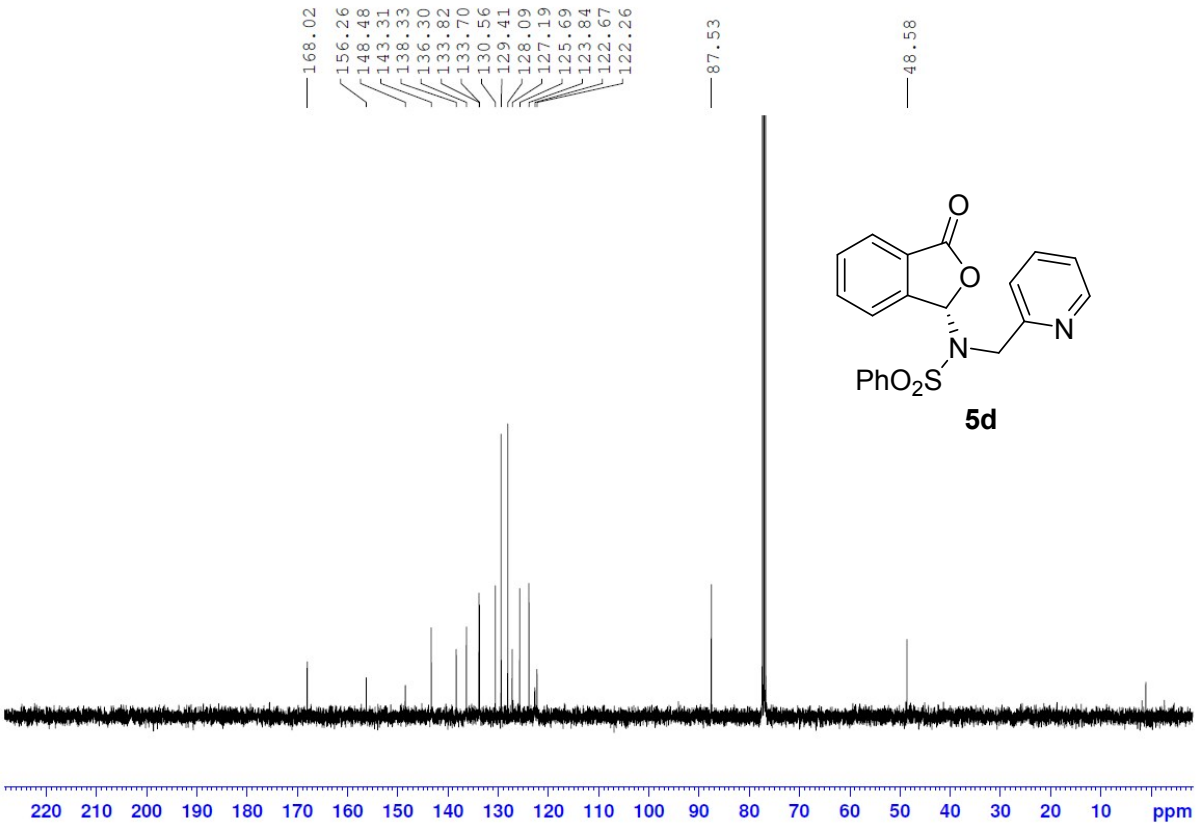
168.02
156.26
148.48
143.31
138.33
136.30
133.82
133.70
130.56
129.41
128.09
127.19
125.69
123.84
122.67
122.26
87.53
48.58
O
O
N
N
PhO2S
5d
220 210 200 190 180 170 160 150 140 130 120 110 100 90 80 70 60 50 40 30 20 10 ppm

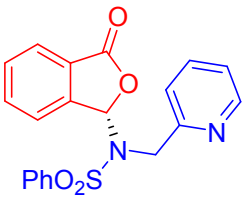

5d

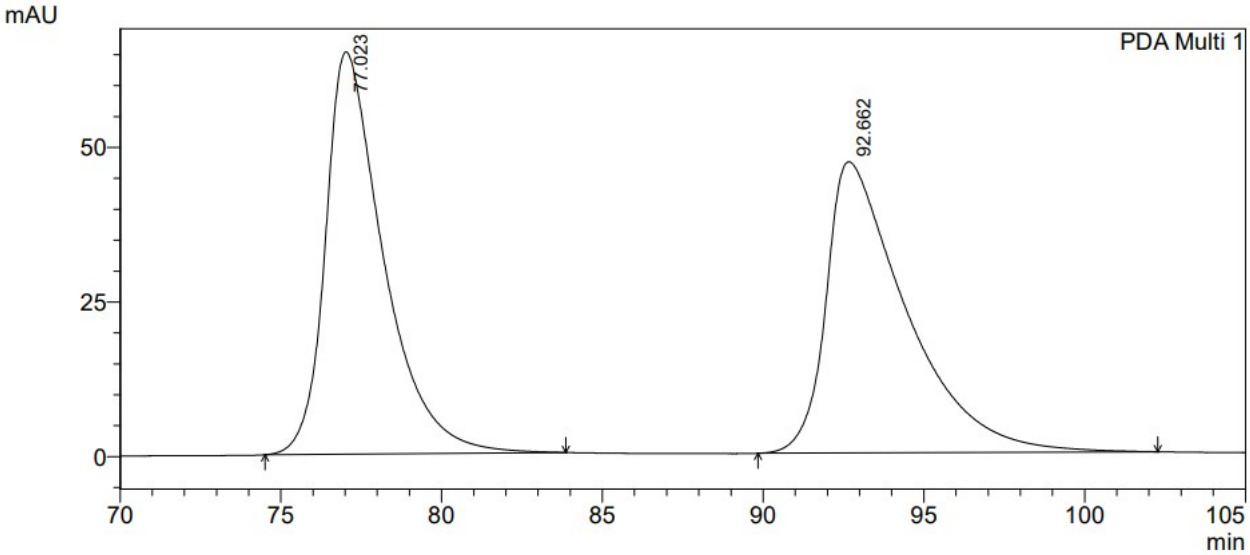

Peak#	Ret. Time	Area	Height	Area %	Height %
1	77.023	8188518	65060	49.964	58.007
2	92.662	8200426	47099	50.036	41.993
Total		16388944	112160	100.000	100.000

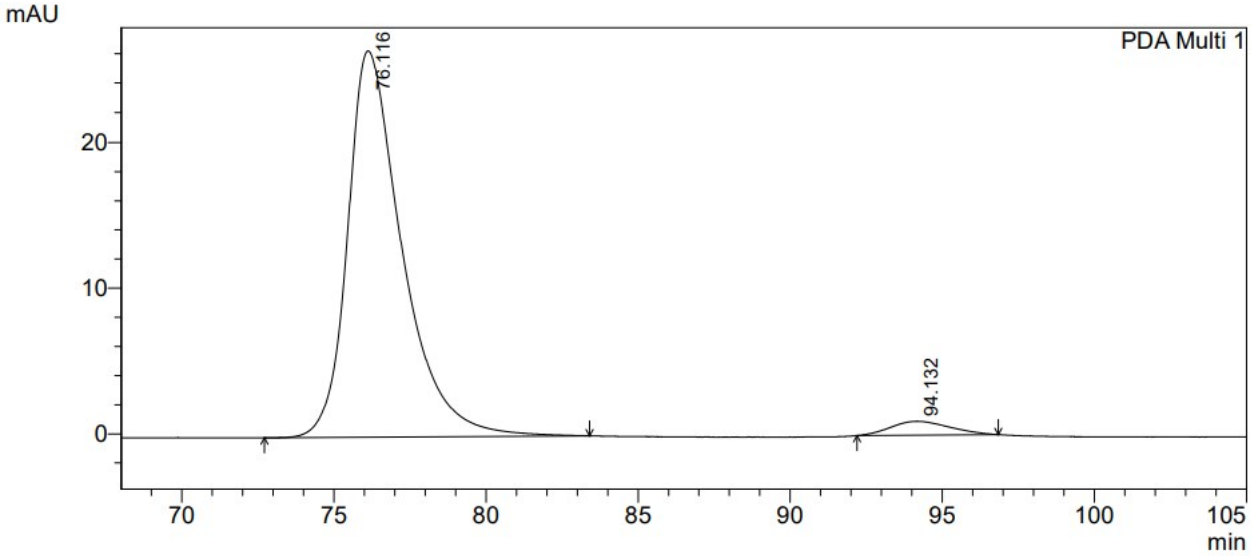

PDA Ch1 254nm 4nm

Peak#	Ret. Time	Area	Height	Area %	Height %
1	76.116	3301182	26427	96.268	96.517
2	94.132	127970	954	3.732	3.483
Total		3429153	27381	100.000	100.000

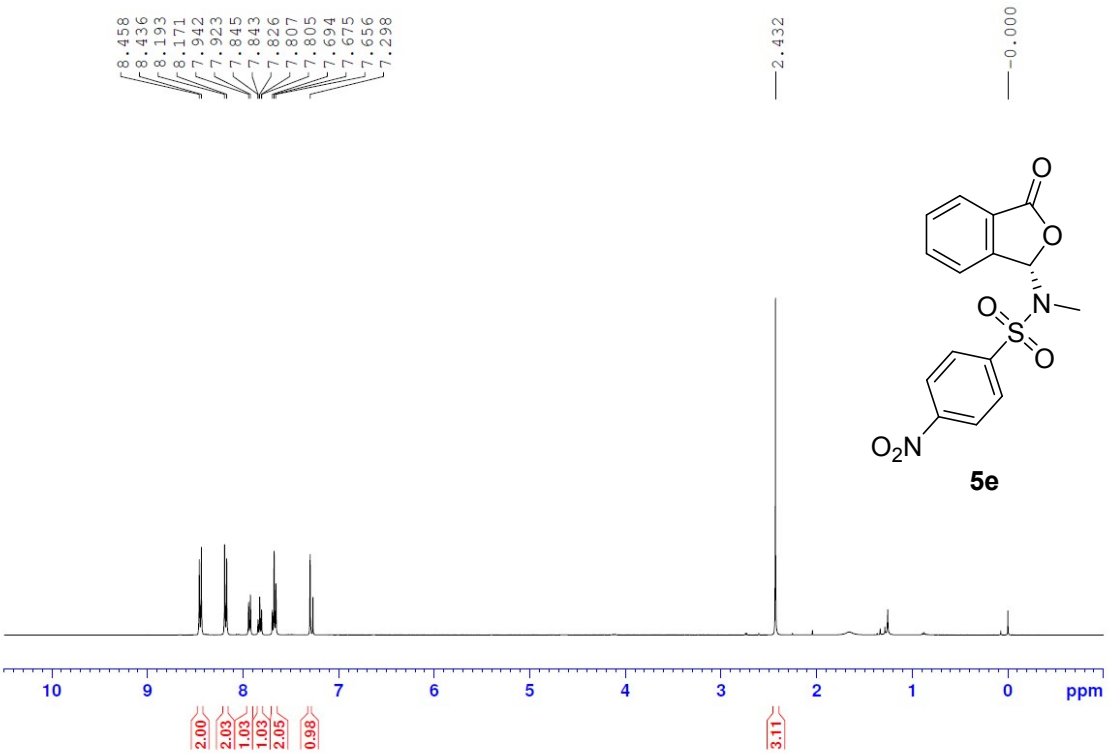
8.458
8.436
8.193
8.171
7.942
7.923
7.845
7.843
7.826
7.807
7.805
7.694
7.675
7.656
7.298
2.432
0.000
10 9 8 7 6 5 4 3 2 1 0 ppm
2.00
2.03
1.03
1.03
2.05
0.98
3.11

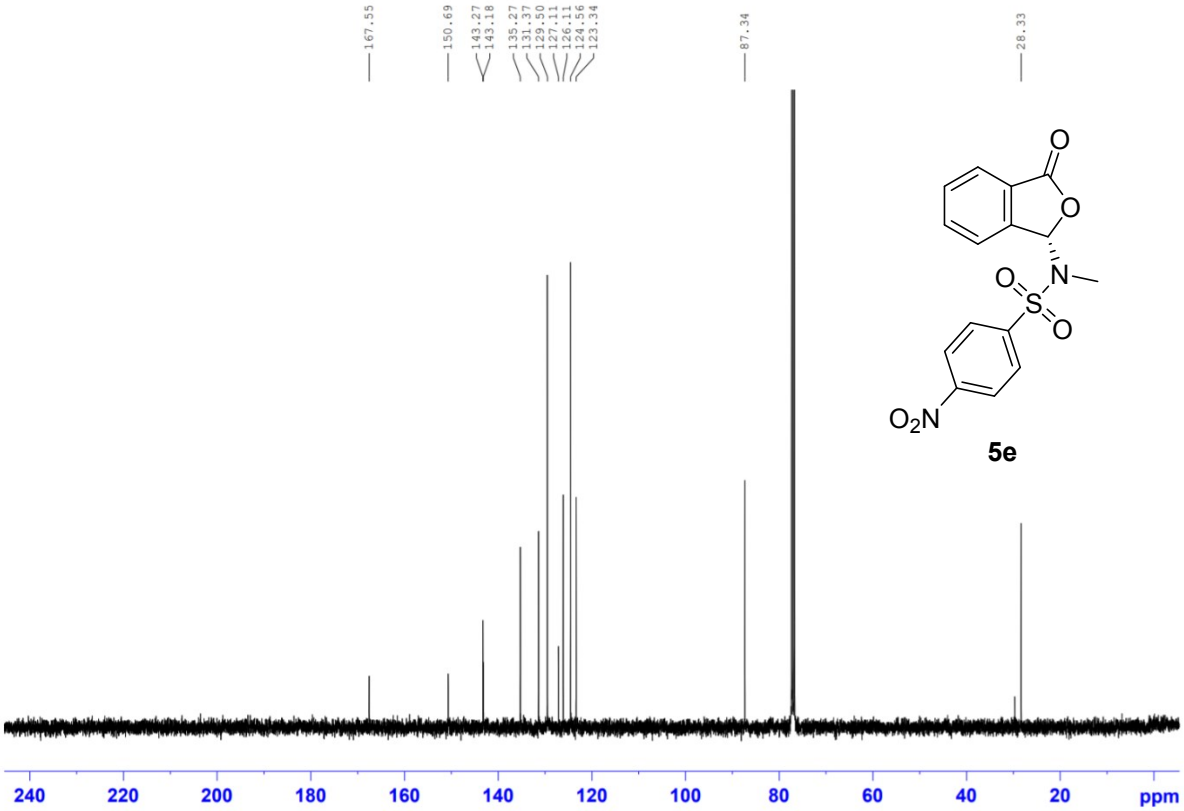
167.55
150.69
143.27
143.18
135.27
131.37
129.50
127.11
126.11
124.56
123.34
87.34
28.33
240 220 200 180 160 140 120 100 80 60 40 20 ppm

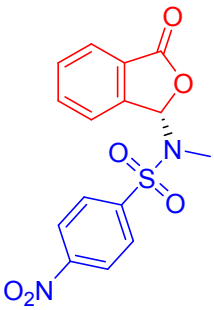

5e

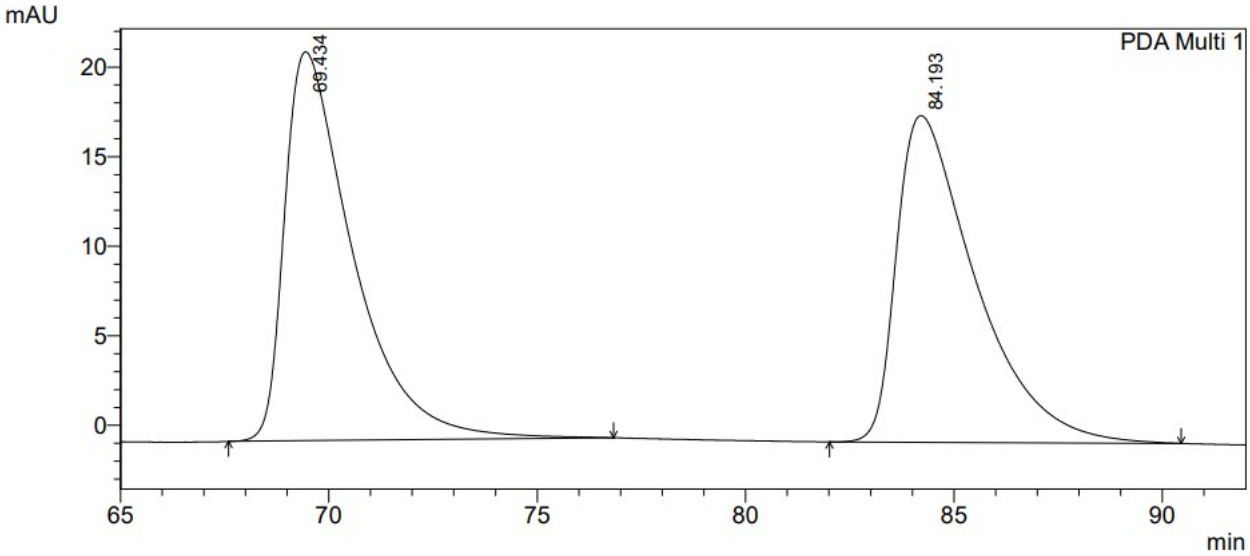

PDA Ch1 254nm 4nm

Peak#	Ret. Time	Area	Height	Area %	Height %
1	69.434	2477247	21704	50.684	54.329
2	84.193	2410368	18245	49.316	45.671
Total		4887614	39950	100.000	100.000

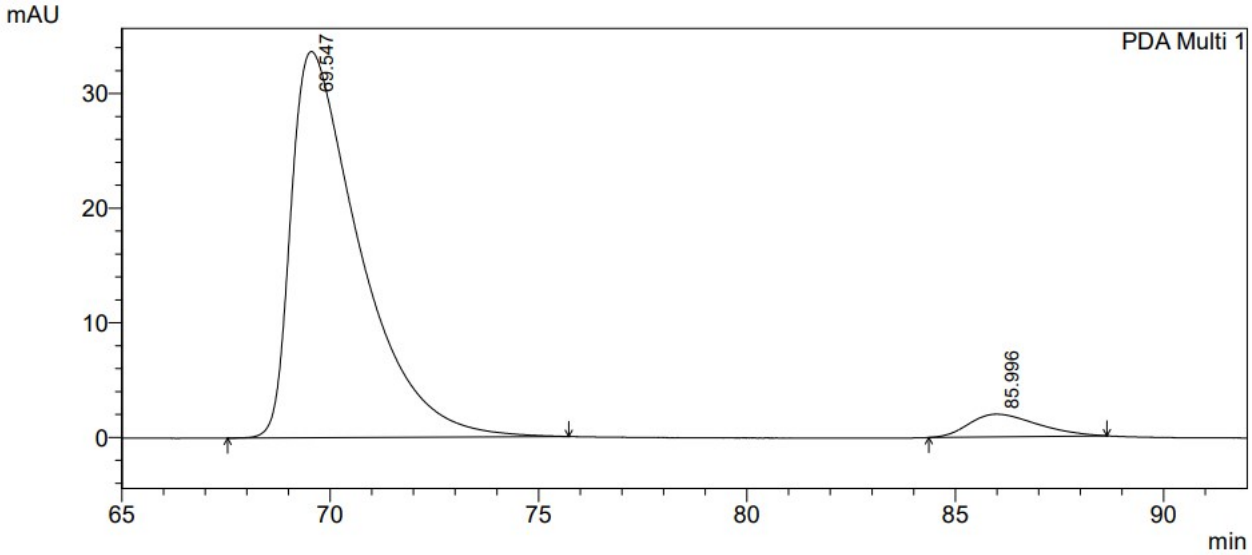

PDA Ch1 254nm 4nm

Peak#	Ret. Time	Area	Height	Area %	Height %
1	69.547	3870488	33691	94.495	94.454
2	85.996	225494	1978	5.505	5.546
Total		4095982	35669	100.000	100.000

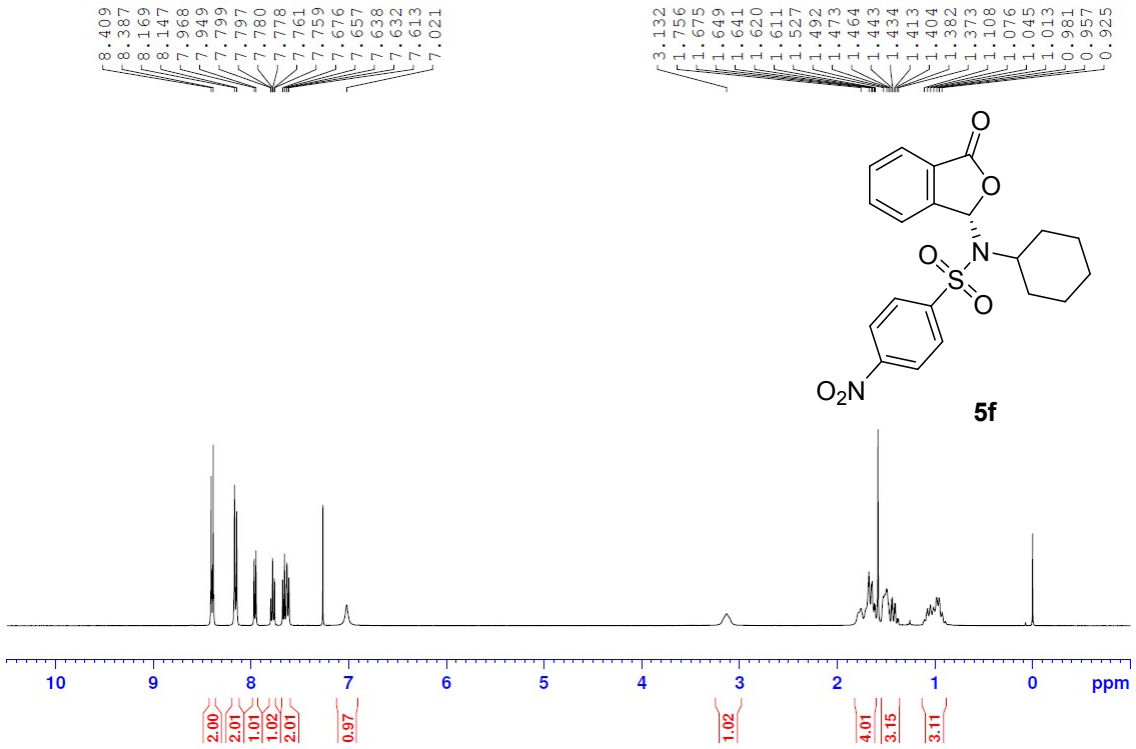
8.409
8.387
8.169
8.147
7.968
7.949
7.799
7.797
7.780
7.778
7.761
7.759
7.676
7.657
7.638
7.632
7.613
7.021
3.132
1.756
1.675
1.649
1.641
1.620
1.611
1.527
1.492
1.473
1.464
1.443
1.434
1.413
1.404
1.382
1.373
1.108
1.076
1.045
1.013
0.981
0.957
0.925
O
O
N
O
S
O
O2N
5f
10
9
8
7
6
5
4
3
2
1
0
ppm
2.00
2.01
1.01
1.02
2.01
0.97
1.02
4.01
3.15
3.11

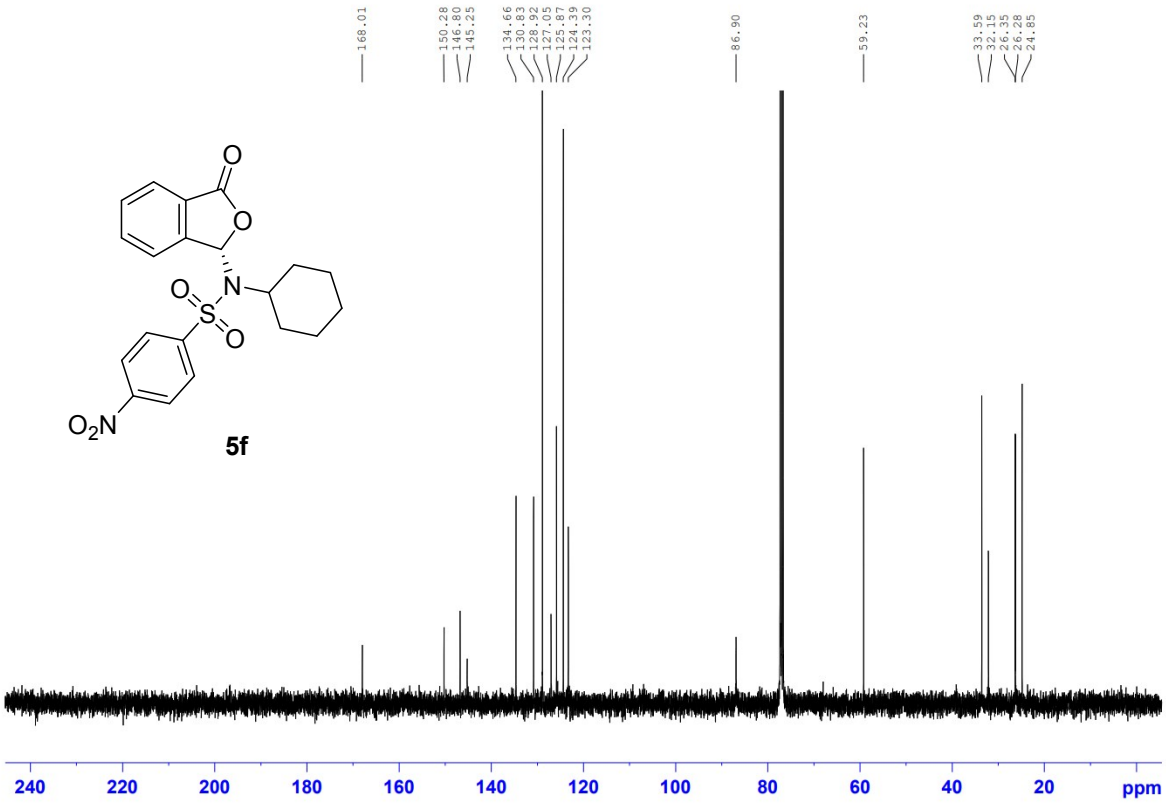
168.01
150.28
146.80
145.25
134.66
130.83
128.92
127.05
125.87
124.39
123.30
86.90
59.23
33.59
32.15
26.35
26.28
24.85
O
O
N
O
S
O
O2N
5f
240
220
200
180
160
140
120
100
80
60
40
20
ppm

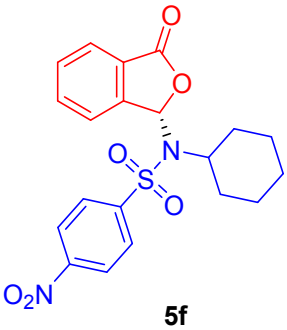

5f

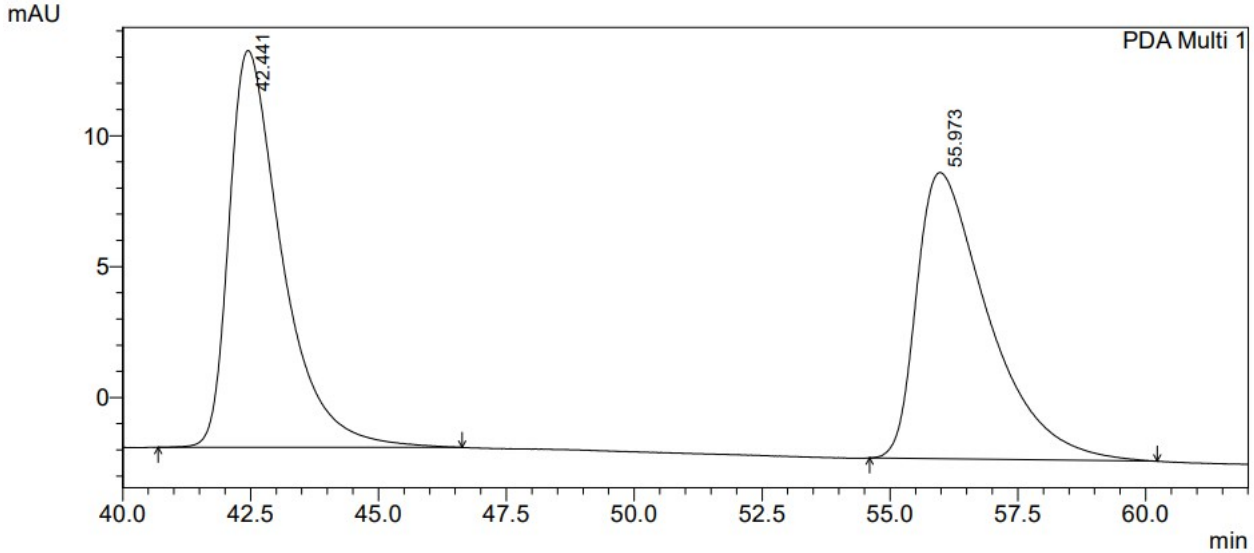

PDA Ch1 254nm 4nm

Peak#	Ret. Time	Area	Height	Area %	Height %
1	42.441	1094385	15155	50.590	58.085
2	55.973	1068846	10936	49.410	41.915
Total		2163231	26091	100.000	100.000

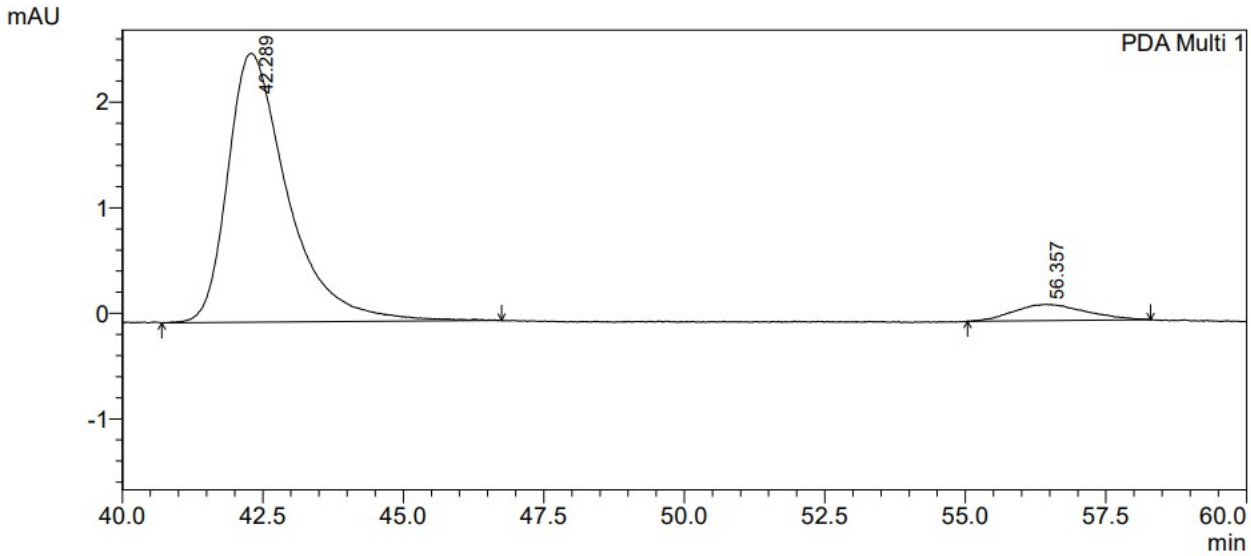

PDA Ch1 254nm 4nm

Peak#	Ret. Time	Area	Height	Area %	Height %
1	42.289	188648	2548	93.188	94.217
2	56.357	13790	156	6.812	5.783
Total		202438	2704	100.000	100.000

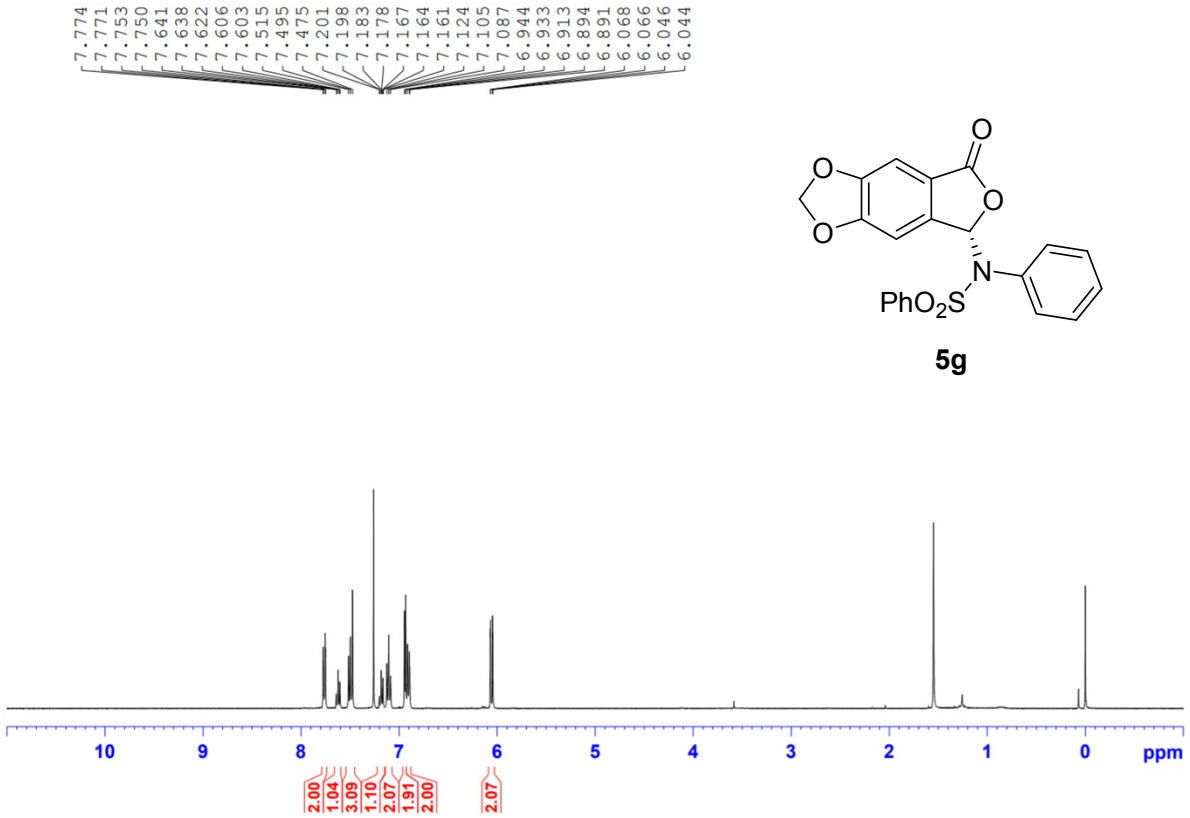
7.774
7.771
7.753
7.750
7.641
7.638
7.622
7.606
7.603
7.515
7.495
7.475
7.201
7.198
7.183
7.178
7.167
7.164
7.161
7.124
7.105
7.087
6.944
6.933
6.913
6.894
6.891
6.068
6.066
6.046
6.044
O
O
O
O
N
PhO2S
5g
10
9
8
7
6
5
4
3
2
1
0
ppm
2.00
1.04
3.09
1.10
2.07
1.91
2.00
2.07

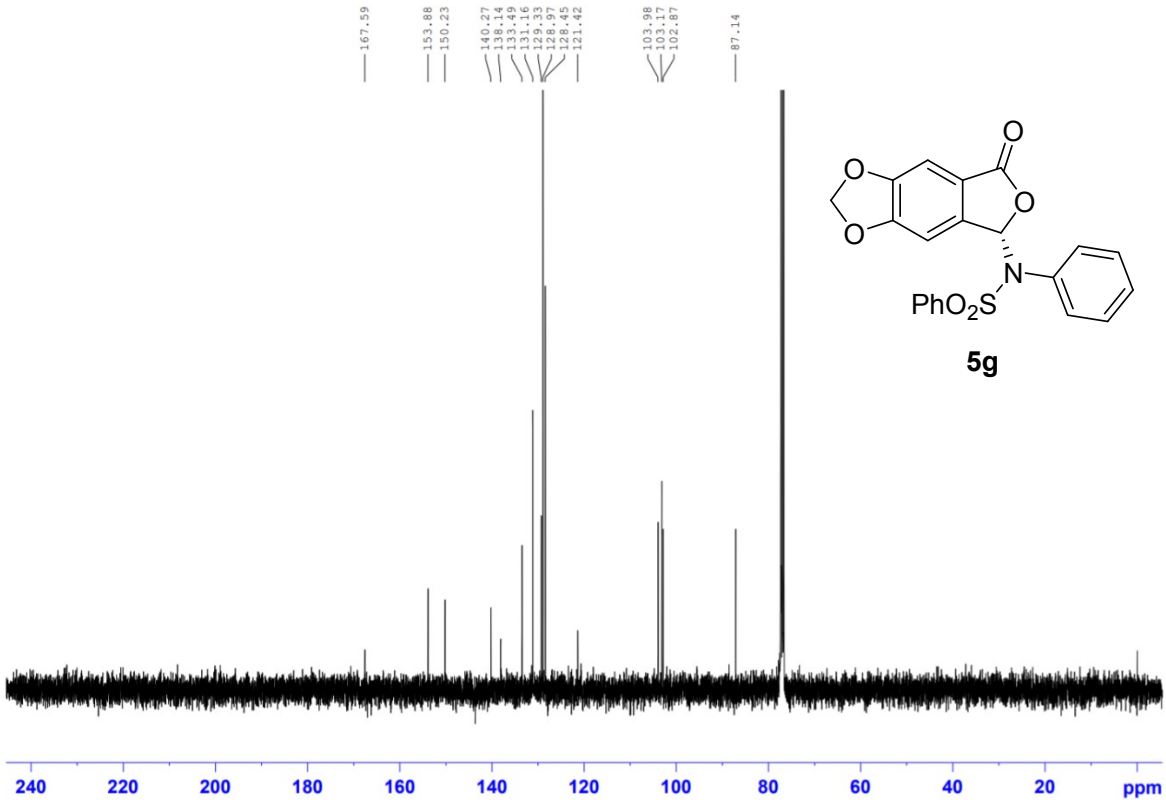
167.59
153.88
150.23
140.27
138.14
133.49
131.16
129.33
128.97
128.45
121.42
103.98
103.17
102.87
87.14
O
O
O
O
N
PhO2S
5g
240
220
200
180
160
140
120
100
80
60
40
20
ppm

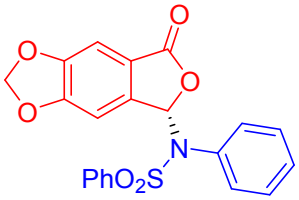

5g

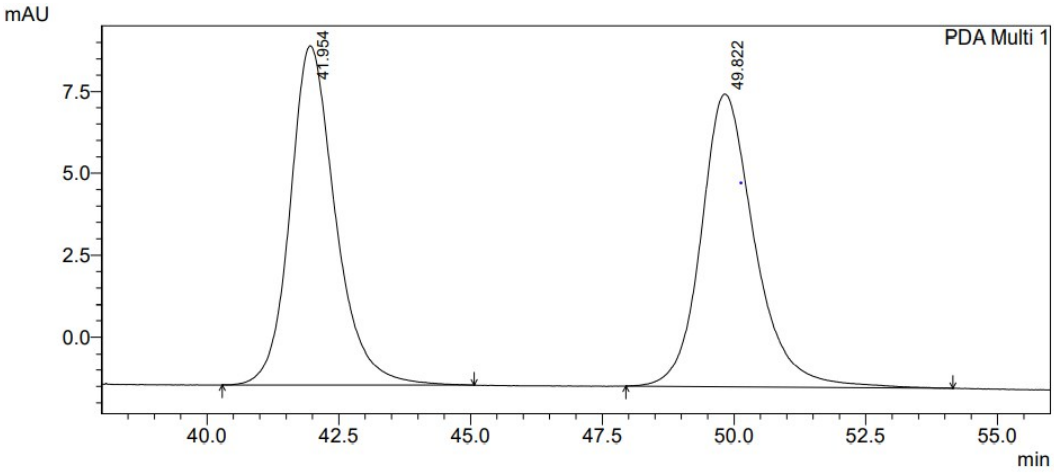

PDA Ch1 254nm 4nm

Peak#	Ret. Time	Area	Height	Area %	Height %
1	41.954	621389	10358	49.521	53.670
2	49.822	633416	8941	50.479	46.330
Total		1254805	19299	100.000	100.000

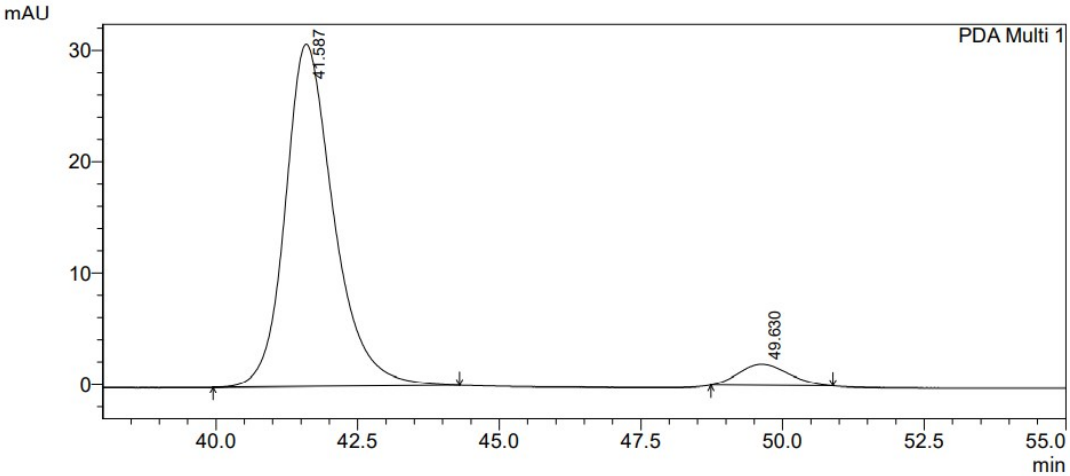

PDA Ch2 220nm 4nm

Peak#	Ret. Time	Area	Height	Area %	Height %
1	41.587	12499924	210689	94.172	94.263
2	49.625	773533	12822	5.828	5.737
Total		13273457	223511	100.000	100.000

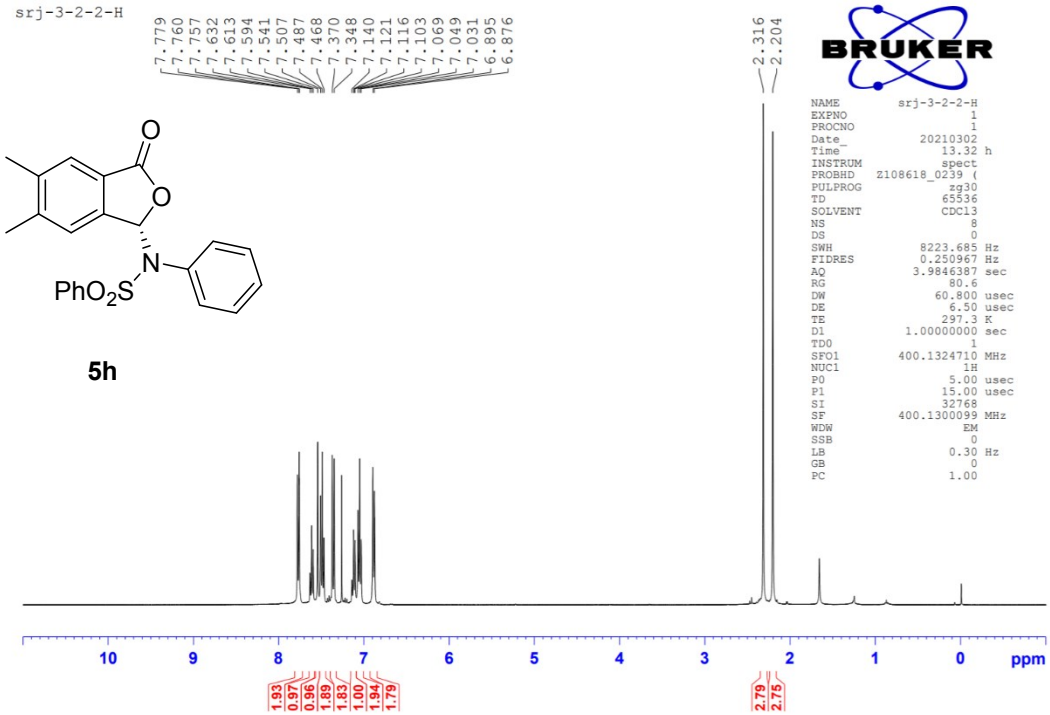
srj-3-2-2-H
7.779
7.760
7.757
7.632
7.613
7.594
7.541
7.507
7.487
7.468
7.370
7.348
7.140
7.121
7.116
7.103
7.069
7.049
7.031
6.895
6.876
2.316
2.204
BRUKER
NAME srj-3-2-2-H
EXPNO 1
PROCNO 1
Date_ 20210302
Time 13.32 h
INSTRUM spect
PROBHD Z108618_0239 (
PULPROG zg30
TD 65536
SOLVENT CDCl3
NS 8
DS 0
SWH 8223.685 Hz
FIDRES 0.250967 Hz
AQ 3.9846387 sec
RG 80.6
DW 60.800 usec
DE 6.50 usec
TE 297.3 K
D1 1.00000000 sec
TD0 1
SFO1 400.1324710 MHz
NUC1 1H
P0 5.00 usec
P1 15.00 usec
SI 32768
SF 400.1300099 MHz
WDW EM
SSB 0
LB 0.30 Hz
GB 0
PC 1.00
O
O
N
PhO2S
5h
10
9
8
7
6
5
4
3
2
1
0
ppm
1.93
0.97
0.96
1.89
1.83
1.00
1.94
1.79
2.79
2.75

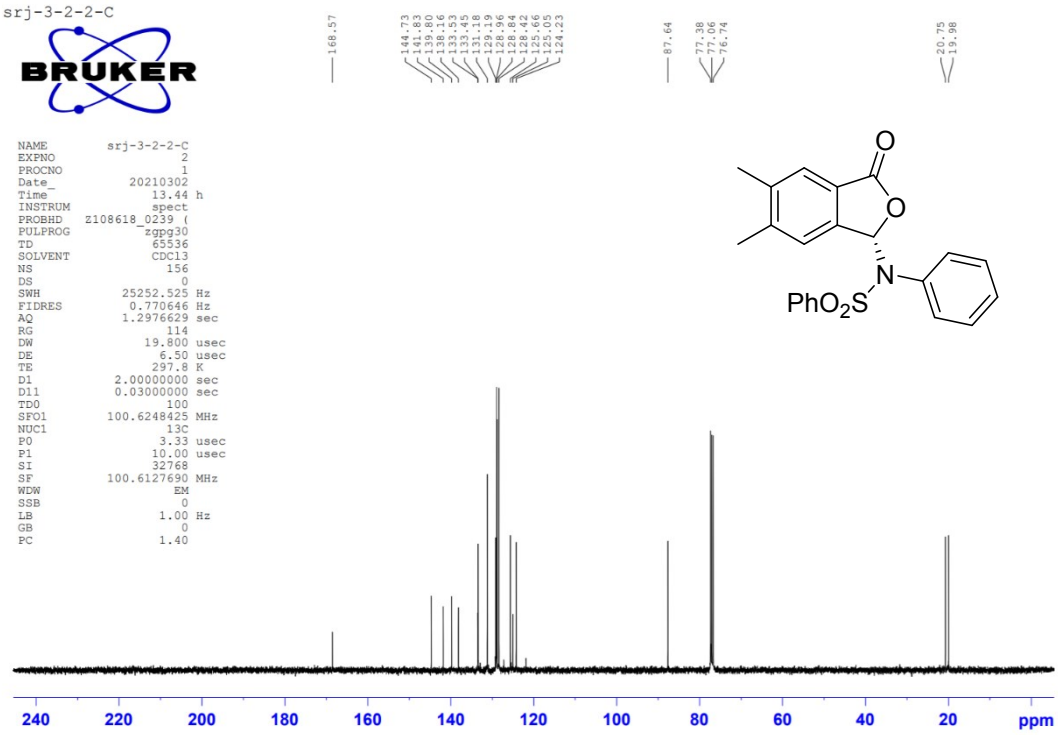
srj-3-2-2-C
BRUKER
168.57
144.73
141.83
139.80
138.16
133.53
133.45
131.18
129.19
128.96
128.84
128.42
125.66
125.55
124.23
87.64
77.38
77.06
76.74
20.75
19.98
NAME srj-3-2-2-C
EXPNO 2
PROCNO 1
Date_ 20210302
Time 13.44 h
INSTRUM spect
PROBHD Z108618_0239 (
PULPROG zgpg30
TD 65536
SOLVENT CDCl3
NS 156
DS 0
SWH 25252.525 Hz
FIDRES 0.770646 Hz
AQ 1.2976629 sec
RG 114
DW 19.800 usec
DE 6.50 usec
TE 297.8 K
D1 2.00000000 sec
D11 0.03000000 sec
TD0 100
SFO1 100.6248425 MHz
NUC1 13C
P0 3.33 usec
P1 10.00 usec
SI 32768
SF 100.6127690 MHz
WDW EM
SSB 0
LB 1.00 Hz
GB 0
PC 1.40
O
O
N
PhO2S
240
220
200
180
160
140
120
100
80
60
40
20
ppm

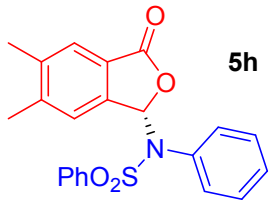

5h

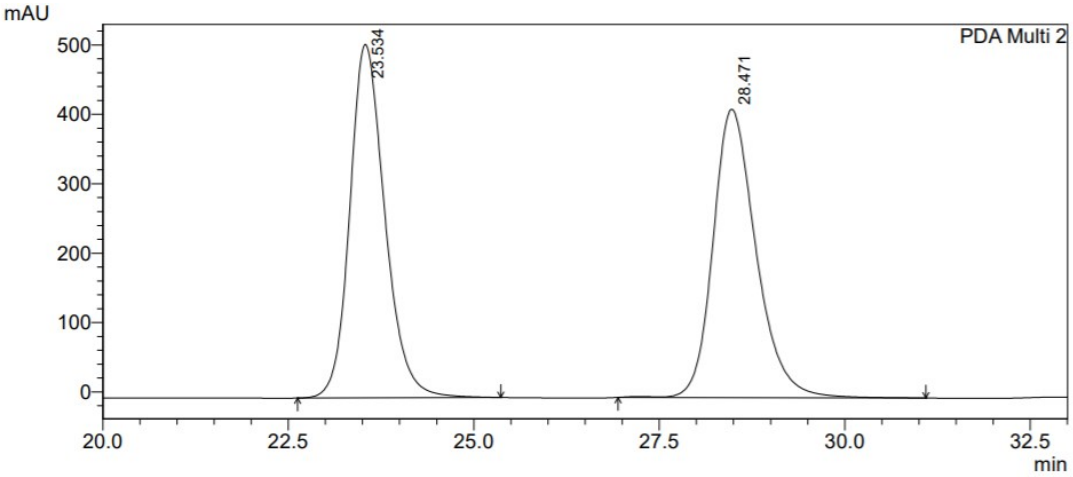

PeakTable

PDA Ch2 220nm 4nm

Peak#	Ret. Time	Area	Height	Area %	Height %
1	23.534	16784381	509611	49.979	55.084
2	28.471	16798690	415547	50.021	44.916
Total		33583070	925158	100.000	100.000

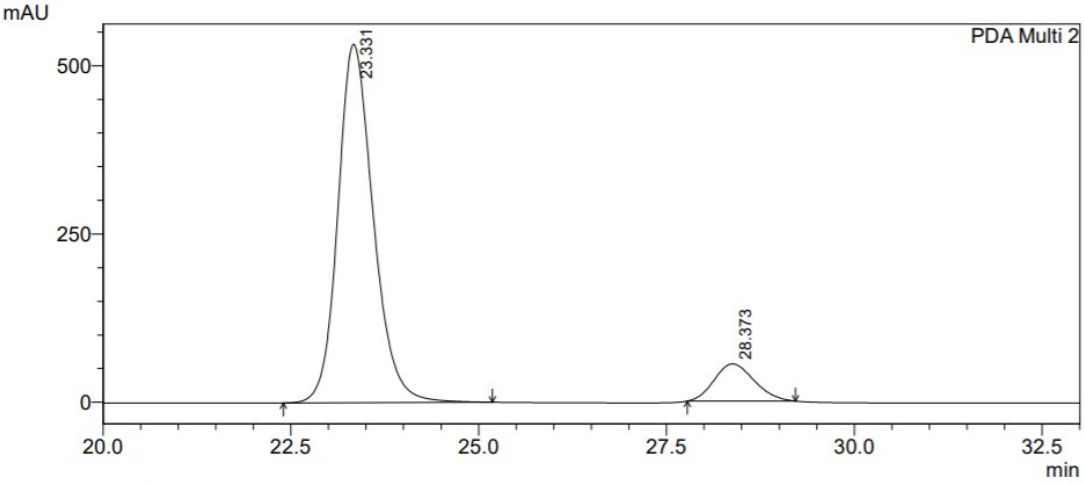

PeakTable

PDA Ch2 220nm 4nm

Peak#	Ret. Time	Area	Height	Area %	Height %
1	23.331	17517146	533054	89.531	90.605
2	28.373	2048238	55276	10.469	9.395
Total		19565385	588330	100.000	100.000

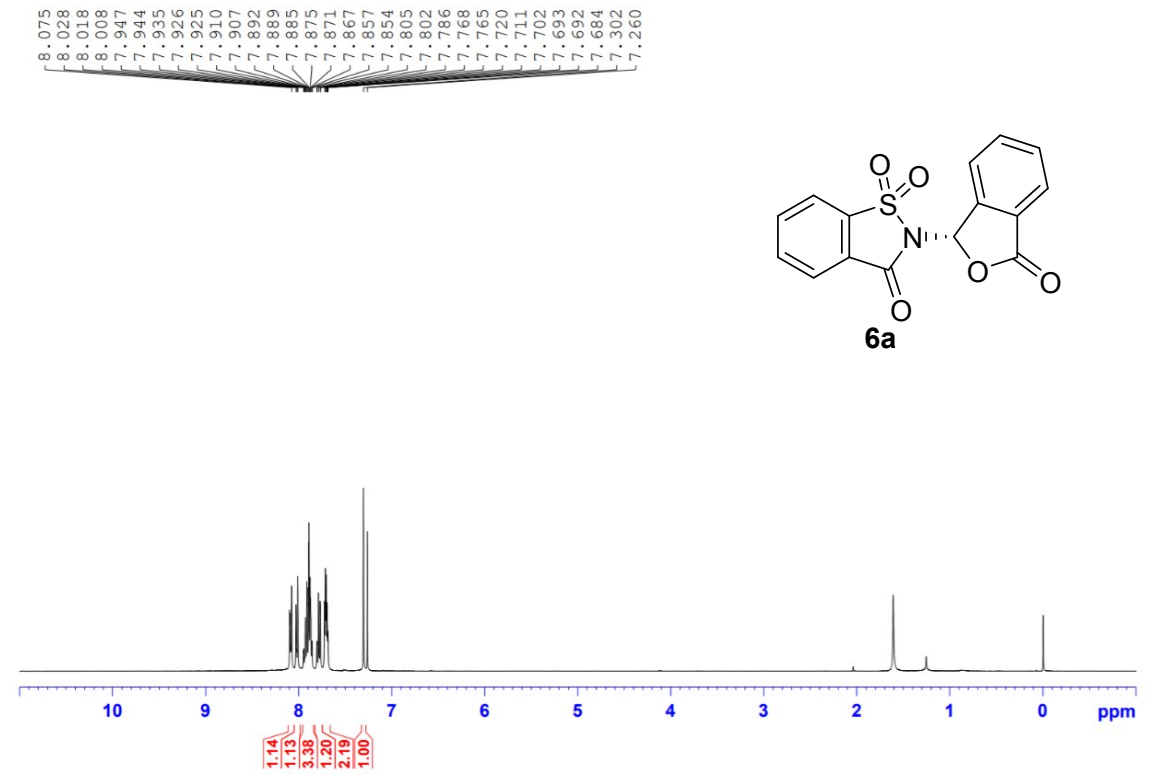
8.075
8.028
8.018
8.008
7.947
7.944
7.935
7.926
7.925
7.910
7.907
7.892
7.889
7.885
7.875
7.871
7.867
7.857
7.854
7.805
7.802
7.786
7.768
7.765
7.720
7.711
7.702
7.693
7.692
7.684
7.302
7.260
6a
10
9
8
7
6
5
4
3
2
1
0
ppm
1.14
1.13
3.38
1.20
2.19
1.00

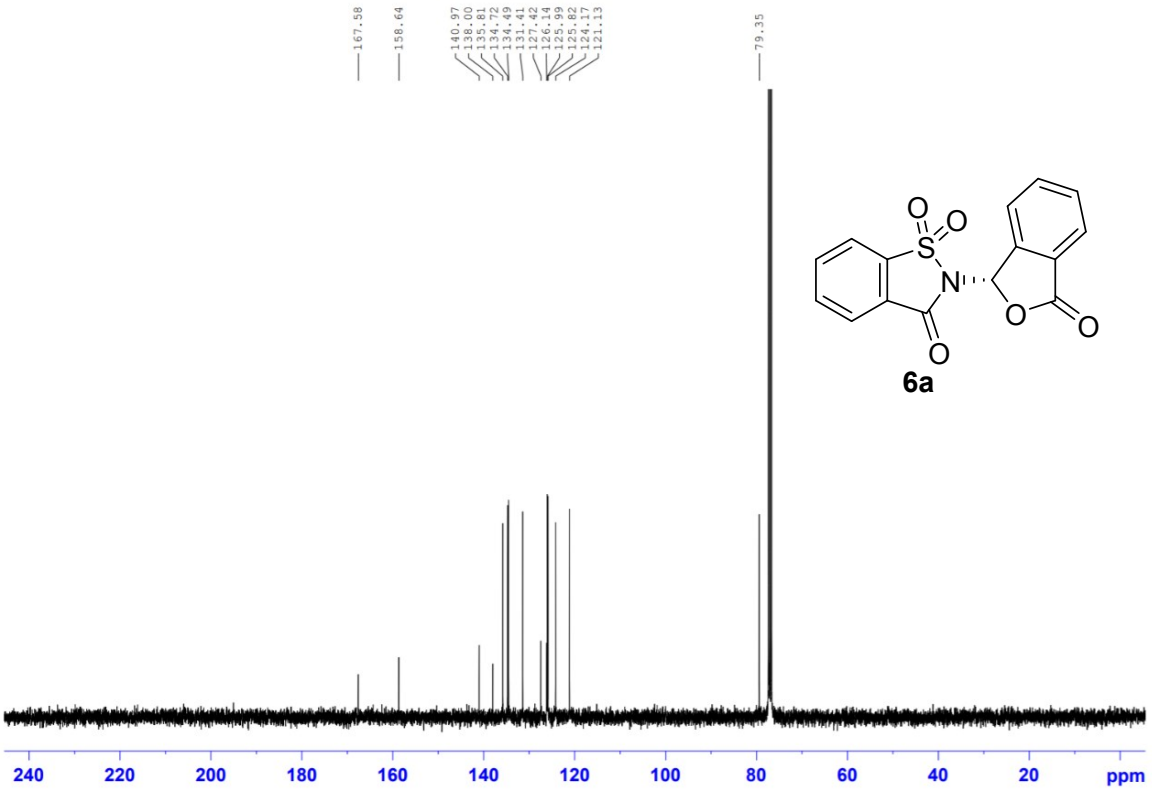
167.58
158.64
140.97
138.00
135.81
134.72
134.49
131.41
127.42
126.14
125.99
125.82
124.17
121.13
79.35
6a
240
220
200
180
160
140
120
100
80
60
40
20
ppm

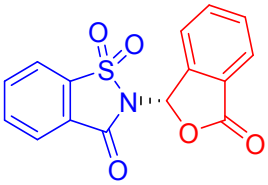

6a

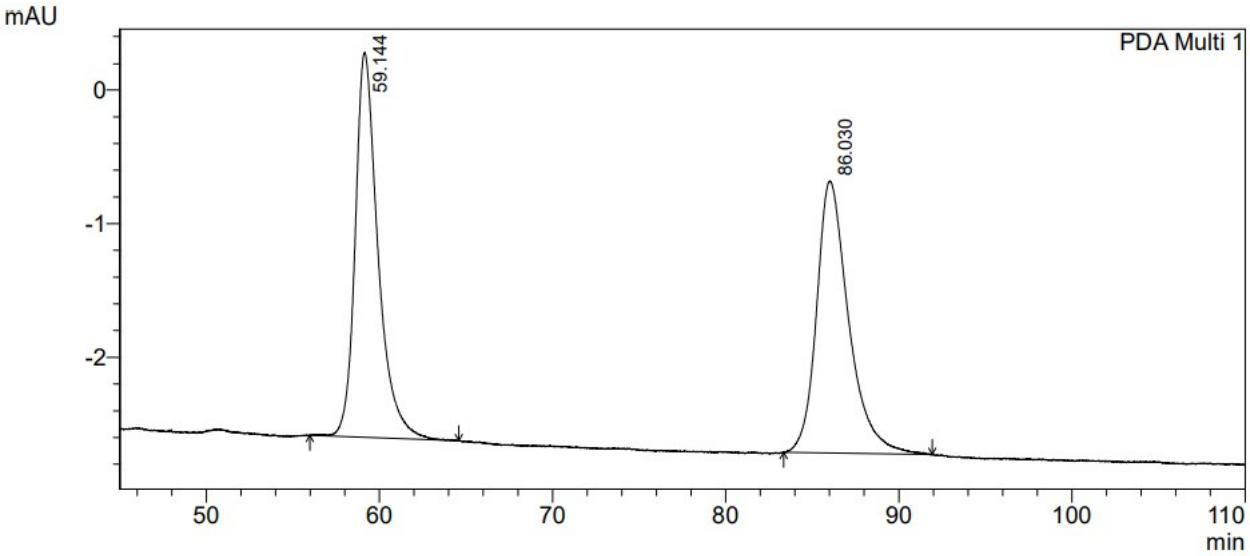

PDA Ch1 254nm 4nm

Peak#	Ret. Time	Area	Height	Area %	Height %
1	59.144	263912	2881	50.146	58.612
2	86.030	262378	2035	49.854	41.388
Total		526291	4916	100.000	100.000

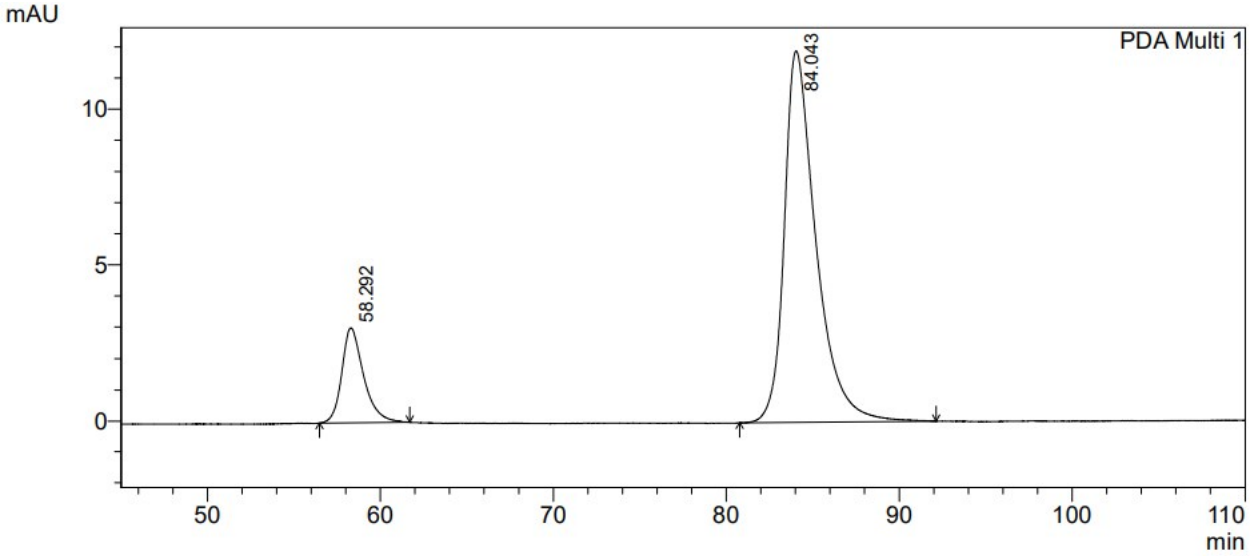

Peak#	Ret. Time	Area	Height	Area %	Height %
1	58.292	267012	3027	14.967	20.261
2	84.043	1516991	11913	85.033	79.739
Total		1784003	14940	100.000	100.000

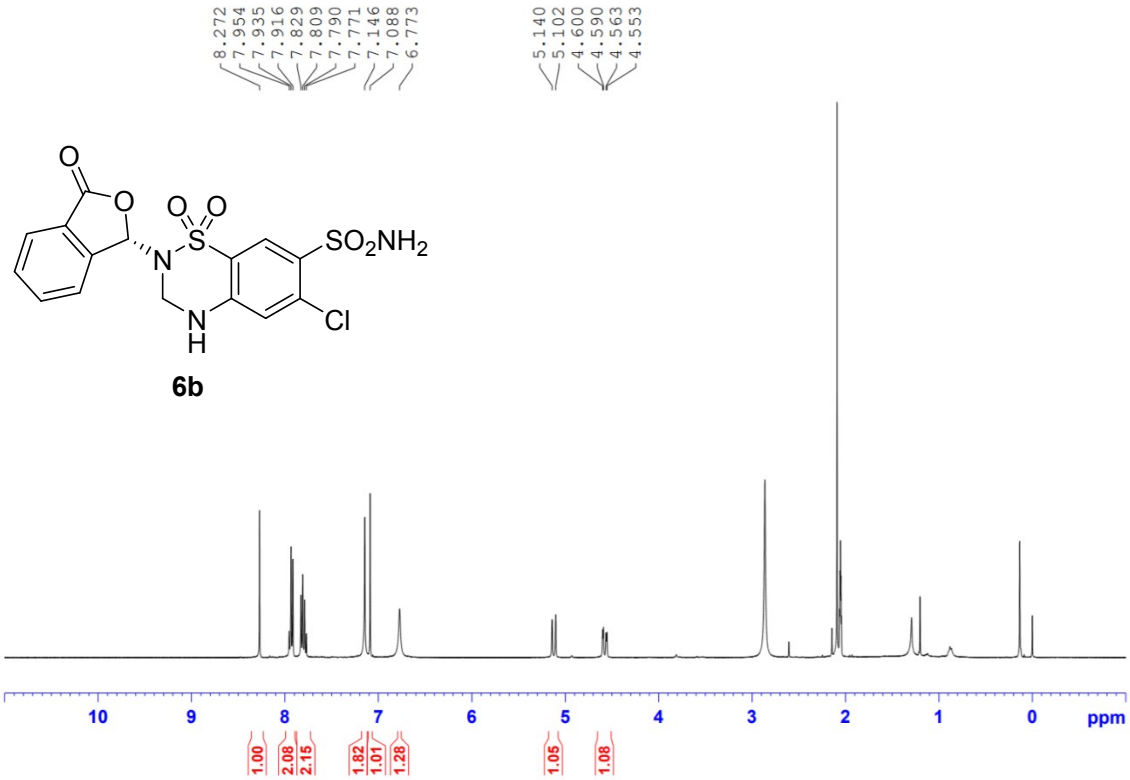
8.272
7.954
7.935
7.916
7.829
7.809
7.790
7.771
7.146
7.088
6.773
5.140
5.102
4.600
4.590
4.563
4.553
SO2NH2
Cl
6b
10
9
8
7
6
5
4
3
2
1
0
ppm
1.00
2.08
2.15
1.82
1.01
1.28
1.05
1.08

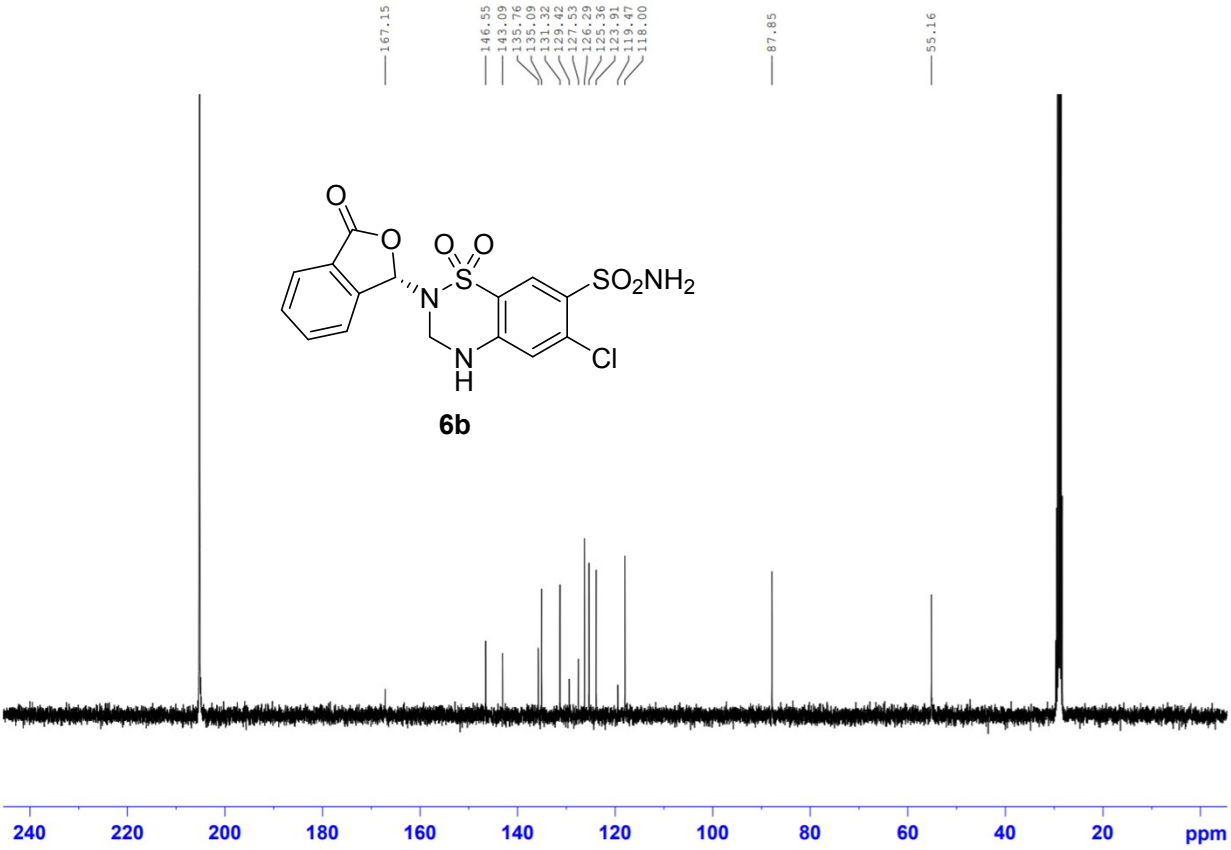
167.15
146.55
143.09
135.76
135.09
131.32
129.42
127.53
126.29
125.36
123.91
119.47
118.00
87.85
55.16
SO2NH2
Cl
6b
240
220
200
180
160
140
120
100
80
60
40
20
ppm

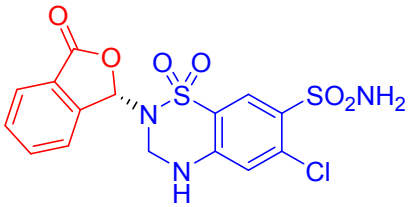

6b

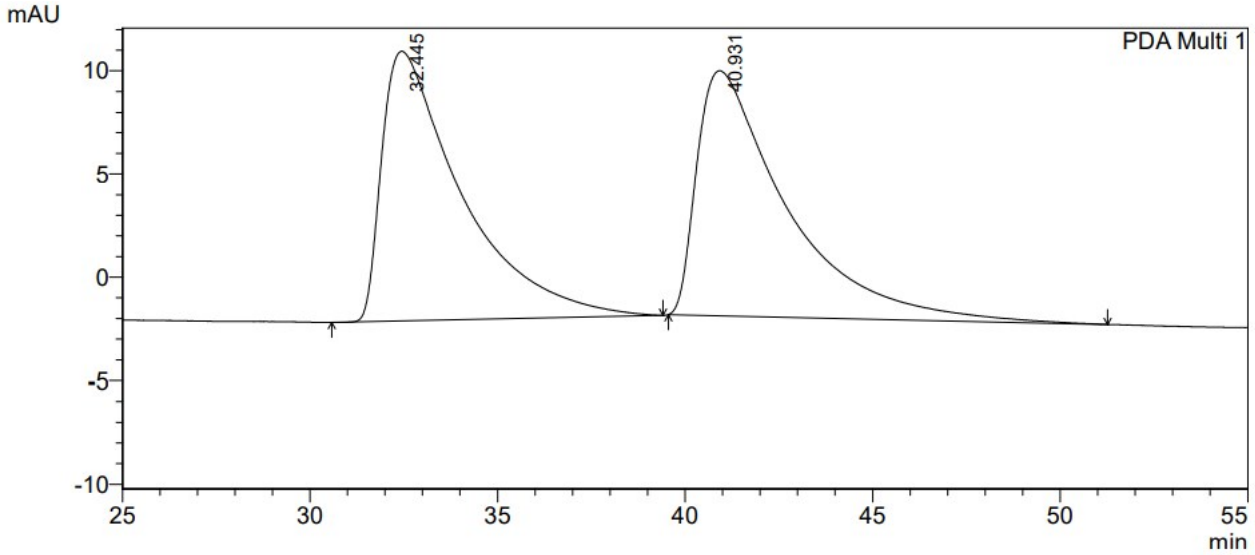

PDA Ch1 254nm 4nm

Peak#	Ret. Time	Area	Height	Area %	Height %
1	32.445	1925471	13068	49.515	52.410
2	40.931	1963172	11866	50.485	47.590
Total		3888643	24934	100.000	100.000

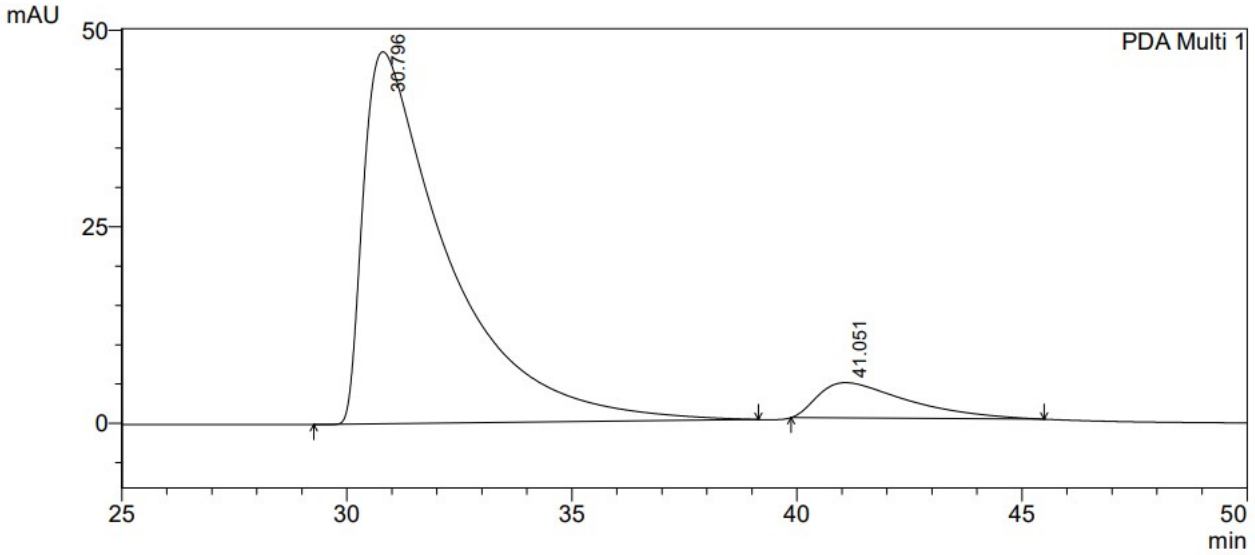

PDA Ch1 254nm 4nm

Peak#	Ret. Time	Area	Height	Area %	Height %
1	30.796	6188663	47299	90.845	91.336
2	41.051	623662	4487	9.155	8.664
Total		6812326	51786	100.000	100.000

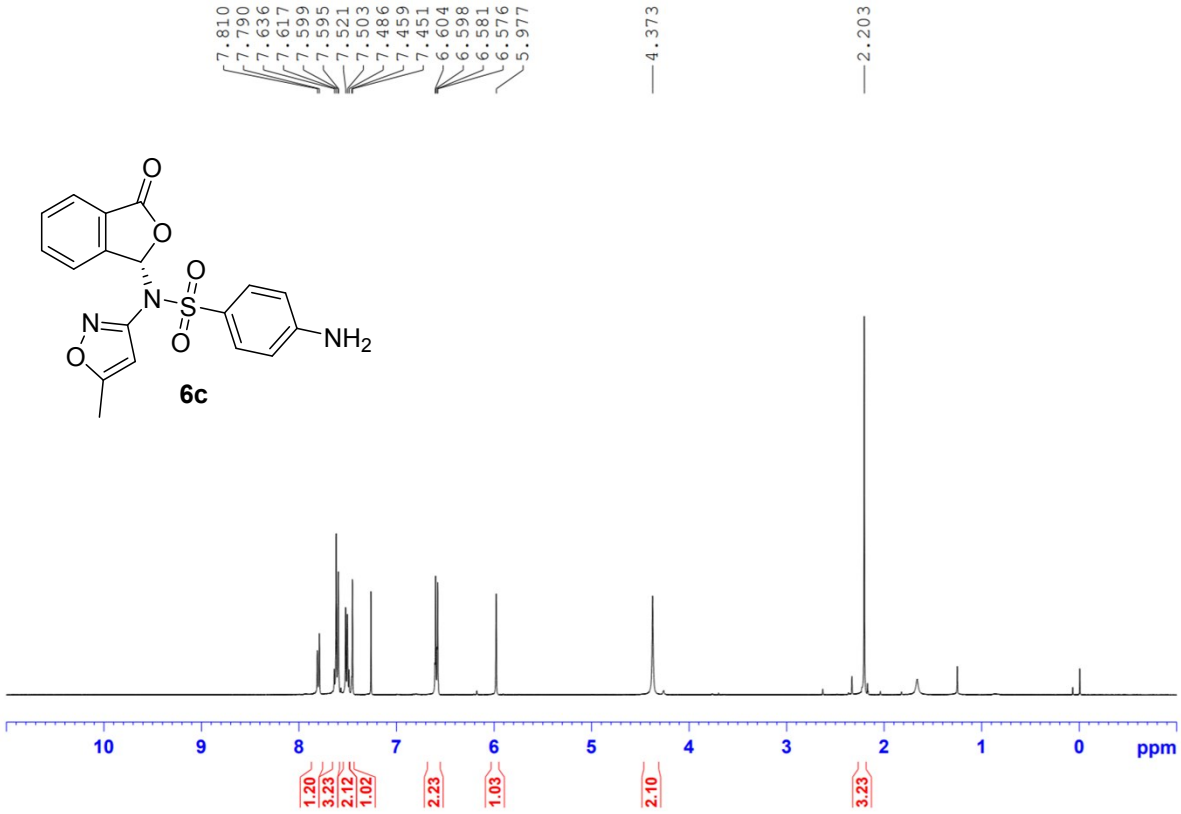
7.810
7.790
7.636
7.617
7.599
7.595
7.521
7.503
7.486
7.459
7.451
6.604
6.598
6.581
6.576
5.977
4.373
2.203
6c
10
9
8
7
6
5
4
3
2
1
0
ppm
1.20
3.23
2.12
1.02
2.23
1.03
2.10
3.23

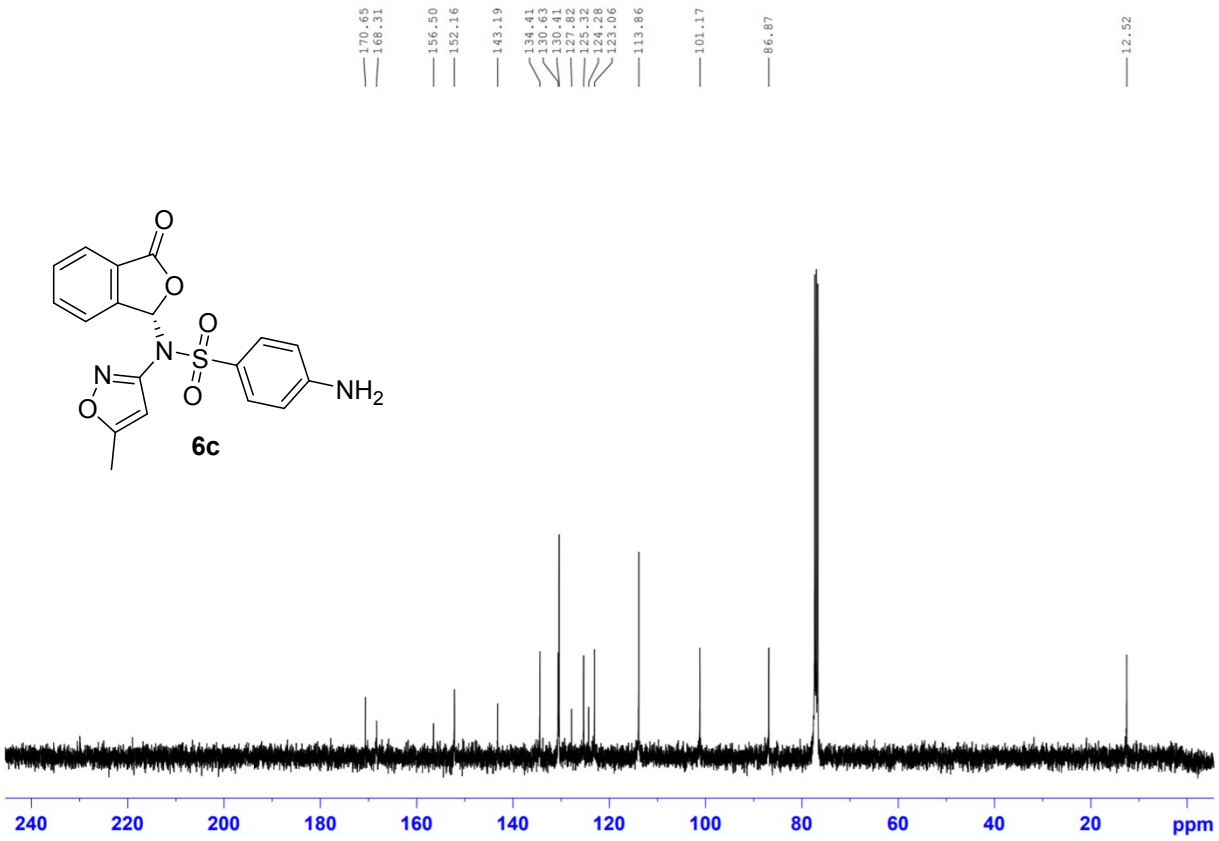
170.65
168.31
156.50
152.16
143.19
134.41
130.63
130.41
127.82
125.32
124.28
123.06
113.86
101.17
86.87
12.52
6c
240
220
200
180
160
140
120
100
80
60
40
20
ppm

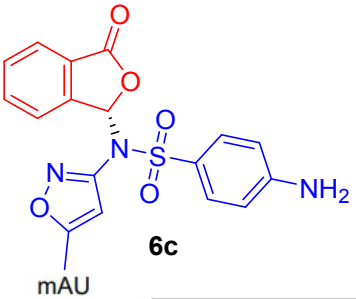

6c

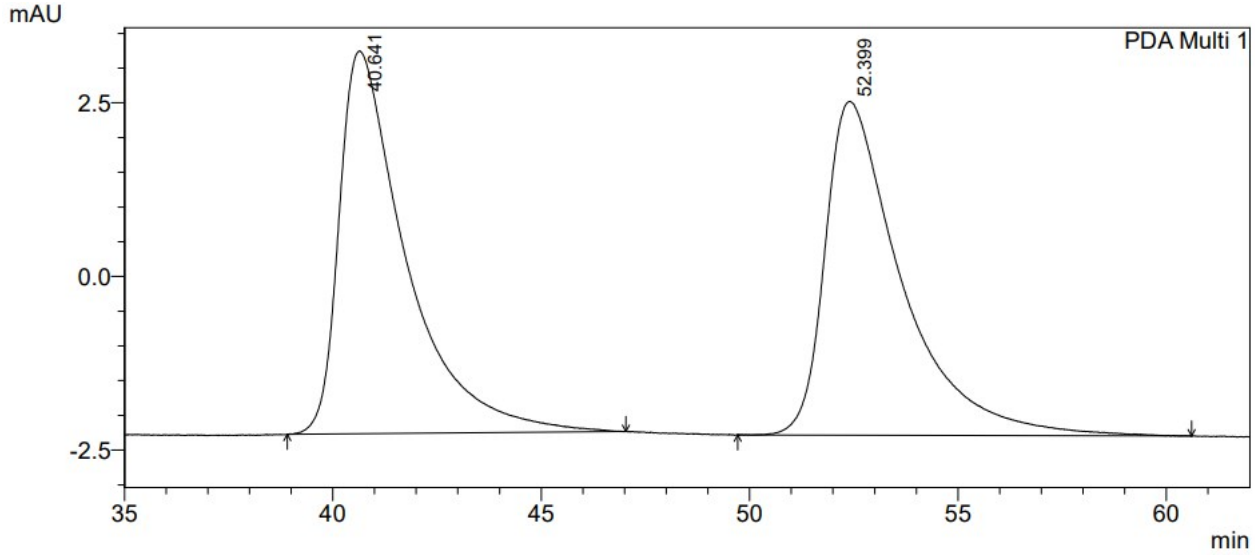

PDA Ch1 254nm 4nm

Peak#	Ret. Time	Area	Height	Area %	Height %
1	40.641	617567	5514	49.942	53.435
2	52.399	618998	4805	50.058	46.565
Total		1236565	10319	100.000	100.000

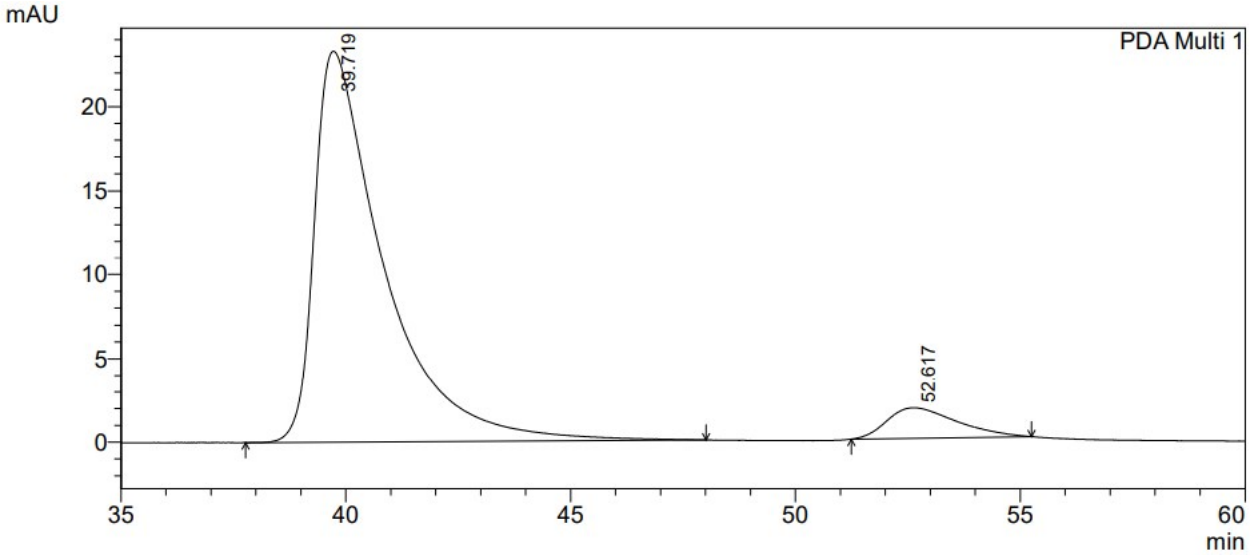

PDA Ch1 254nm 4nm

Peak#	Ret. Time	Area	Height	Area %	Height %
1	39.719	2501997	23302	92.745	92.747
2	52.617	195719	1822	7.255	7.253
Total		2697716	25124	100.000	100.000